Reporte de año Sabático
Periodo: 27 de julio de 2020 al 26 de julio 2021
Dra. Adela Irmene Ortíz López

El plan de actividades incluyó el desarrollo de proyectos de investigación, publicación de resultados, seguimiento de alumnos y consolidación de colaboraciones, todas ellas con el fin de contribuir a mi superación académica en beneficio de la Universidad. Cabe señalar que originalmente se solicitó y aprobó un periodo sabático de 22 meses pero dadas las condiciones sanitarias prevalecientes desde marzo del 2020, se solicitó el regreso anticipado.

A continuación se desglozan los resultados obtenidos en cada uno de los rubros, mientras que los comprobantes se muestran en el Anexo I.

I. Desarrollo de proyectos

1. Se cumplió de manera satisfactoria con la participación en el clúster de biocombustibles gaseosos (SENER-CONACYT) con vigencia de junio 2016 a Febrero del presente año, cumpliendo con todos los productos y entregables comprometidos, tanto a nivel de publicaciones, formación de alumnos y difusión de los resultados obtenidos, así como con la presentación de informes finales.
2. Se concluyó satisfactoriamente el proyecto Divisional Bioprocesos ambientales (**50-S114-15)** el cual tuvo una vigencia de junio de 2015 a junio de 2021 y del cual fungí como responsable. El informe final fue presentado al Consejo Divisional de la DCNI.

II. Publicación en revistas indizadas

1. Duran-Cruz V., Hernandez S., **Ortíz I**. **2021.** Evaluation of Steam Explosion Pretreatment and Enzymatic Hydrolysis Conditions for Agave Bagasse in Biomethane Production. **BioEnergy Research**. https://doi.org/10.1007/s12155-021-10245-9. IF: 2.814
2. Casanova A., Cabrera S., · Díaz-Ruiz G., · Hernández S., · Wacher C., Zubillaga M., **Ortíz I**. **2021**. Evaluation of endosulfan degradation capacity by six pure strains isolated from a horticulture soil. **Folia Microbiologica**. https://doi.org/10.1007/s12223-021-00899-5. IF: 2.099.
3. Tafolla R., Ramírez F., Ortiz R., Cortés E., **Ortíz I.**, Monroy O. **2021.** Treatment of waste activated sludge by steam explosion and alkaline acidogenesis. **Revista Mexicana de Ingeniería Química**. 20 (3) https://doi.org/10.24275/rmiq/IA2388. IF: 2.148.
4. Hernández-Vázquez A., Hernández S., **Ortíz I**. **2020**. Hydrothermal pretreatment of agave bagasse for biomethane production: Operating conditions and energy balance. **Biomass and Bioenergy** 142: 105753. https://doi.org/10.1016/j.biombioe.2020.105753. IF: 3.551

III. Participación en Congresos:

1. Adriana Lizeth Casanova-Olguín, Sonia Cabrera, Sergio Hernández-Jiménez, **Irmene Ortíz**. Evaluación de la capacidad degradadora de endosulfan por cepas bacterianas aisladas de suelo hortícola con historial de uso de plaguicidas. XLI Encuentro Nacional de la Academia Mexicana de Investigación y Docencia en Ingeniería Química A.C. (AMIDIQ). 22-24 octubre **2020**.
2. M. Vital-Jácome, **I. Ortíz,** G. Buitrón. Methane production from Agave bagasse by using chemical, biological, and hydrothermal pretreatments. 2nd. Latin American & Caribbean Young Water Professionals Conference IWA. 8-12 noviembre **2020**.
3. Aceptación del Trabajo "Simulación de la producción de fitasa utilizando un hongo del género *Aspergillus"* Miguel Ángel Tomate Hernández, Sergio Hernández Jiménez, **Irmene Ortíz** López, para ser presentado en el XLII Encuentro Nacional de la Academia Mexicana de Investigación y Docencia en Ingeniería Química A.C. (AMIDIQ) a realizarse del 8 al 11 de septiembre de **2021**.
4. Aceptación del Trabajo "Evaluación técnico-económica del pretratamiento de residuos de poda y vegetación urbana para la producción de etanol" Luis Enrique Angulo Sierra, Sergio Hernández Jiménez, **Irmene Ortíz** López, para ser presentado en el XLII Encuentro Nacional de la Academia Mexicana de Investigación y Docencia en Ingeniería Química A.C. (AMIDIQ) a realizarse del 8 al 11 de septiembre de **2021**.
5. Aceptación del Trabajo "Evaluación de la capacidad de *Achromobacter spanius, Peribacillus Simplex y Bacillus pseudomycoides* para degradar endosulfan" Adriana Casanova, Sonia Cabrera, Marta Zubillaga, Carmen Wacher, Gloria Díaz-Ruiz, Sergio Hernandez, **Irmene Ortíz**, para ser presentado en le XIX congreso nacional de Biotecnología y Bioingeniería a celebrarse del 27 de septiembre al 1 de octubre **2021**.
6. Aceptación del Trabajo "Evaluación de las condiciones de pretratamiento por explosión de vapor e hidrólisis enzimática de bagazo de agave para la producción de biometano" Verónica Duran-Cruz, Sergio Hernández, **Irmene Ortíz**, para ser presentado en le XIX congreso nacional de Biotecnología y Bioingeniería a celebrarse del 27 de septiembre al 1 de octubre **2021**.

IV. Coordinación de libros

Se concluyó con la compilación y edición del libro colectivo Introducción a la Ingeniería Biológica, el cual coordinó junto con el Dr. Rodolfo Quintero. La obra cuenta con 20 capítulos que son contribuciones de 18 profesores del DPT y 3 colaboradores externos. La publicación se presentó al Consejo Editorial de la Unidad Cuajimalpa y se encuentra en revisión externa.

V. Participación en Comités

1. Miembro del Comité Técnico y comité revisor del LXI Encuentro Nacional de la XLI Encuentro Nacional de la Academia Mexicana de Investigación y Docencia en Ingeniería Química A.C. (AMIDIQ). Responsable del Área de Biotecnología. **Enero-Octubre 2020**.

2. Miembro del Comité Técnico y comité revisor del LXII Encuentro Nacional de la Academia Mexicana de Investigación y Docencia en Ingeniería Química A.C. (AMIDIQ). Responsable del Área de Biotecnología. **Marzo-junio 2021**.
3. Miembro del Comité Revisor del Congreso Nacional de Biotecnología y Bioingeniería en el Área de Biotecnología ambiental. **Mayo -julio 2021**
4. Se continuó con la participación como miembro titular del comité de Transparencia de la UAM, nombramiento del segundo periodo de diciembre **2020 a 2022**.

VI. Seguimiento de alumnos

1. Se dio continuidad a la co-dirección de la alumna de maestría, Ing. Carolina Rangel participando en reuniones de comité vía remota para planeación del desarrollo experimental. La alumna tiene un retraso considerable en la obtención del grado debido a problemas tanto personales como académicos, sin embargo, terminó la parte experimental de la tesis y actualmente se encuentra en el análisis de resultados y en la redacción de la ICR.
2. Se participó en el comité doctoral de la alumna Karen Zúñiga que realiza su tesis bajo la dirección del Dr. José Campos. Se realizaron reuniones remotas trimestrales de evaluación de la alumna.
3. Se incorporó a la alumna de Maestría, Verónica Durán Cruz formalizando la dirección de proyecto de investigación.
4. Adicionalmente, participé en los seminarios trimestrales de las tres alumnas anteriores organizado por el PCNI, en julio **2021**.
5. Dirección de Proyecto Terminal "Evaluación técnico-económica del pretratamiento de residuos de poda y vegetación urbana para la producción de etanol". Alumno Luis Enrique Angulo Sierra, Lic. en Ingeniería Biológica de la UAM-C. 16/11/**2020**.
6. Asesoría de Servicio social de la Alumna Adriana Lizeth Casanova Olguín, del 19 de octubre 2020 al 19 abril **2021.**
7. Asesoría del Servicio social del Alumno Miguel Ángel Tomate Hernández, 20 de enero 2021 al 20 de julio **2021**.
8. Se dio seguimiento a los alumnos que solicitarion tutoría para Movilidad, Servicio Social y prácticas profesionales.

VII. Colaboraciones y estancias de investigación

Se tenían planeadas dos estancias de investigación, una en la Universidad Aix-Marseille Université Campus l'Etoile para la consolidación de la colaboración con el Dr. Pierre Christen del Instituto Francés de Investigación para el Desarrollo (**IRD**) y otra en la Universidad del Mar, Oaxaca para continuar con la colabolación con la Dra. Rosario Enríquez. Sin embargo, debido a la emergencia sanitaria causada por el Coronavirus SARS-CoV2, no pudieron realizarse. Sin embargo, las colaboraciones continuan y un producto de ellas es el capítulo Agroecología incluido en el libro Introducción a la Ingeniería Biológica, mencionado en el punto

IV de este informe. Finalmente, existe la posibilidad de realizar las estancias cuando las condiciones sanitarias lo permitan.

VIII. Impartición de seminarios

1. Biodegradación de endosulfan. Centro de Química-ICUAP. Benemérita Universidad Autónoma de Puebla (BUAP). 24 de **junio 2021**

2. Biorrefinerías. Seminario de Ingeniería ambiental. Lic. Ing. Biológica. UAMC. 16 **febrero 2021.**

Anexo I.
Productos generados durante el año sabático

BioEnergy Research
https://doi.org/10.1007/s12155-021-10245-9

Evaluation of Steam Explosion Pretreatment and Enzymatic Hydrolysis Conditions for Agave Bagasse in Biomethane Production

Veronica Duran-Cruz[1] · Sergio Hernández[2] · Irmene Ortíz[2]

Received: 20 October 2020 / Accepted: 5 January 2021

Abstract

The production of biofuels from lignocellulosic biomass includes a pretreatment step to alter the biomass structure and facilitate the enzymatic degradation of the polymers to obtain assimilable compounds. In this study, agave bagasse (AB) was used as a feedstock for obtaining methane, for which AB was pretreated with steam explosion and enzymatically hydrolyzed. The pretreatment conditions corresponded to severity factors (SFs) within a range from 1.65 to 2.89, while enzymatic hydrolysis was performed with enzyme loads of Cellic CTec2 within a range from 0.12 to 3.6 $mg_{protein}\ g^{-1}_{AB}$. The best global yields (including pretreatment and enzymatic hydrolysis) of total carbohydrates (TCs), glucose (GLU), xylose (XYL), and chemical oxygen demand (COD) were 0.7 g TC g^{-1}_{AB}, 0.12 g GLU g^{-1}_{AB}, 0.03 g XYL g^{-1}_{AB}, and 0.20 g O_2 g^{-1}_{AB} obtained using 2.4 $mg_{protein}\ g^{-1}_{AB}$ of Cellic CTec2 with agave bagasse pretreated with an SF of 2.41. The contribution of pretreatment to the global TC yield ranged from 13 to 34% for the different systems evaluated. The biochemical potential of methane (BMP) of hydrolysates (pretreatment at SF 2.41 and 2.4 $mg_{protein}\ g^{-1}_{AB}$ of Cellic CTec2) was 0.284 ± 0.02 in NL $CH_4\ g^{-1}$ COD with a COD removal of 78.4 ± 1.3. This BMP value was 40% higher than the BMP obtained in the system without enzymatic hydrolysis, indicating the impact of this step on conversion to biomethane. The results at the BMP level indicated the potential of this residue for biofuel production.

Keywords Biochemical methane potential (BMP) · Pretreatment · Lignocellulosic biomass · Sugar recovery · Biogas · Severity factor

Introduction

Lignocellulosic agricultural wastes, which are mostly discarded or disposed of, resulting in a variety of environmental problems, can be used as feedstock for second-generation biofuel production. The growing interest in biofuel production is related to a concern about the depletion of oil reserves and a possible crisis due to fuel shortages and, from an environmental point of view, due to the potential reduction of greenhouse gas emissions [1].

In Mexico, the projections by 2030 for the development of second-generation biofuels include at least the use of 4% in transportation and 35% in electricity [2]. Agave bagasse (AB) is a lignocellulosic residue from tequila production with potential as feedstock since it is one of the most important mexican industries, generating approximately 540,000 tons of AB per year that are disposed of in fields or burned at tequila factories [3].

Lignocellulosic biomass has a recalcitrant structure due to its composition of cellulose, hemicellulose, and lignin; therefore, pretreatment and enzymatic hydrolysis are required to obtain carbohydrates that can be converted into biofuels. Pretreatment is a critical step since the structure of lignocellulosic matter is altered to facilitate the access of enzymes to chains of polymers. Physicochemical, chemical, and biological pretreatments can be applied to lignocellulosic biomass; among these pretreatments, one of the most studied in the laboratory, demonstration, and commercial plants is steam explosion [4]. In this hydrothermal pretreatment, the biomass is processed with saturated steam at temperatures between 160 and 280 °C for times ranging from seconds to minutes, followed by sudden depressurization [5, 6]. The main effects of the steam explosion process on biomass are as follows: (a)

✉ Irmene Ortíz
irmene@cua.uam.mx

[1] Licenciatura en Ingeniería Biológica, Universidad Autónoma Metropolitana-Cuajimalpa, Mexico City, Mexico

[2] Departamento Procesos y Tecnología, Universidad Autónoma Metropolitana-Cuajimalpa, Av. Vasco de Quiroga 4871, Col. Santa Fe. C.P, 05348 Mexico City, Mexico

Published online: 16 January 2021

reduction of the degree of polymerization due to acidic degradation and thermal degradation; (b) mechanical breakage of fibers to a certain extent due to the sudden decompression of the system, the consequent deconstruction of the amorphous regions, and the partial destruction of the crystalline regions; and (c) destruction of the hydrogen bonds and structural rearrangement due to temperature and pressure conditions [7, 8]. In addition to the above, this pretreatment uses almost no chemical products since it requires only water to solubilize and depolymerize the hemicellulose in the liquid phase (hydrolysates). In this way, steam explosion can be considered an environmentally friendly process and was selected for this study [9]. Other advantages of steam explosion include a significantly lower environmental impact and a lower capital investment compared with other leading pretreatments. However, the main disadvantage is the energy requirement to achieve the operational conditions. However, it has recently been shown that steam explosion pretreatment of AB for the production of methane is energetically feasible [3, 8]. After pretreatment, enzyme complexes, mainly cellulases and hemicellulases, act on the β-1,4-glycosidic bonds that join the cellulose and hemicellulose molecules to release the monomers, allowing further processing [10].

The potential of AB for the production of gaseous biofuels has been explored by Valdez-Vazquez et al. [11], who reported a comparison of biological, enzymatic, chemical, and hydrothermal pretreatments. Similarly, Galindo-Hernández et al. [12] pretreated AB with alkaline hydrogen peroxide and performed enzymatic saccharification to evaluate hydrogen and methane production. García-Amador et al. [13] evaluated the feasibility of bioelectrohydrogen production from steam explosion–pretreated AB. Other studies such as ethanol performing autohydrolysis at severity factors (SF) ranging from 2.35 to 4.12, as well as enzymatic hydrolysis (EH) and fermentation with *S. cerevisiae* [14], have been performed for the production of liquid biofuels.

In this study, AB was pretreated by steam explosion with temperatures below the temperatures commonly reported in the literature, which resulted in less severe conditions and lower energy requirements. In this context, the objective of this work was to evaluate the yields of total carbohydrates (TCs), glucose (GLU), and xylose (XYL) obtained by enzymatic hydrolysis of steam explosion–pretreated agave bagasse under different operating conditions and enzymatic cocktails for their later conversion to biomethane.

Methodology

Biomass

Bagasse of *Agave tequilana* Weber, blue variety, obtained from a tequila factory from Amatitán, state of Jalisco, was donated by the Institute for Scientific and Technological Research of San Luis Potosi (IPICYT). The bagasse was sun-dried, sieved (< 1.7 mm), and stored at room temperature [15]. The composition of AB was 46.0 ± 1.0% cellulose, 23.1 ± 1.0% hemicellulose, 15.3 ± 1.0% lignin, 6.8 ± 1.4% total extractives, 4.3 ± 1.2% moisture content, and 2.9 ± 1.2% ash [3].

Pretreatment

Unground dried agave bagasse was pretreated by steam explosion at a solid:liquid ratio of 55:2000 (wt/wt) and temperatures of 116, 142, and 154 °C for 15 and 20 min. These operational conditions were selected based on our previous study, where the energy balance at different operational conditions was evaluated [3].

The SF was used for the comparison of pretreatments since it includes the operational parameters of temperature and time of pretreatment and is consequently related to the energy requirements. The SF was calculated for each pretreatment according to Eq. 1, which is based on first-order kinetics and obeys Arrhenius's law [16]. The conditions of the pretreatments employed are shown in Table 1.

$$\mathrm{SF} = \mathrm{Log}\left(t^{*}e^{\frac{(T-100)}{14.75}}\right) \quad (1)$$

where T is the temperature in °C, and t is the time in minutes.

Two fractions were obtained from the pretreatment, one solid fraction consisting of the pretreated (humid) bagasse and one liquid fraction, the hydrolysates. The solid fraction was dried at 38 °C for preservation, whereas the hydrolysates were refrigerated at 4 °C until used for EH (Table 2). As described below, the solid fraction was characterized after acid hydrolysis [17] and analyzed, as were the hydrolysates.

Table 1 Experimental conditions and severity factor values of the pretreatments

Temperature (°C)	Pressure (MPa)	Time (min)	SF
116	0.28	15	1.65
142	0.47	15	2.41
142	0.47	20	2.54
154	0.67	15	2.77
154	0.67	20	2.89

SF, severity factor

Solid: liquid ratio (wt/wt) in all cases 55:2000

Table 2 Experimental conditions for enzymatic hydrolysis

SF	Enzyme	Concentration ($mg_{protein}\ g^{-1}_{AB}$)	Aqueous phase
Control	Cellic CTec2	0.12-2.40	0.1 M Acetate Buffer, pH 5
2.54	Cellic CTec2	0.12	0.1 M Acetate Buffer, pH 5
2.77			
2.89			
2.41	Cellic CTec2	0.12	Hydrolysates, pH 5
2.54			
2.41	Cellic CTec2	1.20	
1.65	Cellic CTec2	2.40	
2.41[a]			
2.54			
2.77			
2.89			
2.41	Cellic CTec2	3.60	
2.41[a]	Celluclast 1.5 L-Viscozyme L	3.7–19.4	50 mM Citrate Buffer, pH 3.5

[a] Selected for BMP tests; *SF*, severity factor

Enzymatic Hydrolysis

The EH of the solid fraction obtained with the different pretreatments studied was evaluated using buffer and different concentrations of the Cellic CTec2 cocktail (Novozymes), as shown in Table 2. Simultaneous EH of the solid and liquid fractions resulting from the different pretreatments studied was also performed as described in Table 2. The aqueous phase obtained after EH is referred to as enzymatic hydrolysates, and its BMP was evaluated for selected experiments (described later). In the first set of experiments, an enzymatic concentration of 0.12 $mg_{protein}\ g^{-1}_{AB}$ with different SF levels was evaluated; in another set of experiments, different concentrations of the Cellic CTec2 cocktail were tested with materials pretreated with SF 2.41. Finally, the concentration of 2.4 $mg_{protein}\ g^{-1}_{AB}$ of Cellic CTec2 with different SF levels was tested. Temperature, pH, stirring speed, and time were set according to the manufacturers' specifications at 50 °C, initial pH 5, 120 rpm, and 34 h, using a ratio of 25 g_{AB} per liter of buffer or hydrolysate. When needed, the initial pH of 5 was adjusted using 0.1 M NaOH; there was no significant change in pH during EH, and it was therefore not controlled.

A comparison with the enzymatic mix consisting of Celluclast 1.5 L-Viscozyme L mixture (Novozymes) donated by Dr. Felipe Alatriste-Mondragón from IPICYT was used. This mixture has previously been optimized for AB hydrolysis using the same AB batch as in this study [15]. Therefore, the enzymatic concentration and the operational conditions were fixed at the optimized values: 3.7 $mg_{protein}\ g^{-1}_{AB}$ of Celluclast 1.5 L, 19.4 Viscozyme L, 40 °C, and 120 rpm for 12 h, with a ratio of 64.84 g_{AB} per liter of the buffer (Table 2).

Control assays were carried out with AB without pretreatment under the conditions mentioned previously for each enzymatic cocktail. Negative control assays were carried out without adding AB under the same conditions. All experiments were performed in triplicate.

Biochemical Methane Potential Tests

Based on the results obtained, the enzymatic hydrolysates obtained with Cellic CTec2 at 2.4 $mg_{protein}\ g^{-1}_{AB}$, those obtained with Celluclast 1.5 L-Viscozyme L, and the control without EH were selected to be subjected to a BMP test, and the three were pretreated with SF 2.41. These analyses were carried out at the Center for Exact Sciences and Engineering (CUCEI) of the University of Guadalajara using the Automatic Methane Potential Test System (AMPTS II, Bioprocess Control, Sweden). Anaerobic sludge from a UASB reactor employed to treat tequila vinasses was used as inoculum for anaerobic digestion under the following conditions: 37 °C, 150 rpm, initial pH of 7.5, 10 g volatile solids total per liter of sludge as inoculum, and the initial COD values were fixed to 5 g COD L^{-1} [18].

Analytical Methods

The protein concentration of the enzymatic cocktails was determined by the Lowry assay according to the Instruction Manual, DC Protein Assay and quantified by spectrophotometry at 750 nm (Biotraza, model 752) [19].

Periodic aqueous samples of enzymatic hydrolysates were taken from each experiment. The analyses performed were as follows: (a) TC by the phenol-sulfuric acid method and quantified by spectrophotometry at 485 nm (Biotraza, model 752) [20], (b) GLU and XYL concentrations using a Biochemistry Analyzer YSI-2700, and (c) COD according to the HACH

Method 8000 using a Hach DRB200 reactor for COD digestion and quantified spectrophotometrically at 600 nm (Biotraza, model 752) [21]. Acetic acid was quantified by high-performance liquid chromatography (HPLC, Varian ProStar 210) with a UV–vis detector (Varian ProStar PS 325, 278 nm) using an AMinex HPX-87H column [3].

Yield Calculations and Data Analysis

The EH yields of TC, GLU, and XYL expressed as g g^{-1}_{AB} were calculated by subtracting the initial concentration of carbohydrates from the final carbohydrate concentrations and considering the volume of the hydrolysates and the mass of AB on a dry basis. The global yield included sugar recovery from both the pretreatment and EH, in all cases referring to the initial content in the AB.

The experimental EH and BMP data were fitted by the Gompertz model using OriginPro 8 software. This logistic model has the parameters A, t_r, and k related by Eq. 2.

$$Sc = Ae^{-e(-k(t-t_r))} \quad (2)$$

where Sc is the TC concentration (g L^{-1}) or methane concentration (NmL); k is the production rate (h^{-1}); A is a parameter related to final concentration values; t is time (h); and t_r is the time at the inflection point of the curve (h). The maximum production rate (V_{max}) can be estimated by derivation of Eq. 2, resulting in Eq. 3:

$$V_{max} = 0.386\, A\, k \quad (3)$$

One-way analysis of variance (ANOVA) was performed, and statistical significance was determined at a level of $p < 0.05$ using IBM SPSS software.

Results and Discussion

Total Carbohydrates After Pretreatment

The characterization of the pretreated bagasse and the hydrolysates obtained after steam explosion is shown in Table 3. In all cases, higher TC yields were found in the residual solid fraction (0.59 to 0.76 g g^{-1}_{AB}) than in the hydrolysates (0.04 to 0.08 g g^{-1}_{AB}) for the different pretreatments tested. The glucose content in the solid fraction after pretreatment ranged from 0.54 to 0.75 g GLU g^{-1} TC (Table 1S in Electronic Supplementary Material), indicating that they were the main carbohydrates present in that fraction. These TC contents were affected by the severity of the pretreatment; the highest value was found at the lowest SF, while the lowest value was observed under the most severe conditions (Table 3). The sums of the solid fraction and the hydrolysates were not significantly different, except for more severe conditions (SF 2.89), which could be attributable to the degradation of sugars by acid hydrolysis or temperature [6]. However, 0.04 to 0.05 g g^{-1} TC, GLU, and XYL were in the hydrolysates. Therefore, the main effect of the pretreatment was found in the hemicellulose fraction, whereas the cellulose fraction mainly remained in the solid fraction, requiring further hydrolysis via enzymatic reactions. This approach was also supported by the presence of acetic acid (0.45–0.55 g L^{-1}) in the liquid fraction of all pretreatment conditions (Table 1S in the Electronic Supplementary Material). The formation of this compound during pretreatment has been related to xylan deacetylation after depolymerization, and as a result of these reactions, accessibility to carbohydrates in the solid residual fraction is favored [3, 22].

Effect of SF on Enzymatic Hydrolysis

The highest TC yield obtained from the EH (0.12 $mg_{protein}$ g^{-1}_{AB} Cellic CTec2) of the solid fraction pretreated at SF 2.89 was 13 and 27% higher than the TC yield of the control and SF 2.54, respectively (Fig. 1). The GLU yield obtained at SF 2.54 was 15 to 188% higher than the GLU yields of the other SFs. However, the XYL yield remained the same for the control as well as SF 2.54 and 2.89 pretreatments, in agreement with the characterization of the solid fraction and hydrolysates after pretreatment (discussed in the previous section), where we observed that cellulose remained mainly in the solid fraction, while hemicellulose was released as disaccharides and oligosaccharides in the hydrolysates. The increment in SF from 2.54 to 2.89 (due to an increment of temperature from 142 to 154 °C) promoted a higher TC yield, but the GLU yield was reduced at SF 2.89 compared with 2.54, indicating the possible recovery of other carbohydrates and the modification of the AB fibers due to the higher temperature resulting in the degradation of structural sugars. Furthermore, when using both fractions (liquid and solid) resulting from the pretreatment at SF 2.54, the TC and XYL yields increased by 40 and 155%, respectively, compared to the experiments where only the solid fraction was enzymatically hydrolysate, while no

Table 3 TC contents in the pretreated bagasse and hydrolysates after pretreatment

	Solid fraction	Hydrolysates	
SF	TC (g g^{-1}_{AB})		pH
1.65	0.76 ± 0.03	0.040 ± 0.001	5.1 ± 0.1
2.41	0.66 ± 4 × 10^{-3}	0.055 ± 2 × 10^{-4}	4.0 ± 0.1
2.54	0.74 ± 0.02	0.057 ± 0.006	4.1 ± 0.1
2.77	0.61 ± 0.04	0.079 ± 0.007	4.7 ± 0.1
2.89	0.59 ± 0.02	0.073 ± 0.009	4.8 ± 0.1

SF, severity factor, *TC*, total carbohydrates

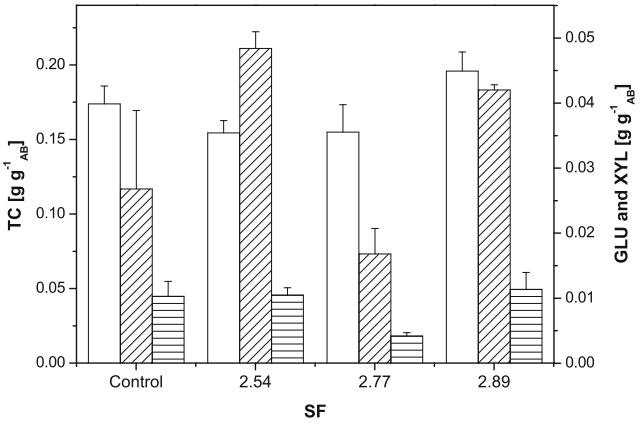

Fig. 1 Comparison of sugar yields after enzymatic hydrolysis with 0.12 $mg_{protein}\ g^{-1}{}_{AB}$ with different SF values. (□) TC; (▨) GLU; (▤) XYL

significant difference was observed for GLU yield (data not shown).

The TC yields obtained (Fig. 1) are comparable with the TC yields reported previously (~ 0.15 ± 0.02 g TC $g^{-1}{}_{AB}$) when 0.7 $mg_{protein}\ g^{-1}{}_{AB}$ of Celluclast 1.5 L was used [23]. However, the values of 0.19 ± 0.02 g TC $g^{-1}{}_{AB}$ obtained for SF 2.89 are comparable with the values obtained when using alkaline peroxide hydrogen as pretreatment and EH (20 $mg_{protein}\ g^{-1}{}_{AB}$ of Celluclast 1.5 L) [12]. However, the GLU yields were six times lower than the GLU yields reported in a study using ionic liquid pretreatment and EH with Cellic CTec2 (70 $mg_{protein}\ g^{-1}{}_{AB}$) [24]. Therefore, we applied increased enzyme concentrations, as discussed in the following section.

Effect of Enzyme Concentration

Figures 2a, b, and c show the evolution of TC, GLU, and XYL concentrations obtained during the EH of pretreated AB at SF 2.41 and Cellic CTec2 concentrations tested. Increasing the enzymatic concentration from 0.12 and 1.2 $mg_{protein}\ g^{-1}{}_{AB}$ (10X) did not result in significantly different TC, GLU, or XYL yields. However, the increase in enzymatic concentration by 20X and 30X increased the final TC concentration by 8 and 48%, respectively. A similar behavior was observed for the GLU and XYL concentrations with the 20X enzymatic concentration, where significant differences of 24 and 16% were found. The GLU and XYL yields obtained at the highest enzymatic concentration tested were not significantly different from those obtained with 20X (GLU and XYL yields of 0.12 and 0.03 g $g^{-1}{}_{AB}$, respectively).

The fit of these experimental data to the Gompertz model (R^2 0.904 to 0.990) is shown in Fig. 3. In general, the increase in the enzymatic concentration resulted in an increase in V_{max} and k. The highest values of V_{max} (0.73 g $h^{-1}\ L^{-1}$) and k (0.71 h^{-1}) were obtained at an enzymatic concentration of 30X.

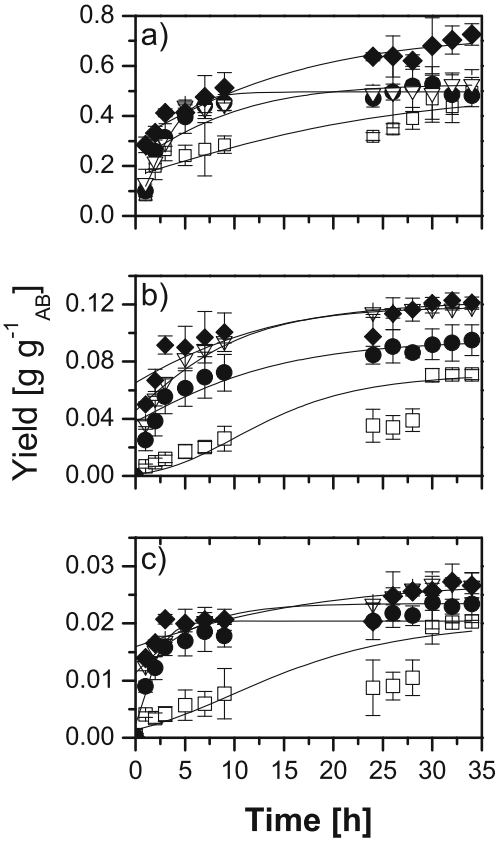

Fig. 2 Yields of (**a**) TC, (**b**) GLU, and (**c**) XYL of the enzymatic hydrolysis of AB pretreated at SF 2.41 at Cellic CTec2 concentrations in $mg_{protein}\ g^{-1}{}_{AB}$ of 0.12 (□), 1.2 (●), 2.4 (▽), and 3.6 (◆). Gompertz model fit (continuous line)

However, as discussed previously, this increase in enzymatic concentrations did not entail significant increases in TC, GLU, or XYL yields, and therefore, the higher costs are not justified.

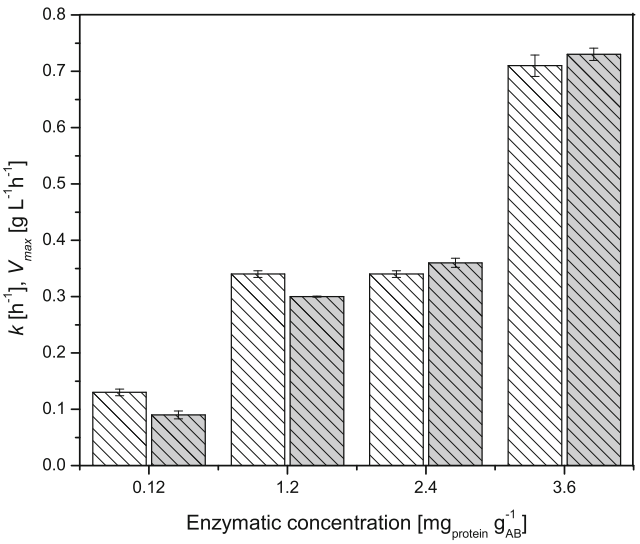

Fig. 3 Kinetic parameters of the test fitted by the Gompertz model: k (open), V_{max} (gray fill)

Therefore, we decided to continue the EH experiments with an enzymatic concentration of 2.4 $mg_{protein}\ g^{-1}_{AB}$ (20X).

Global TC, GLU, and XYL Yields for Different Systems Tested

The global yields, i.e., those obtained after pretreatment and EH, are shown in Fig. 4. The contribution of pretreatment to the global TC yield ranged from 13 to 34% (Fig. 4a) for the different systems, while this contribution was marginal for GLU and XYL global yields (Fig. 4b, c). The highest global TC yield (0.7 g g^{-1}_{AB}) was obtained at SF 2.54 and was statistically similar to the global TC yield obtained at 2.41 and significantly higher than the global TC yield of the other systems. This result indicated that the pretreatment time did not have a significant effect on the TC yield since both pretreatments were performed at 142 °C, and the increment in SF was attributable to the increment in time from 15 to 20 min. However, the highest GLU yield (0.12 g g^{-1}_{AB}) was obtained at SFs 2.41 and 2.89 and was significantly higher than the GLU yield obtained at SFs 1.65 and 2.54. The global XYL yields remained between 0.010 and 0.038 g g^{-1}_{AB}; with increasing SF values, the XYL yields also increased, except for the most severe conditions, which is attributable to the degradation of sugars due to higher temperatures and longer pretreatment times (154 °C and 20 min).

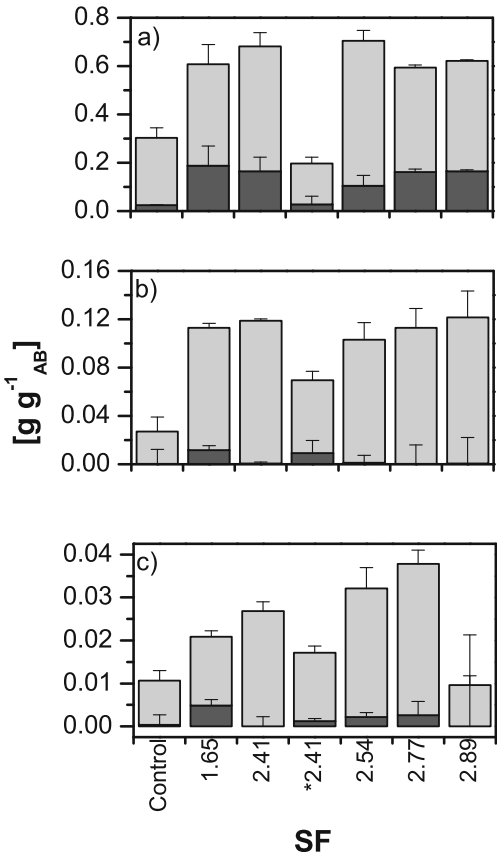

Fig. 4 Global yields of (**a**) TC, (**b**) GLU, and (**c**) XYL from pretreatment (dark gray) and enzymatic hydrolysis (light gray) as a function of SF. Enzyme concentration in all cases 2.4 $mg_{protein}\ g^{-1}_{AB}$ of Cellic CTec2, except (*) 23.1 $mg_{protein}\ g^{-1}$ of Celluclast 1.5 L-Viscozyme L

Therefore, the best yields were obtained with pretreatment at SF 2.41 and EH with Cellic CTec2 (2.4 $mg_{protein}\ g^{-1}_{AB}$), and this system was compared to the system pretreated at the same SF and enzymatically hydrolyzed with Celluclast 1.5 L-Viscozyme L mixture (23.1 $mg_{protein}\ g^{-1}_{AB}$) using previously optimized conditions. The analysis of Gompertz model parameters obtained for these two systems indicated that the values of V_{max} (g L^{-1} h^{-1}) and k (h^{-1}) for Celluclast 1.5 L-Viscozyme L mixture was 45% and 15% higher than the Cellic CTec2 system. In contrast, the TC, GLU, and XYL yields (g g^{-1}_{AB}) observed were significantly lower (38, 59, and 64%) than the TC, GLU, and XYL yields obtained with Cellic CTec2 (Fig. 4a, b, and c) despite the 9.6 times higher enzymatic concentration, which can be explained by the 2.6 lower ratio of AB to aqueous phase used in the Cellic CTec2 system.

In a previous study, 312.54 ± 46.89 mg of reducing sugars g^{-1}_{AB} under the optimized conditions was reported [15]. However, in this study, only GLU and XYL were considered. The global TC yield obtained was 43 and 59% higher than the global TC yield reported for AB pretreated with alkaline hydrogen peroxide and sequential EH with Viscozyme L and Celluclast 1.5 L and AB only with binary EH [12, 25]. This value was also 49% higher than the value obtained by EH with Stonezyme [25]. In contrast, the highest global GLU yields were 57, 58, and 50% lower than the global GLU yields obtained with pretreated AB with ammonia fiber expansion, autohydrolysis, or ionic liquid and EH with Cellic CTec2 and Cellic HTec2, respectively [26]. The highest global yield of XYL was also significantly lower than the global yield of XYL obtained from ammonia fiber expansion, autohydrolysis, or ionic liquid pretreatment followed by EH with Cellic CTec2 and Cellic HTec2 [26]. TC yields higher than the yields previously reported but the GLU and XLY yields lower indicates that other carbohydrates were released. In the following section, the effects of these other carbohydrates on anaerobic digestion are discussed.

COD Evaluation

All cases exhibited an increase in COD with respect to the initial value (Fig. 5), indicating the release of organic matter to the aqueous phase. The pretreatments SFs 2.77 and 2.89 resulted in increases in the final COD of 44.56 and 24.35%, respectively, in relation to the control. However, the EH of the solid fraction from pretreatment SF 2.54 with 0.12 $mg_{protein}\ g^{-1}_{AB}$ Cellic CTec2 showed no significant differences when compared to the control (without pretreatment). However, the final COD after EH with 0.12 $mg_{protein}\ g^{-1}_{AB}$ of Cellic CTec2 in both fractions of the pretreatment at SF 2.54 was 27%

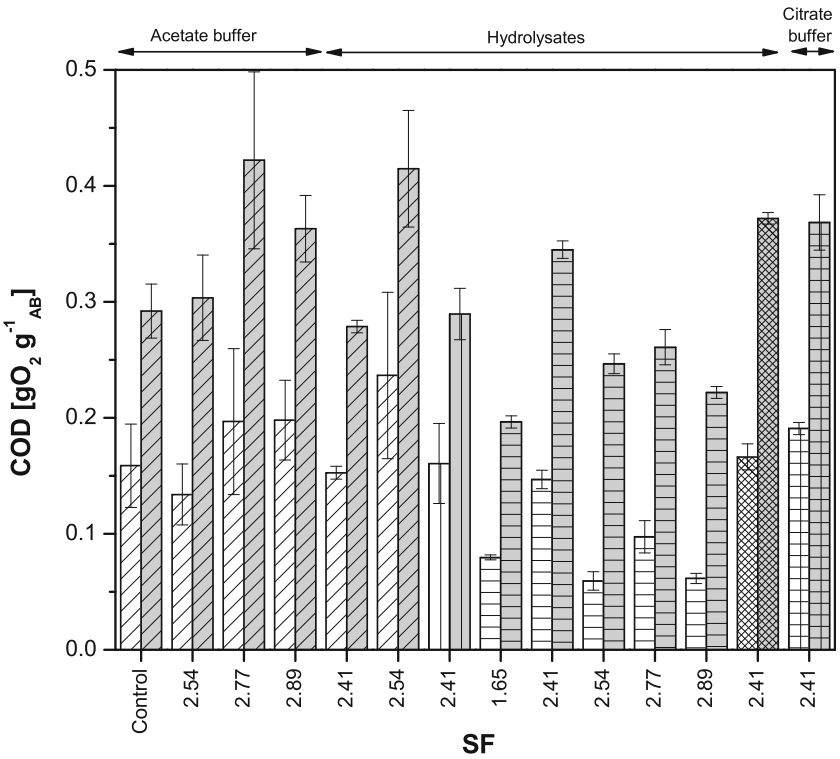

Fig. 5 Initial COD (open) and final COD (gray fill) yields. Enzymatic concentrations in mg-$_{protein}$ g^{-1}_{AB} of Cellic CTec2: 0.12 (▨), 1.2 (▥), 2.4 (▤), 3.6 (▩), and Celluclast 1.5 L-Viscozyme: 23.1 (▦)

higher than the EH of only the solid fraction. In contrast, the increase in enzymatic concentration up to 3.6 $mg_{protein}$ g^{-1}_{AB} of Cellic CTec2 in systems with solid and liquid fractions pretreated at SF 2.41 did not entail an increase in the final COD, which may be related to the yields of GLU and XYL also not showing a significant increase from 2.4 to 3.6 mg-$_{protein}$ g^{-1}_{AB}.

Regarding systems using both fractions after pretreatments at a fixed concentration of 2.4 $mg_{protein}$ g^{-1}_{AB} of Cellic CTec2 and different SF values, the highest concentration of the final COD in the pretreatment SF 2.41 (0.34 ± 0.03 g O_2 g^{-1}_{AB}) was 41% higher than the highest concentration of the final COD in the pretreatment SF 1.65. The value is comparable to the value obtained using alkaline peroxide hydrogen as pretreatment and EH with Viscozyme L (22 $mg_{protein}$ g^{-1}_{AB}), as well as EH with Cellulase 50XL (~ 14 FPU g^{-1}_{AB}) and AB pretreated with rumen fluid or diluted acid [11, 12, 27]. In contrast, the value is lower than the 0.7 g O_2 g^{-1}_{AB} obtained with EH (Celluclast 1.5 L, 0.7 $mg_{protein}$ g^{-1}_{AB}) and 1.1 g O_2 g^{-1}_{AB} obtained after alkaline peroxide hydrogen and EH with Celluclast 1.5 L and Viscozyme L (14 and 2 $mg_{protein}$ g^{-1}_{AB}) [12, 23]. Nevertheless, no significant differences were seen between SF 1.65 and pretreatments having higher SF values (2.54, 2.77, and 2.89). The comparison of the COD in the systems hydrolyzed with Cellic CTec2 or Celluclast 1.5 L-Viscozyme L mixture showed no significant differences. The system with 2.4 $mg_{protein}$ g^{-1}_{AB} and pretreatment SF 2.41 exhibited an increase in COD of 0.20 ± 0.01 g O_2 g^{-1}_{AB} without significant differences with respect to higher enzymatic concentrations. Similar to the behavior for global TC, GLU, and XYL yields for different systems tested discussed above, a decrease in the COD obtained was observed with increasing SF.

BMP studies

Based on the results obtained, AB pretreated with SF 2.41 (142 °C for 15 min) was evaluated for BMP, and the results with and without EH are shown in Table 4, where these results are compared with data reported in the literature. The BMP of enzymatic hydrolysates of the pretreated materials was 68% greater than the BMP of the system without EH. In comparison, the BMP of the hydrolysate system with Cellic CTec2 was 17% greater than the BMP of the Celluclast 1.5 L-Viscozyme L mixture, and no significant differences were found ($p < 0.05$). The fit of the BMP tests by the Gompertz model is presented in Figure 1S in the Electronic Supplementary Material, while the kinetic parameters are reported in Table 5. The V_{max} obtained with the enzymatic hydrolysates using Cellic CTec2 was 45 and 20% higher than the V_{max} without HE and with the mixture Celluclast 1.5 L-Viscozyme L, respectively. However, t_r also increased, meaning that the maximum methane production requires a longer process time to achieve the maximum concentration (30 to 37% higher). During anaerobic digestion of enzymatic hydrolysates with Cellic CTec2, 78.4% removal of COD was achieved, slightly superior to the values previously reported (72.8 and 60%) [28, 29]. The value of BMP obtained was

Table 4 Comparison of BMP values reported in this study and in the literature for bagasse agave with different pretreatments and enzymes

Pretreatment type/conditions	Enzymatic hydrolysis enzyme/conditions	BMP ($NLCH_4$ g^{-1} COD_{add})	Reference
Steam explosion 142 °C, 15 min	—	0.169 ± 0.03	This study
Steam explosion 142 °C, 15 min	Cellic CTec2 2.4 $mg_{protein}$ g^{-1}_{AB}, 50 °C, 25 g_{AB} L^{-1}	0.284 ± 0.02	This study
Steam explosion 142 °C, 15 min	Celluclast 1.5 L-Viscozyme L 3.7/19.4 $mg_{protein}$ g^{-1}_{AB}, 40 °C, 64.84 g_{AB} L^{-1}	0.236 ± 0.05	This study
Steam explosion 142 °C, 5 cycles	—	0.260	[31]
Steam explosion 142 °C, 3 cycles	—	0.317	[31]
Steam explosion 158 °C, 20 min	—	0.168 ± 0.007	[11]
Steam explosion 178 °C, 24 min, 5 cycles	—	0.220	[11]
Acid hydrolysis 1.4% (wt/v) HCl, 123 °C, 126 min	—	0.260	[28]
Acid hydrolysis 2.7% (wt/v) HCl, 124 °C, 78 min	Celluclast 1.5 L 40 FPU g^{-1}_{AB}, 40 °C, 40 g_{AB} L^{-1}	0.240	[29]
Acid hydrolysis 1.8% (wt/v) HCl, 119 °C, 103 min	—	0.280	[30]
Acid hydrolysis 1.9% (wt/v) HCl, 130 °C, 193.2 min	—	0.230	[11]
Alkaline hydrogen peroxide 2% (wt/v), 50 °C, 90 min	Celluclast 1.5 L-Viscozyme 1.84 $mg_{protein}$ mL^{-1}, 0.1 $mg_{protein}$ mL^{-1}, 40 °C, 50 g_{AB} L^{-1}	0.200 ± 0.02	[12]
Biological pretreatment with rumen fluid 25 g_{AB} L^{-1} S_0/X_0 ratio 0.33 (g_{vs}/g_{vs}) 37 °C, 15 days	—	0.175	[11]
Biological pretreatment with native microbiota 40.5 g_{AB} L^{-1} S_0/X_0 ratio 0.7 (g_{vs}/g_{vs}) 37 °C, 4 days	—	0.241	[11]
—	Cellulase 50 XL 10.67 $mg_{protein}$ g^{-1}_{AB}, 42.7 °C, 87.5 g_{AB} L^{-1}	0.220	[11]
Ozone pretreatment 90 mg O_3 g^{-1}_{AB}, 60 min	Celluclast 1.5 L 4.72 UI g^{-1}_{AB}, 50 °C, 50 g_{AB} L^{-1}	0.210	[11]
Liquid ionic [Ch][Lys] 20% (wt/v) 124 °C, 205 min	Cellic CTec2 8 FPU g^{-1}_{AB}, 50 °C, 40 g_{AB} L^{-1}	0.300	[32]

N, normalized data (1 atm and 0 °C); *BMP*, biochemical methane potential; *FPU*, filter paper units; *S0/X0*, initial substrate/biomass; *[Ch][Lys]*, cholinium lysinate; —, not applicable; *vs*, volatile solids

0.284 NL CH_4 g^{-1} COD, comparable to the values found in other studies where acid hydrolysis was used as pretreatment [28–30]. In this sense, the pretreatment used herein has the advantage of not employing acid catalysts and of using a ratio of 25 g_{AB} per liter, while in the studies mentioned above, ratios between 40 and 50 g_{AB} per liter were used. However, the BMP values were 10% lower than the values obtained when three cycles of steam explosion were used and 6% lower than the values reported for pretreatment with ionic liquids [31, 32]. However, compared to alkaline and biological pretreatments, the BMP obtained herein was between 15 and 38% greater [11, 12].

The steam explosion conditions employed in this study, compared with the conditions in the literature for AB pretreatment, have the advantage of a shorter pretreatment time and, in some cases, a lower temperature without the use of catalysts, possibly resulting in diminished environmental impacts, but the achievement of similar BMP values requires the application of EH. Since the BMP values obtained with different pretreatments with and without EH, in general, reached the same range, the differentiation between them should include data on operating time and costs, the energy use required, and its performance in anaerobic digestion reactors.

Conclusions

In all cases, pretreatment resulted in higher TC yields after EH, indicating the relevance of this first step for the use of AB for biofuel production. The systems where both fractions generated by the pretreatments were used for EH favored higher TC and XYL yields. The pretreatment conditions that favored the highest TC, GLU, and XYL yields after EH did not correspond to the most severe conditions, implicating a reduction in the energy and time invested in this process and directly affecting the costs of biogas production. Likewise, the increase in enzymatic concentration of CellicTec2 enhanced the yields of TC, GLU, and XYL, as well as the V_{max}. However, there were no significant differences between the two highest enzymatic concentrations tested. Furthermore, pretreatment and EH significantly increased the BMP values of the hydrolysates compared to the BMP values of the controls (without EH or pretreatment). The BMP values obtained for the hydrolysates are comparable to the values reported in the literature for other pretreatment systems such as acid hydrolysis, biological and chemical systems, and other enzymatic formulations.

Table 5 Kinetic parameters of the BMP test fitted by the Gompertz model

Enzymatic cocktail	R^2	k (h^{-1})	V_{max} (NmL h^{-1})	t_r (h)
None (control)	0.984	0.048 ± 0.001	7.4 ± 4x10^{-4}	16.3 ± 0.3
Cellic Ctec 2	0.986	0.056 ± 0.001	13.4 ± 5x10^{-4}	21.3 ± 0.3
Celluclast 1.5 L-Viscozyme L	0.997	0.063 ± 0.001	10.8 ± 3x10^{-4}	19.7 ± 0.1

Supplementary Information The online version contains supplementary material available at https://doi.org/10.1007/s12155-021-10245-9.

Acknowledgments The Cluster Biocombustibles Gaseosos is acknowledged for the grant received by V. Duran-Cruz.

Author Contributions V Duran-Cruz carried out the research, analyzed the data, prepared the visuals, and wrote the first draft.

S Hernández supervised the pretreatment experimentation and analyzed the data.

I Ortíz did the conceptualization, supervised the research, analyzed the data, and wrote the final draft.

Funding This work was financed by the Mexican Department of Energy (SENER) through the Gaseous Biofuels Cluster Project 247006.

Compliance with Ethical Standards

Conflict of Interest The authors declare that they have no conflict of interest.

References

1. Manieniyan V, Thambidurai M, Selvakumar R (2009) Study on energy crisis and the future of fossil fuels. Proceedings of SHEE 10: 2234-3689 https://doi.org/10.13140/2.1.2234.3689
2. Eisentraut A (2010) Sustainable production of second-generation biofuels: potential and perspectives in major economies and developing countries. IEA Energy Papers. https://doi.org/10.1787/5kmh3njpt6r0-en
3. Hernández-Vázquez A, Hernández S, Ortíz I (2020) Hydrothermal pretreatment of agave bagasse for biomethane production: operating conditions and energy balance. Biomass Bioenergy 142: 105753. https://doi.org/10.1016/j.biombioe.2020.105753
4. Bajpai P (2016) Pretreatment of lignocellulosic biomass for biofuel production 2016: 17–70. https://doi.org/10.1007/978-981-10-0687-6_4
5. Wang K, Chen J, Sun S, Sun R (2015) Steam explosion. In: Pandey A, Negi S, Binod P, Larroche C (eds) Pretreatment of Biomass Processes and Technologies. Elsevier, Ámsterdam, pp 75–104
6. Ruiz HA, Conrad M, Sun S, Sanchez A, Rocha GJM, Romaní A, Castro E, Torres A, Rodríguez-Jasso RM, Andrade LP, Smirnova I, Sun R, Meyer AS (2020) Engineering aspects of hydrothermal pretreatment: From batch to continuous operation, scale-up and pilot reactor under biorefinery concept. Bioresour Technol 229: 122685. https://doi.org/10.1016/j.biortech.2019.122685
7. Chen H, Sui W (2017) Steam explosion as a hydrothermal pretreatment in the biorefinery concept. In: Ruiz HA, Thomsen M, Trajano HL (eds) Hydrothermal Processing in Biorefineries: Production of Bioethanol and High Added-Value Compounds of Second and Third Generation Biomass. Springer, Cham, pp 317–332
8. Chen HZ, Liu ZH (2015) Steam explosion and its combinatorial pretreatment refining technology of plant biomass to bio-based products. Biotechnol J 10:866–885. https://doi.org/10.1002/biot.201400705
9. Aguilar DL, Rodríguez-Jasso RM, Zanuso E, Jasso de Rodríguez D, Amaya-Delgado L, Sanchez A, Ruiz HA (2018) Scale-up and evaluation of hydrothermal pretreatment in isothermal and non-isothermal regimen for bioethanol production using agave bagasse. Bioresour Technol 263:112–119. https://doi.org/10.1016/j.biortech.2018.04.100
10. Pino MS, Rodríguez-Jasso RM, Michelin M, Ruiz HA (2019) Enhancement and modeling of enzymatic hydrolysis on cellulose from agave bagasse hydrothermally pretreated in a horizontal bioreactor. Carbohydr Polym 211:349–359. https://doi.org/10.1016/j.carbpol.2019.01.111
11. Valdez-Vazquez I, Alatriste-Mondragón F, Arreola-Vargas J, Buitrón G, Carrillo-Reyes J, León-Becerril E, Mendez-Acosta HO, Ortíz I, Weber B (2020) Comparison of biological, enzymatic, chemical and hydrothermal pretreatments for producing biomethane from Agave bagasse. Ind Crop Prod 145:112160. https://doi.org/10.1016/j.indcrop.2020.112160
12. Galindo-Hernández KL, Tapia-Rodríguez A, Alatriste-Mondragón F, Celis LB, Arreola-Vargas J, Razo-Flores E (2018) Enhancing saccharification of *Agave tequilana* bagasse by oxidative delignification and enzymatic synergism for the production of hydrogen and methane. Int J Hydrog Energy 43:22116–22125. https://doi.org/10.1016/j.ijhydene.2018.10.071
13. García-Amador R, Hernández S, Ortiz I, Cercado B (2019) Assessment of microbial electrolysis cells fed hydrolysate from agave bagasse to determine the feasibility of bioelectrohydrogen production. Rev Mex Ing Quim 18:865–874. https://doi.org/10.24275/uam/izt/dcbi/revmexingquim/2019v18n3/Garcia
14. Rios-González J, Morales-Martínez TK, Rodríguez-Flores MF, Rodríguez-De la Garza JA, Castillo-Quiroz D, Castro-Montoya AJ, Martinez A (2017) Autohydrolysis pretreatment assessment in ethanol production from agave bagasse. Bioresour Technol 242: 184–190. https://doi.org/10.1016/j.biortech.2017.03.039
15. López-Gutiérrez I, Razo-Flores E, Méndez-Acosta HO, Amaya-Delgado L, Alatriste-Mondragón F (2020) Optimization by response surface methodology of the enzymatic hydrolysis of non-pretreated agave bagasse with binary mixtures of commercial enzymatic preparations. Biomass Convers Biorefin. https://doi.org/10.1007/s13399-020-00698-x
16. Pielhop T, Amgarten J, Studer MH, von Rohr PR (2017) Pilot-scale steam explosion pretreatment with 2-naphthol to overcome high softwood recalcitrance. Biotechnol Biofuels 10:130. https://doi.org/10.1186/s13068-017-0816-y
17. Sluiter A, Hames B, Ruiz R, Scarlata C, Sluiter J, Templeton D, Crocker D (2012) Determination of structural carbohydrates and lignin in biomass. NREL/TP-510-42618.
18. Angelidaki I, Alves M, Bolzonella D, Borzacconi L, Campos JL, Guwy AJ, Kalyuzhnyi S, Jenicek P, van Lier JB (2009) Defining the biomethane potential (BMP) of solid organic wastes and energy crops: a proposed protocol for batch assays. Water Sci Technol 59: 927–934. https://doi.org/10.2166/wst.2009.040

19. Bio-Rad Laboratories (*s. f.*) *DC* Protein Assay Instruction Manual, technical bulletin LIT448. IOP Published Bio-Rad Laboratories. http://www.bio-rad.com/webroot/web/pdf/lsr/literature/LIT448.pdf. Accessed 30 September 2020.
20. Dubois M, Gilles KA, Hamilton JK, Rebers PA, Smith F (1956) Colorimetric method for determination of sugars and related substances. Anal Chem 28:350–356. https://doi.org/10.1021/ac60111a017
21. Hach Company (2014) Oxygen demand, chemical Method 8000. IOP Published Hach Company. https://www.hach.com/asset-get.download.jsa?id = 7639983816 Accessed 15 June 2020
22. Dalli SS, Rakshit SK (2015) Utilization of hemicelluloses from lignocellulosic biomass-potential products. In: Pittman KL (ed) Lignocellulose: Biotechnology, chemical, composition and future prospects. Nova Publisher Inc., NewYork, pp 85–118
23. Montiel CV, Razo-Flores E (2018) Continuous hydrogen and methane production from *Agave tequilana* bagasse hydrolysate by sequential process to maximize energy recovery efficiency. Bioresour Technol 249:334–341. https://doi.org/10.1016/j.biortech.2017.10.032
24. Pérez-Pimienta JA, Mojica-Álvarez RM, Sánchez-Herrera LM, Mittal A, Sykes RW (2018) Recalcitrance assessment of the agro-industrial residues from five agave species: ionic liquid pretreatment, saccharification and structural characterization. Bioenerg Res 11:551–561. https://doi.org/10.1007/s12155-018-9920-5
25. Montoya-Rosales JJ, Olmos-Hernández DK, Palomo-Brionesa R, Montiel-Corona V, Marib AG, Razo-Flores E (2019) Improvement of continuous hydrogen production using individual and binary enzymatic hydrolysates of agave bagasse in suspended-culture and biofilm reactors. Bioresour Technol 283:251–260. https://doi.org/10.1016/j.biortech.2019.03.072
26. Perez-Pimienta JA, Flores-Gómez CA, Ruiz HA, Sathitsuksanoh N, Balan V, Costa SL, Dale BE, Singh S, Simmons BA (2016) Evaluation of agave bagasse recalcitrance using AFEXTM, autohydrolysis, and ionic liquid pretreatments. Bioresour Technol 211:216–223. https://doi.org/10.1016/j.biortech.2016.03.103
27. Tapia-Rodriguez A, Ibarra-Faz E, Razo-Flores E (2019) Hydrogen and methane production potential of agave bagasse enzymatic hydrolysates and comparative technoeconomic feasibility implications. Int J Hydrog Energy 44:17792–17801. https://doi.org/10.1016/j.ijhydene.2019.05.087
28. Arreola-Vargas J, Ojeda-Castillo V, Snell-Castro R, Corona-González RI, Alatriste-Mondragón F, Méndez-Acosta HO (2015) Methane production from acid hydrolysates of *Agave tequilana* bagasse: evaluation of hydrolysis conditions and methane yield. Bioresour Technol 181:191–199. https://doi.org/10.1016/j.biortech.2015.01.036
29. Arreola-Vargas J, Flores-Larios A, González-Álvarez V, Corona-González RI, Méndez-Acosta HO (2016) Single and two-stage anaerobic digestion for hydrogen and methane production from acid and enzymatic hydrolysates of *Agave tequilana* bagasse. Int J Hydrog Energy 41:897–904. https://doi.org/10.1016/j.ijhydene.2015.11.016
30. Breton-Deval L, Méndez-Acosta HO, González-Álvarez V, Snell-Castro R, Gutiérrez-Sánchez D, Arreola-Vargas J (2018) *Agave tequilana* bagasse for methane production in batch and sequencing batch reactors: acid catalyst effect, batch optimization and stability of the semi-continuous process. J Environ Manage 224:156–163. https://doi.org/10.1016/j.jenvman.2018.07.053
31. Weber B, Estrada-Maya A, Sandoval-Moctezuma AC, Martínez-Cienfuegos IG (2019) Anaerobic digestion of extracts from steam exploded *Agave tequilana* bagasse. J Environ Manage 245:489–495. https://doi.org/10.1016/j.jenvman.2019.05.093
32. Pérez-Pimienta JA, Icaza-Herrera JPA, Méndez-Acosta HO, González-Álvarez V, Méndoza-Pérez JA, Arreola-Vargas J (2020) Bioderived ionic liquid-based pretreatment enhances methane production from *Agave tequilana* bagasse. RSC Adv 10:14025–14032. https://doi.org/10.1039/D0RA01849J

Folia Microbiologica
https://doi.org/10.1007/s12223-021-00899-5

ORIGINAL ARTICLE

Evaluation of endosulfan degradation capacity by six pure strains isolated from a horticulture soil

Adriana Casanova[1] · Sonia Cabrera[2] · Gloria Díaz-Ruiz[3] · Sergio Hernández[4] · Carmen Wacher[3] · Marta Zubillaga[2] · Irmene Ortíz[4]

Received: 22 February 2021 / Accepted: 2 July 2021

Abstract
Endosulfan is an organochlorine pesticide included in the Stockholm Convention for Persistent Organic Compounds. The utilization of endosulfan as the sole source of carbon and its mineralization was evaluated using pure strains of *Bacillus subtilis*, *Bacillus pseudomycoides*, *Peribacillus simplex*, *Enterobacter cloacae*, *Achromobacter spanius*, and *Pseudomonas putida*, isolated from soil with historical pesticide use. The consumption of the α isomer of endosulfan by five of the six strains studied was higher than 95%, while *B. subtilis* degraded only 76% of the initial concentration (14 mg/L). On the other hand, the degradation of the β isomer was approximately 86% of the initial concentration (6 mg/L) by *B. subtilis*, *P. simplex*, and *B. pseudomycoides* and 95% by *P. putida*, *E. cloacae*, and *A. spanius*. The ability of *A. spanius*, *P. simplex*, and *B. pseudomycoides* to degrade endosulfan has not been previously reported. The production of endosulfan lactone by the *Bacillus* strains, as well as *A. spanius* and *P. putida*, indicated that endosulfan was degraded by the hydrolytic pathway.

Introduction

In 2018, the Food Agriculture Organization (FAO) registered the use of 4.1 million tons of pesticides worldwide (FAO 2020). In Latin America, Argentine and Mexico are the second- and third-largest pesticide consumers, with 172.9 and 53.1 thousand tons, respectively (FAO 2020). The indiscriminate use of pesticides, mainly organophosphates and organochlorine, has surpassed its benefits, invoking health and environmental problems (Mahmood et al. 2016). Organochlorine pesticides are classified as persistent organic pollutants (POPs) that bioaccumulate in aquatic and terrestrial organisms (Jayaraj et al. 2016).

Endosulfan is the common name for pesticide 6,7,8,9,10,10-hexachloro-1,5,5a,6,9,9a-hexahydro-6,9-methano-2,4,3-benzodioxathiepine-3-oxide. The commercial preparation of endosulfan (a mixture of the α and β stereoisomers in a ratio of 7:3) was used worldwide until its inclusion in the Stockholm Convention in 2011. Endosulfan is commonly used in coffee-producing countries for the control of coffee borers (*Hypothenemus hampei*) and insects, mainly, *Nezara viridula* and caterpillars, which affect soybean crops. It is worth noticing that soybean production is one of the most profitable activities in the Argentine economy, as coffee production is in Mexico (González et al. 2009). Endosulfan is ubiquitous, it has a half-life in soil of 60 and 800 days for *α* and β isomers; therefore, it can persist in the environment for several months (Kataoka and Takagi 2013). The presence of endosulfan in the environment affects the biodiversity and fertility of soils (Khan 2012). The α isomer is asymmetric and thermodynamically stable, while the β isomer is symmetric and easily transforms into the α isomer. β-Endosulfan has been reported to be more toxic than its α counterpart, indicating enzymatic specificity (Kwon et al. 2005). The degradations rates of the two isomers in the environment can vary from hours to months depending

✉ Irmene Ortíz
irmene@cua.uam.mx

1 Licenciatura en Ingeniería Biológica, Universidad Autónoma Metropolitana-Cuajimalpa, Mexico City, Mexico

2 Depto. de Ingeniería Agrícola y uso de la tierra, Facultad de Agronomía, Universidad de Buenos Aires, Buenos Aires, Argentine

3 Depto. de Alimentos y Biotecnología, Facultad de Química, Universidad Nacional Autónoma de México, Mexico City, Mexico

4 Depto. de Procesos y Tecnología, Universidad Autónoma Metropolitana-Cuajimalpa. Av. Vasco de Quiroga 4871, Col. Santa Fe. C.P. 05348, México City, Mexico

Published online: 14 July 2021

on the soil type, pH, temperature, and microbial activity (Schmidt et al. 1997; Singh et al. 2014).

In the environment, endosulfan isomers can be transformed abiotically by the attack of the sulfite group or biotically by the action of microorganisms (Kataoka et al. 2011). Biological degradation can occur via hydrolytic and oxidative pathways either through consecutive oxidation and hydrolysis reactions or hydrolysis (Kamei et al. 2011; Kataoka et al. 2010; Katayama and Matsumura 1993; Kullman and Matsumura 1996; Shetty et al. 2000). The primary metabolites produced by oxidation and hydrolysis are endosulfan sulfate and endosulfan diol, respectively (Sutherland et al. 2004). Endosulfan monoalcohol is produced by further oxidation of endosulfan sulfate by the enzymatic action of monooxygenases. In contrast, the hydrolysis of endosulfan by some microorganisms produces endosulfan diol (Kwon et al. 2005). Endosulfan sulfate has been reported to be even more toxic than endosulfan, whereas endosulfan diol can be further transformed into less toxic metabolites such as endosulfan ether, endosulfan hydroxyether, endosulfan lactone, and hydroycarbolate of endosulfan (Verma et al. 2011).

Some microorganisms have been reported to use endosulfan as a carbon or sulfur source or both (Siddique et al. 2003). *Pseudomonas putida* is commonly used in bioremediation processes because of its ability to degrade a wide range of compounds, including endosulfan (Loh and Cao 2008). A *P. putida* strain isolated from contaminated soil from a coffee-cultivated area has been reported to degrade 11.66 mg/L per day of endosulfan with the production of endosulfan sulfate, endosulfan diol, and endosulfan lactone (Sunitha et al. 2012). *Pseudomonas* sp. KS-2P has been reported to degrade 2.5 mg/L per day of endosulfan and 2.9 mg/L per day of endosulfan sulfate (Lee et al. 2003). The degradation and mineralization of endosulfan by the *Enterobacter* genus have also been reported (Abraham and Silambarasan 2014). In particular, *Enterobacter cloacae* has been reported to tolerate up to 1300 mg/L and degrade 100 mg/kg per day of endosulfan and 111.11 mg/kg per day of endosulfan sulfate (Abraham and Silambarasan 2015). Furthermore, a strain of *E. cloacae* isolated from agricultural soil degraded both isomers with a degradation rate of 0.143 mg/L per day and 0.085 mg /L per day for α and β-endosulfan, respectively (Jimenez-Torres et al. 2016). On the other hand, a study of utilization of endosulfan as the energy source by *Bacillus subtilis* reported a degradation rate of 6.72 mg/L per day with the production of endosulfan diol, endosulfan lactone, and endosulfan sulfate, as well as the consumption of 8.3 mg/L per day of α-endosulfan and 9.7 mg/L per day of β-endosulfan with the production of 1,2,3,4,7,7-hexachloro-5,6-dihydroxybicyclo[2.2.1]-2-heptene and 1,2,3,4,7,7-hexachloro-formaldehyde-6-methylbi-cyclo[2.2.1]-2-heptene (Ishag et al. 2017; Kumar et al. 2014).

Peribacillus simplex, *Bacillus pseudomycoides*, and *Achromobacter spanius* were also studied in this work, and to the best of our knowledge, these microorganisms have not been previously reported as degraders of endosulfan. However, *Achromobacter* sp. degraded endosulfan and *Peribacillus simplex* (formerly *Bacillus simplex*) has been studied for metal absorption and degradation of metolachlor and trifluralin (Erguven et al. 2016; Munoz et al. 2011; Patel and Gupta 2020; Sunitha et al. 2012; Valentine et al. 1996). *Bacillus pseudomycoides* has been reported as a malathion and azo dye acid black 24 degrader (Li et al. 2016; Tamer and Medhat 2013). *Achromobacter spanius* has been known to degrade kerosene and TNT (Gumuscu et al. 2015; Stancu 2020).

Therefore, the objective of this study was to evaluate the ability of *P. putida*, *E. cloacae*, *A. spanius*, *B. subtilis*, *P. simplex*, and *B. pseudomycoides* to degrade and mineralize endosulfan.

Table 1 Physicochemical characteristics of the soil

Parameter	Value
CEC (meq/100 g)	16.8
EC (meq/100 g)	11.89
Mg	3.1
K	2.67
Na	0.79
ES (%)	4.7
pH	6.8
TOC	2.04
N total (%)	0.23
FC (%)	59.85

CEC cation exchange capacity, *EC* exchangeable cations, *ES* exchangeable sodium, *TOC* total organic carbon, *FC* field capacity

Materials and methods

Soil sample collection and characterization

Soil samples were collected from the horticulture region known as "Cinturón hortícola Platense" in Buenos Aires, Argentine, where tomato, pepper, aubergine, parsley, broccoli, cabbage, lettuce, and artichoke, among others, have been cultivated traditionally for more than 20 years with intensive use of organic and inorganic fertilizers and pesticides, including endosulfan. Five soil samples were collected randomly from a depth of up to 15 cm and preserved at 5 °C until analysis.

The soil was classified as loamy with a composition of 33% sand, 46.64% silt, and 20.36% clay; their physicochemical characteristics are shown in Table 1 (Cabrera et al. 2018). Endosulfan sulfate was detected in the soil indicating the previous presence of endosulfan (data not shown).

Isolation, purification, selection, and acclimation of strains

Strain isolation was performed using 25 g of soil and 250 mL of mineral medium (in g/L) 5.97 Na_2HPO_4, 0.01 $CaCl_2{\cdot}H_2O$, 2.27 KH_2PO_4, 0.99 $(NH4)_2SO_4$, 0.025 $FeSO_4{\cdot}7H_2O$, and 0.5 $MgSO_4{\cdot}7H_2O$ (Jimenez-Torres et al. 2016), and 22 mg/L or 2000 mg/L of commercial endosulfan (Tridane 350) was added. The culture was incubated at room temperature (24–28 °C) and 150 rpm. After 7 days, 50 mL of the cultures were mixed with 200 mL of fresh mineral medium and the corresponding amount of endosulfan to restore the concentrations. After another 7 days, an aliquot of each culture was streaked in plates with Luria–Bertani agar (LB) or potato dextrose agar (PDA) and incubated at 30 °C for 48 h. The cultivated colonies were observed under a microscope and classified according to their morphology, color, edge, and surface. Different colonies were successively cultured for strain purification under the same conditions.

Inhibition tests in the presence of endosulfan were performed on the seven pure strains obtained following a previously reported protocol (Hernández-Ramos et al. 2019). The strains that did not exhibit inhibition were selected for acclimation, identification, and degradation tests, as described in the following paragraph.

In the acclimation process, the selected strains were cultured in LB broth and 2.5 mg/L of endosulfan at 30 °C and 150 rpm for 72 h and reseeded three times using 10% (v/v) of inoculum each time. The final culture cells were centrifuged three times. The pellet was washed with sterile water each time. The final pellet was resuspended in a known volume of sterile water and then cryo-preserved at −4 °C in a 20% (v/v) glycerol solution. The purified strains are deposited and available in the internal UAM collection of microorganisms.

The inoculum for biodegradation tests was prepared in 250 mL of LB broth using 1.5 mL of the preserved strains.

DNA extraction, amplification of 16S rRNA gene, and sequence analysis

Total DNA was extracted from the pure strains following the method described by (Lawson et al. 2001). The quality of the extracts was verified on 1% (wt/vol) agarose-TBE 1X gels. The gels were stained with ethidium bromide (10 ng/mL) and documented using the Chemidoc system (Bio-Rad, Richmond, CA). DNA was quantified using a spectrophotometer (Epoch, BioTek, USA). The 16S rRNA gene sequence was amplified with pA 5-AGA GTT TGA TCC TGG CTC AG 3′ and pH 3-′AAG GAG GTG ATC CAG CCG CA 5′ primers. The PCR was performed in a Thermocycler T-Personal Combi (Biometra, Germany) using the following conditions: preheating at 94 °C for 5 min, followed by 35 cycles of denaturation at 94 °C for 30 s, annealing at 56 °C for 30 s, extension at 72 °C for 1 min; and a final extension step at 72 °C for 5 min. The amplified products were examined by electrophoresis on a 1% agarose gel, as previously described.

The amplicons were purified using the MONTAGE GENOMICS Kit, according to the manufacturer's instructions. Sequencing was performed at the "Laboratorio de Secuenciación Genómica de la Biodiversidad y de la Salud" at the Universidad Nacional Autónoma de México. The quality of the sequences was verified using the Chromas software (version 2.6.6) and then analyzed for bacterial identification in the National Center for Biotechnology Information (NCBI) database using the online BLAST program (https://blast.ncbi.nlm.nih.gov/Blast.cgi).

The evolutionary history was inferred using the neighbor-joining method (Saitou and Nei 1987). The bootstrap consensus tree constructed from 1000 replicates was used to represent the analyzed taxa's evolutionary history (Felsenstein 1985). Evolutionary analyses were conducted using MEGA X (Kumar et al. 2018). The analysis involved seven nucleotide sequences. The included codon positions were the 1st + 2nd + 3rd + noncoding positions. All ambiguous positions were removed for each sequence pair (pairwise deletion option). For the root identification, *Sulfolobus acidocaldarius*, an Archaea, was included as a phylogenetically distant microorganism (outgroup) as the phyla of the studied microorganisms were Proteobacteria and Firmicutes.

Degradation tests

Degradation tests were performed in triplicate for each strain in hermetic amber flasks (125 mL) using 27 mL of mineral media (previously described), 3 mL of inoculum, and 20 mg/L of endosulfan (Sigma-Aldrich, isomers α and β, ratio 7:3, 99.9% purity). They were incubated at 150 rpm and 30 °C for approximately 800 h. The flasks were provided with a precision sampling valve (Mininert®) that allowed periodical headspace sampling. The final content of each flask was analyzed for residual endosulfan, metabolites, and biomass, as described in the next section.

Analytical methods

Carbon dioxide quantification

Headspace gas samples (100 µL) were analyzed in a gas chromatograph (550 Gow-Mac series, USA) with a thermal conductivity detector (GC-TCD) using a CTR1 column (Alltech) and helium as a carrier gas, as described previously (Hernández-Ramos et al. 2019).

Biomass quantification

After the test period, the complete content of each flask was membrane-filtered (0.45 μm) to recover the final biomass. Solvent washing was performed for endosulfan recovery. The membranes were dried at 50 °C until a constant weight was achieved. The mass was quantified by the difference between the wet and dry weights. The recovered liquid phase was analyzed for residual endosulfan and metabolites as follows.

Liquid–liquid extraction

The liquid phase recovered after filtration was subjected to a liquid–liquid extraction procedure (US EPA 1996; 3510C). Briefly, 33 mL of dichloromethane was added, followed by 10 min of magnetic agitation and phase decantation. The final volume of the organic phase, collected after repeating this procedure three times, was concentrated. The solvent was changed to hexane by rotoevaporation (Hernández-Ramos et al. 2019).

Quantification of residual endosulfan

The concentrated extracts were analyzed by US EPA Method 8270D using gas chromatography with a mass spectrum detector (Agilent 6890 N, MSD 5975B, USA) with a 5MS SGE capillary column. The initial and final oven temperatures were 90 °C and 250 °C; the temperature was increased at a rate of 5 °C min^{-1}, and helium was used as the carrier gas. The detector and injector temperatures were 250 °C and 220 °C, respectively. For metabolite analysis, a scan method in the range of 50–450 z/m at 70 eV was performed, while the identification was performed using the NIST05 Mass Spectral Library.

Data analysis

The CO_2 experimental data were fitted by the Gompertz model using OriginPro 8 software to obtain kinetic parameters, such as the maximum production rate (Vmax) and production rate (k), which are related to the degradation of endosulfan. One-way analysis of variance (ANOVA) with a 95% confidence level and post hoc (Tukey) tests were performed to establish the differences between tests and controls and between strains in the IBM SPSS 22 software.

Results and discussion

Isolation and identification of strains

Seven strains were isolated on media containing endosulfan. The inhibition tests indicated that one gram-positive strain exhibited moderate growth inhibition in the presence of endosulfan. Therefore, no further experiments were performed using this strain. Three strains were isolated from media containing 2000 mg endosulfan per L of culture (B1, B2, and C2 in Table 2), and three from the culture with endosulfan concentration 22 mg/L (A1, A2, and C1 in Table 2). There are few reports where endosulfan concentrations of 500, 1000, and 2100 mg/L were used for isolation of fungal and bacterial strains or even in degradation tests (Bhalerao and Puranik 2007; Kumar and Philip 2006; Silambarasan and Abraham 2014). The identification of the six isolated strains, using 16S rRNA gene sequencing, is presented in Table 2.

Degradation of endosulfan isomers and specific rates

The α-endosulfan consumption was 76% for *B. subtilis* and above 95% for the other strains (initial concentration 14 m/L). On the other hand, the β isomer (initial concentration 6 mg/L) was approximately 95% for *P. putida*, *E. cloacae*, and *A. spanius*, and 86% for *B. subtilis*, *P. simplex*, and *B. pseudomycoides*. These results are consistent with those reported in the literature, where the β isomer has been reported as being more toxic due to the specificity of the enzymes required for its degradation (Kwon et al. 2002).

The specific degradation rates (i.e., the mass of the isomer eliminated per volume of culture per biomass) for

Table 2 Identification of bacterial isolates from soil using 16S rRNA gene sequencing

Isolate label	Organism	Identity (%)	Sequence length (bp)	Accession number
A1	*Pseudomonas putida*	99.00	1378	MZ147607
A2	*Enterobacter cloacae*	98.00	1483	MZ147605
B1	*Achromobacter spanius*	98.00	1451	MZ147606
B2	*Bacillus subtilis*	98.00	1449	MZ147602
C1	*Peribacillus simplex*	99.65	1419	MZ147604
C2	*Bacillus pseudomycoides*	99.70	1437	MZ147603

α-and β-endosulfan are presented in Fig. 1a, b, respectively. The biomass of the tests was corrected using the biomass quantified from the endogenous controls of each strain. The specific degradation rate for both isomers by *P. putida* was significantly ($p > 0.05$) higher, four times higher than those of *E. cloacae* and *B. subtilis*, three times higher than that of *P. simplex*, and two times higher than those of *A. spanius* and *B. pseudomycoides.*

Global degradation

The volumetric rates (mg/L per day) of endosulfan degradation and the degradation of its isomers are presented in Table 3. The highest volumetric degradation rate was observed for *E. cloacae*, which was approximately twice those of *P. putida* and *B. pseudomycoides*. However, no significant differences were observed for *E. cloacae*, *A. spanius*, *P. simplex*, and *B. subtilis*. The rate of total endosulfan obtained for *P. putida* was four times lower than that reported by (Sunitha et al. 2012). The total endosulfan rate for *B. subtilis* observed in this study was similar to the values of 6.72 mg/L per day and 2.5 times lower than those previously reported (Ishag et al. 2017; Kumar et al. 2014). On the other hand, the *E. cloacae* values for both isomers were one order of magnitude higher than those reported by (Jimenez-Torres et al. 2016).

As previously mentioned, endosulfan degradation *by A. spanius*, *P. simplex*, and *B. pseudomycoides* has not been previously reported. However, the observed rates are comparable to those reported for *P. aeruginosa*, *B. megaterium*, and *Klebsiella pneumoniae* (Kumar 2011; Kwon et al. 2002; Ozdal et al. 2016; Seralathan et al. 2014).

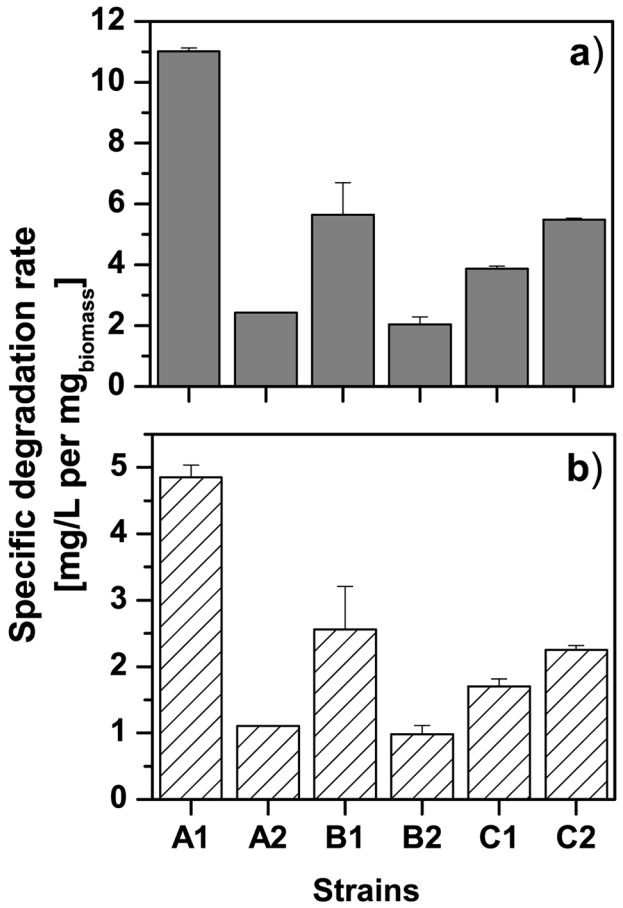

Fig. 1 Specific degradation rate for **a** α—endosulfan and **b** β—endosulfan for the isolated strains. A1 *Pseudomonas putida*, A2 *Enterobacter cloacae*, B1 *Achromobacter spanius*, B2 *Bacillus subtilis*, C1 *Peribacillus simplex*, and C2 *Bacillus pseudomycoides*. Bars represent the standard deviation of $n = 6$

CO_2 production as an indirect measure of microbial activity

The microbial activities related to CO_2 production for each strain are shown in Fig. 2a–f. Except for *B. pseudomycoides*, in all cases, the CO_2 produced was significantly higher ($P = 0.05$) in the tests than in the endogenous controls, indicating the utilization of endosulfan isomers as the sole carbon source and its mineralization. The CO_2 production by *B. pseudomycoides* indicated that the microorganism utilized endosulfan for growth or metabolite production rather than CO_2 production, which was consistent with its highest biomass production among all the studied strains.

The rate values (k) obtained by fitting the CO_2 production by the Gompertz model for *E. cloacae*, *A. spanius*, and *B. subtilis* were approximately 0.012 h^{-1}. While, the rates for *P. putida*, *P. simplex*, and *B. pseudomycoides* were approximately half, suggesting that the first mineralize the endosulfan twice as fast despite the specific rates of *P. putida* being the highest. Furthermore, the values of V_{max} (~0.1 mg/h) obtained for *A. spanius* and *B. subtilis* were significantly higher ($P = 0.05$) than those obtained for the other strains (Table 4).

Table 3 Volumetric degradation rate of total endosulfan and its α- and β-isomers

Strain	Degradation rate (mg/L per day)		
	Total	α-Isomer	β-Isomer
Pseudomonas putida	2.80 ± 0.06	1.99 ± 0.04	1.06 ± 0.15
Enterobacter cloacae	5.58 ± 0.08	4.61 ± 0.04	1.97 ± 0.03
Achromobacter spanius	5.43 ± 0.21	3.80 ± 0.16	1.62 ± 0.05
Bacillus subtilis	4.79 ± 0.88	3.99 ± 0.36	1.55 ± 0.36
Peribacillus simplex	5.19 ± 0.34	2.07 ± 0.08	0.81 ± 0.11
Bacillus pseudomycoides	2.66 ± 0.11	1.99 ± 0.04	0.68 ± 0.07

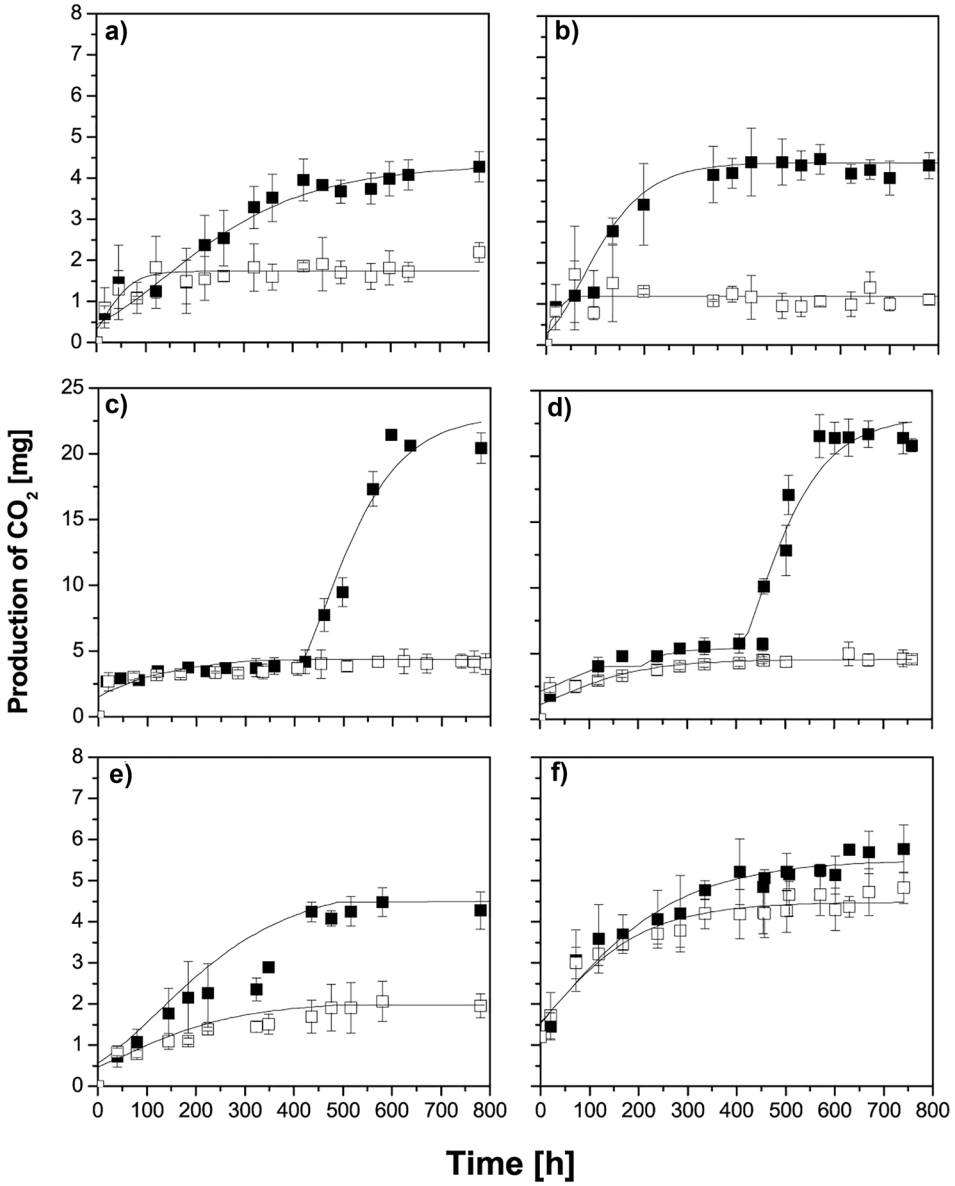

Fig. 2 CO_2 production for **a** *Pseudomonas putida*, **b** *Enterobacter cloacae*, **c** *Achromobacter spanius*, **d** *Bacillus subtilis*, **e** *Peribacillus simplex*, and **f** *Bacillus pseudomycoides*. Black square indicates the addition of endosulfan, white square endogenous control (without endosulfan), and (—) the Gompertz model fit. Bars represent the standard deviation of $n = 6$

Evolutionary relationships of taxa

The evolutionary taxa relationship analysis had a total of 1557 positions in the final dataset. The percentage of replicate trees in which the associated taxa clustered together in the bootstrap test (1000 replicates) is shown next to the branches (Fig. 3). These data indicate that at least 63% of the replications for *B. subtilis* and *B. pseudomycoides* belonged to the same common ancestor and a common ancestor of *B. pseudomycoides*, *B. subtilis*, and *P. simplex* existed in 100% of the replications. The branches corresponding to the partitions, reproduced in less than 50% of the bootstrap replicas, collapsed (*A. spanius* and *E. cloacae*). As expected, the *Bacillus* spp. genus strains were more closely related. The *A. spanius* strain was not evolutionarily related to any of the other strains.

Finally, the evolutionary distances of the strains did not indicate any relationship with the parameters studied

Table 4 Kinetics parameters for CO_2 obtained by Gompertz fitting

Organism	k (h^{-1})	V_{max} (mg/h)
Pseudomonas putida	0.0059 ± 0.0009	0.0095 ± 0.0002
Enterobacter cloacae	0.0138 ± 0.0012	0.0225 ± 0.0002
Achromobacter spanius	0.0116 ± 0.0028	0.0978 ± 0.0003
Bacillus subtilis	0.0127 ± 0.0033	0.1077 ± 0.0053
Peribacillus simplex	0.0063 ± 0.0016	0.0115 ± 0.0008
Bacillus pseudomycoides	0.0067 ± 0.0011	0.0135 ± 0.0017

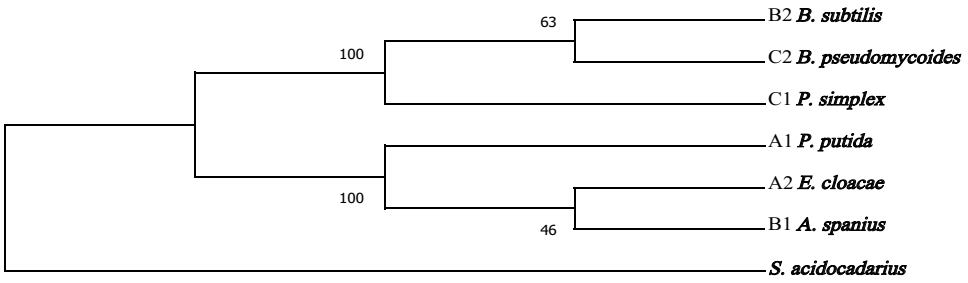

Fig. 3 Identification of strains isolated from soil. Neighbor-joining dendrogram constructed by analysis and comparison of partial sequences of 16S rRNA gene from soil strains. *Sulfolobus acidocaldarius*: outgroup microorganism. Bootstrap = 1000

(volumetric or specific rates and production of CO_2). For *E. cloacae* and *A. spanius*, the bootstrap percentages lower than 50% had the highest endosulfan degradation rates. However, due to their lower replication percentage, the relationship between their evolutionary line and degrading capabilities could not be established. Therefore, the ability to degrade endosulfan is related to processes of the envelope of the organisms through natural selection, which allows them to adapt to the conditions imposed by the environment, including the presence of pollutants; in this case, endosulfan.

Metabolite identification

The metabolites identified for each strain are presented in Table 5. Although endosulfan sulfate is one of the most commonly reported metabolites, it was not found in any of the tested strains (Kataoka and Takagi 2013; Sutherland et al. 2004; Thangadurai and Suresh 2014). For *E. cloacae*, the identified compounds (not shown) in the final samples were also present in the abiotic control samples. Therefore, they were not related to biological degradation. On the other hand, endosulfan diol (retention time (RT) = 20.124) and endosulfan ether (RT = 20.143 min) were detected in the *P. putida* and *B. pseudomycoides* degradation tests, indicating a hydrolytic pathway consistent with previous reports of pure and mixed *P. putida* cultures (Sunitha et al. 2012).

Endosulfan lactone (RT = 20.474 min) was detected in the final *B. subtilis* samples of the degradation tests, in agreement with previous studies (Kumar et al. 2014). However, this metabolite was also found in *P. simplex* and *B. pseudomycoides* strains that have not been reported for endosulfan degradation (Ahmad 2020; Ishag et al. 2017). This compound is produced from endosulfan hydroxyether by endosulfan hydroxyether dehydrogenase, suggesting degradation by the hydrolytic pathway (Lee et al. 2003).

Table 5 Identified metabolites on final samples of the degradation experiments

RT (min)	Compound	Formula	#CAS	Quality (%)
Pseudomonas putida				
20.124	Bicyclo (2.2.1) hept-5-ene-2,3-dimethanol, 1,4,5,6,7,7-hexachloro-(endosulfan diol)	$C_9H_8Cl_6O_2$	002,157–19-9	90
20.143	4,7-methanoisobenzofuran, 4,5,6,7,8,8-hexachloro-1,3,3a,4,7,7a-hexahydro-(endosulfan ether)	$C_9H_6Cl_6O$	003,369–52-6	84
Achromobacter spanius				
22.210	1,2-benzenedicarbocylic acid, butyl 2-methylpropyl ester	$C_{16}H_{22}O_4$	017,851–53-5	93
Bacillus subtilis				
22.210	1,2-benzenedicarbocylic acid, butyl 2-methylpropyl ester	$C_{16}H_{22}O_4$	017,851–53-5	93
25.474	4,7-methanoisobenzofuran-1[3H]-one, 4,5,6,7,8,8-hexachloro-3a,4,7,7a-tetrahydro-(endosulfan lactone)	$C_9H_4Cl_6O_2$	003,868–61-9	90
Peribacillus simplex				
25.458	4,7-methanoisobenzofuran-1[3H]-one, 4,5,6,7,8,8-hexachloro-3a,4,7,7a-tetrahydro-(endosulfan lactone)	$C_9H_4Cl_6O_2$	003,868–61-9	86
Bacillus pseudomycoides				
20.124	Bicyclo (2.2.1) hept-5-ene-2,3-dimethanol, 1,4,5,6,7,7-hexachloro-(endosulfan diol)	$C_9H_8Cl_6O_2$	002,157–19-9	89
20.143	4,7-methanoisobenzofuran, 4,5,6,7,8,8-hexachloro-1,3,3a,4,7,7a-hexahydro-(endosulfan ether)	$C_9H_6Cl_6O$	003,369–52-6	92
25.458	4,7-methanoisobenzofuran-1[3H]-one, 4,5,6,7,8,8-hexachloro-3a,4,7,7a-tetrahydro-(endosulfan lactone)	$C_9H_4Cl_6O_2$	003,868–61-9	90

RT residence time

Conclusions

Five of the six isolated strains showed the capacity to degrade both isomers of endosulfan and mineralize them (i.e., conversion to CO_2). Furthermore, *A. spanius*, *P. simplex*, and *B. pseudomycoides* have not been previously reported for endosulfan degradation. However, *B. pseudomycoides* utilizes endosulfan for growth or metabolite production rather than CO_2 production. The degradation rates observed for the α isomer were higher than those for the β isomer, concurring with its higher toxicity. The presence of endosulfan lactone indicated that the *Bacillus* strains (*B. subtilis*, *P. simplex*, and *B. pseudomycoides*), as well as *A. spanius* and *P. putida*, degraded endosulfan by the hydrolytic pathway.

Acknowledgements The financial support of the Universidad Autónoma Metropolitana Project 47401023 of the Program "Apoyo a la Investigación 2019" is acknowledged. This work was also financially supported by the Universidad de Buenos Aires for the S. Cabrera doctoral fellowship and UBACyT Proyects 20220140100042BA and 22320200100758BA.

Author contribution A. Casanova carried out the research, analyzed the data, prepared the visuals, contributed to the first draft, and read and approved the final manuscript. S. Cabrera carried out the sampling and characterization of the soil, isolation and purification of the strains, preliminary degradation tests, and read and approved the final manuscript. G. Díaz-Ruiz carried out the identification of strains, contributed to the first draft, and read and approved the final manuscript. S. Hernández supervised the experimentation, analyzed the data, contributed to the final draft, and read and approved the final manuscript. C. Wacher analyzed the data and read and approved the final manuscript. M. Zubillaga analyzed the data and read and approved the final manuscript. I. Ortíz performed the conceptualization, supervised the research, analyzed the data, and wrote and approved the final draft.

Funding This work was financed by the Program "Apoyo a la Investigación 2019" of the Universidad Autónoma Metropolitana Project 47401023.

Availability of data and materials The datasets used and/or analyzed during the current study are available from the corresponding author upon reasonable request.

Declarations

Competing interests The authors declare no competing interests.

References

Abraham J, Silambarasan S (2014) Biomineralization and formulation of endosulfan degrading bacterial and fungal consortiums. Pest Biochem Physiol 116:24–31. https://doi.org/10.1016/j.pestbp.2014.09.006

Abraham J, Silambarasan S (2015) Plant growth promoting bacteria *Enterobacter asburiae* JAS5 and *Enterobacter cloacae* JAS7 in mineralization of endosulfan. Appl Biochem Biotechnol 175:3336–3348. https://doi.org/10.1007/s12010-015-1504-7

Ahmad KS (2020) Remedial potential of bacterial and fungal strains (*Bacillus subtilis, Aspergillus niger, Aspergillus flavus* and *Penicillium chrysogenum)* against organochlorine insecticide Endosulfan. Folia Microbiol 65:801–810. https://doi.org/10.1007/s12223-020-00792-7

Bhalerao TS, Puranik PR (2007) Biodegradation of organochlorine pesticide, endosulfan, by a fungal soil isolate, *Aspergillus niger*. Int Biodeterior Biodegrad 59:315–321. https://doi.org/10.1016/j.ibiod.2006.09.002

Cabrera S, Zubillaga MS, Montserrat JM Degradación comparativa de plaguicidas en suelos con diferente historia de uso del cinturón hortícola de La Plata. In: XXVI Congreso Argentino de Ciencias del Suelo, 2018. Asociación Argentina de la Ciencia del Suelo, pp 1562–1568

Erguven GO, Bayhan H, Ikizoglu B, Kanat G, Nuhoglu Y (2016) The capacity of some newly bacteria and fungi for biodegradation of herbicide trifluralin under agiated culture media. Cell and Mol Biol 62:74–79. https://doi.org/10.14715/cmb/2016.62.6.14

Felsenstein J (1985) Confidence limits on phylogenies: an approach using the bootstrap. Evolution 39:783–791. https://doi.org/10.1111/j.1558-5646.1985.tb00420.x

Food and Agriculture Organization of the United Nations FAO (2020) FAOSTAT statistical database. http://www.fao.org/faostat/en/#data/RP. Accessed 6 February 2021

González FB et al. (2009) El endosulfán y sus alternativas en América Latina. RAP-AL, Chile https://rap-al.org/articulos_files/Alternativas_12_Julio.pdf

Gumuscu B, Cekmecelioglu D, Tekinay T (2015) Complete dissipation of 2,4,6-trinitrotoluene by in-vessel composting. RSC Adv 5:51812–51819. https://doi.org/10.1039/c5ra07997g

Hernández-Ramos AC, Hernández S, Ortíz I (2019) Study on endosulfan-degrading capability of *Paecilomyces variotii, Paecilomyces lilacinus* and *Sphingobacterium* sp. in liquid cultures. Bioremediation J 23:251–258. https://doi.org/10.1080/10889868.2019.1671794

Ishag ASA, Abdelbagi AO, Hammad AMA, Elsheikh EAE, Elsaid OE, Hur JH (2017) Biodegradation of endosulfan and pendimethalin by three strains of bacteria isolated from pesticides-polluted soils in the Sudan. Appl Biol Chem 60:287–297. https://doi.org/10.1007/s13765-017-0281-0

Jayaraj R, Megha P, Sreedev P (2016) Organochlorine pesticides, their toxic effects on living organisms and their fate in the environment. Interdiscip Toxicol 9:90–100. https://doi.org/10.1515/intox-2016-0012

Jimenez-Torres C, Ortiz I, San-Martin P, Hernandez-Herrera RI (2016) Biodegradation of malathion, α- and β-endosulfan by bacterial strains isolated from agricultural soil in Veracruz, Mexico. J Environ Sci Health Part B 51:853–859. https://doi.org/10.1080/03601234.2016.1211906

Kamei I, Takagi K, Kondo R (2011) Degradation of endosulfan and endosulfan sulfate by white-rot fungus *Trametes hirsuta*. J Wood Sci 57:317–322. https://doi.org/10.1007/s10086-011-1176-z

Kataoka R, Takagi K (2013) Biodegradability and biodegradation pathways of endosulfan and endosulfan sulfate. Appl Biol Chem 97:3285–3292. https://doi.org/10.1007/s00253-013-4774-4

Kataoka R, Takagi K, Sakakibara F (2010) A new endosulfan-degrading fungus, *Mortierella species*, isolated from a soil contaminated with organochlorine pesticides. J Pest Sci 35:326–332. https://doi.org/10.1584/jpestics.G10-10

Kataoka R, Takagi K, Sakakibara F (2011) Biodegradation of endosulfan by *Mortieralla* sp. strain W8 in soil: Influence of different substrates on biodegradation. Chemosphere 85:548–552. https://doi.org/10.1016/j.chemosphere.2011.08.021

Katayama A, Matsumura F (1993) Degradation of organochlorine pesticides, particularly endosulfan, by *Trichoderma harzianum*. Environ Toxicol Chem 12:1059–1065. https://doi.org/10.1002/etc.5620120612

Khan KH (2012) Impact of endosulfan on living beings. Int J Biosci 2:9–17. https://www.researchgate.net/publication/257429504

Kullman SW, Matsumura F (1996) Metabolic pathways utilized by *Phanerochaete chrysosporium* for degradation of the cyclodiene pesticide endosulfan. App Environ Microbiol 62:593–600. https://doi.org/10.1128/AEM.62.2.593-600.1996

Kumar A, Bhoot N, Soni I, John PJ (2014) Isolation and characterization of a *Bacillus subtilis* strain that degrades endosulfan and endosulfan sulfate. 3 Biotech 4:467–475. https://doi.org/10.1007/s13205-013-0176-7

Kumar M, Philip L (2006) Enrichment and isolation of a mixed bacterial culture for complete mineralization of endosulfan. J Environ Sci Health Part B 41:81–96. https://doi.org/10.1080/03601230500234935

Kumar S (2011) Isolation, characterization and growth response study of endosulfan degrading bacteria from cultivated soil. Intern J Adv Eng Technol 3:178–182

Kumar S, Stecher G, Li M, Knyaz C, Tamura K (2018) MEGA X: molecular evolutionary genetics analysis across computing platforms. Mol Biol Evol 35:1547–1549. https://doi.org/10.1093/molbev/msy096

Kwon G-S, Kim J-E, Kim T-K, Sohn H-Y, Koh S-C, Shin K-S, Kim D-G (2002) *Klebsiella pneumoniae* KE-1 degrades endosulfan without formation of the toxic metabolite, endosulfan sulfate. FEMS Microbiol Lett 215:255–259. https://doi.org/10.1111/j.1574-6968.2002.tb11399.x

Kwon G-S, Sohn H-Y, Shin K-S, Kim E, Seo B-I (2005) Biodegradation of the organochlorine insecticide, endosulfan, and the toxic metabolite, endosulfan sulfate, by *Klebsiella oxytoca* KE-8. App Microbiol Biotechnol 67:845–850. https://doi.org/10.1007/s00253-004-1879-9

Lawson PA, Falsen E, Truberg-Jensen K, Collins MD (2001) *Aerococcus sanguicola* sp. *nov*., isolated from a human clinical source. Internat J System Evol Microbiol 51:475–479. https://doi.org/10.1099/00207713-51-2-475

Lee S-E, Kim J-S, Kennedy IR, Park J-W, Kwon G-S, Koh S-C, Kim J-E (2003) Biotransformation of an organochlorine insecticide, endosulfan, by *Anabaena* species. J Agric Food Chem 51:1336–1340. https://doi.org/10.1021/jf0257289

Li J, Deng M, Wang Y, Chen W (2016) Production and characteristics of biosurfactant produced by *Bacillus pseudomycoides* BS6 utilizing soybean oil waste. Int Biodeterior Biodegrad 112:72–79. https://doi.org/10.1016/j.ibiod.2016.05.002

Loh K-C, Cao B (2008) Paradigm in biodegradation using *Pseudomonas putida*—a review of proteomics studies. Enzyme Microb Technol 43:1–12. https://doi.org/10.1016/j.enzmictec.2008.03.004

Mahmood I, Imadi SR, Shazadi K, Gul A, Hakeem KR (2016) Effects of pesticides on environment. In:Hakeem KR, Akhtar MS, Abdullah SNA (eds) Plant, soil and microbes. pp 253–269

Munoz A, Koskinen WC, Cox L, Sadowsky MJ (2011) Biodegradation and mineralization of metolachlor and alachlor by *Candida xestobii*. J Agric Food Chem 59:619–627. https://doi.org/10.1021/jf103508w

Ozdal M, Ozdal OG, Algur OF (2016) Isolation and characterization of α-endosulfan degrading bacteria from the microflora of cockroaches. Pol J Microbiol 65:63–68. https://doi.org/10.5604/17331331.1197325

Patel S, Gupta RS (2020) A phylogenomic and comparative genomic framework for resolving the polyphyly of the genus *Bacillus*: proposal for six new genera of *Bacillus species*, *Peribacillus gen*. nov., *Cytobacillus gen.* nov., *Mesobacillus gen*. nov., *Neobacillus gen*. nov., *Metabacillus gen*. nov. and *Alkalihalobacillus gen*. nov. Int J Syst Evol Microbiol 70:406–438. https://doi.org/10.1099/ijsem.0.003775

Saitou N, Nei M (1987) The neighbor-joining method: a new method for reconstructing phylogenetic trees. Mol Biol Evol 4:406–425. https://doi.org/10.1093/oxfordjournals.molbev.a040454

Schmidt WF, Hapeman CJ, Fettinger JC, Rice CP, Bilboulian S (1997) Structure and asymmetry in the isomeric conversion of β- to α-endosulfan. J Agric Food Chem 45:1023–1026. https://doi.org/10.1021/jf970020t

Seralathan MV, Sivanesan S, Bafana A, Kashyap SM, Patrizio A, Krishnamurthi K, Chakrabarti T (2014) Cytochrome P450 BM3 of *Bacillus megaterium* - a possible endosulfan biotransforming gene. J Environ Sci 26:2307–2314. https://doi.org/10.1016/j.jes.2014.09.016

Shetty PK, Mitra J, Murthy NBK, Namitha KK, Savitha KN, Raghu K (2000) Biodegradation of cyclodiene insecticide endosulfan by *Mucor thermo-hyalospora* MTCC 1384. Curr Sci 79:1381–1383

Siddique T, Okeke BC, Arshad M, Frankenberger WT (2003) Enrichment and isolation of endosulfan-degrading microorganisms. J Environ Qual 32:47–54. https://doi.org/10.2134/jeq2003.0047

Silambarasan S, Abraham J (2014) Halophilic bacterium JAS4 in biomineralisation of endosulfan and its metabolites isolated from Gossypium herbaceum rhizosphere soil. J Taiwan Chem Eng 45:1748–1756. https://doi.org/10.1016/j.jtice.2014.01.013

Singh P, Volger B, Gordon E (2014) Endosulfan. In: Wexler P (ed) Encyclopedia of toxicology, 3rd edn. Academic Press, Oxford, pp 341–343

Stancu MM (2020) Kerosene tolerance in *Achromobacter* and *Pseudomonas species*. Ann Microbiol 70:13. https://doi.org/10.1186/s13213-020-01543-2

Sunitha S, Murthy VK, Riaz M (2012) Characterization strains of endosulfan and endosulfan sulphate degradation with *Pseudomonas putida*. Int J Environ Sci 3:859–869. https://doi.org/10.6088/ijes.2012030132013

Sutherland TD, Horne I, Weir KM, Russell RJ, Oakeshott JG (2004) Toxicity and residues of endosulfan isomers. Rev Environ Contam Toxicol 183:99–113. https://doi.org/10.1007/978-1-4419-9100-3_4

Tamer MAT, Medhat AHE-N (2013) Malathion degradation by soil isolated bacteria and detection of degradation products by GC-MS. Int J Environ Sci 3:1467–1476. https://doi.org/10.6088/ijes.2013030500017

Thangadurai P, Suresh S (2014) Biodegradation of endosulfan by soil bacterial cultures. Int Biodeterior Biodegrad 94:38–47. https://doi.org/10.1016/j.ibiod.2014.06.017

Valentine NB, Bolton H, Kingsley MT, Drake GR, Balkwill DL, Plymale AE (1996) Biosorption of cadmium, cobalt, nickel and strontium by a *Bacillus simplex* strain isolated from the vadose zone. J Ind Microbiol 12:189–196. https://doi.org/10.1007/BF01570003

Verma A, Ali D, Farooq M, Pant AB, Ray RS, Hans RK (2011) Expression and inducibility of endosulfan metabolizing gene in *Rhodococcus* strain isolated from earthworm gut microflora for its application in bioremediation. Bioresour Technol 102:2979–2984. https://doi.org/10.1016/j.biortech.2010.10.005

Vol. 20, No. 3(2021) IA2388
Revista Mexicana de Ingeniería Química

Treatment of waste activated sludge by steam explosion and alkaline acidogenesis

Tratamiento de lodos activados de purga por explosión de vapor y acidogénesis alcalina

R. Tafolla[1], F. Ramírez[1], R. Ortiz[2], E. Cortés[2], I. Ortiz[3], O. Monroy[1]*

[1]*Biotechnology,* [2]*Health Sciences and* [3]*Processes & Technology Departments, Universidad Autónoma Metropolitana,* [1,2]*Av. San Rafael Atlixco 186, Col. Vicentina, 09340 Iztapalapa,* [3]*Av. Vasco de Quiroga 4871, Col. Santa Fé, 05348 Cuajimalpa, CDMX, México.*

Received: February 26, 2021; Accepted: July 13, 2021

Abstract

A process improvement of the anaerobic digestion of waste activated sludge (WAS) is needed to produce energy and chemicals to compensate the costs of the full wastewater treatment process. Alkaline steam explosion (A-SE) @160°C and 0.67 MPa absolute pressure, followed by thermophilic alkaline acidogenesis (50°C, pH 9) improves the WAS digestibility and the methane yields by breaking the cell walls and the extracellular polymers. This work studies the treatment time and alkalinity effects on the number of destroyed solids measured as cell damage and particle size reduction. To monitor the process a flow cytometer (FCM), through light scattering signals, proved to be an alternative to the measurement of total suspended solids by gravimetry.

The effect of alkaline acidogenesis on the volatile fatty acids (VFA) yield is studied with the A-SE suspension which is cooled down to 50°C and fed to a continuous acidogenic reactor at pH 9 under several organic loads to find the optimum (6 g COD_{VSS}/L·d) with the highest soluble COD and VFA production rates (1.4 and 0.8 g COD/L,d respectively). This effluent can be fed to a methanogenic reactor to produce 0.5 L_{CH4}/L·d or the VFA can be separated for the chemical industry.

Keywords: Anaerobic digestion, flow cytometry, scanning electronic microscopy, particle size reduction, cell wall.

Resumen

Es necesario mejorar la digestión anaerobia de los lodos activados de purga (LAP) para producir energía y productos químicos y así compensar los costos del proceso de tratamiento de aguas residuales. La explosión por vapor alcalina (A-SE) a 160°C y 0.67 MPa absoluta, seguida de acidogénesis alcalina termofílica (50 ° C, pH 9) mejora la digestibilidad de los LAP y los rendimientos de metano al romper la pared celular y los polímeros extracelulares. Este trabajo estudia los efectos del tiempo de tratamiento y la alcalinidad en la cantidad de sólidos destruidos, medidos como daño celular y reducción del tamaño de las partículas. Para monitorear el proceso, un citómetro de flujo (FCM) mediante de señales de dispersión de luz demostró ser una alternativa a la determinación de los sólidos suspendidos totales por gravimetría.

El efecto de la acidogénesis alcalina sobre el rendimiento de ácidos grasos volátiles (AGV) se estudia con material A-SE que se enfría a 50°C y se alimenta a un reactor acidogénico continuo a pH 9 bajo varias cargas orgánicas para encontrar el óptimo (6 g DQOVSS/L·d) con las mayores tasas de producción de DQO soluble y VFA (1.4 y 0.8 g DQO/L·d respectivamente). Este efluente se puede alimentar a un reactor metanogénico para producir 0.5 L_{CH4}/L·d o se pueden separar los AGV para la industria química.

Palabras clave: Digestión anaerobia, citometría de flujo, microscopía electrónica de barrido, reducción del tamaño de partículas, pared celular.

* *Corresponding author. E-mail*: monroy@xanum.uam.mx
https://doi.org/10.24275/rmiq/IA2388
ISSN:1665-2738, *issn-e*: 2395-8472

1 Introduction

Waste activated sludge (WAS) is the byproduct of the most used wastewater treatment process worldwide. It is formed by floccules of aggregated microbial cells bound by extracellular polymeric substances (EPS) which constitute 80% of the floc. It is produced at a yield of 0.6 g of volatile suspended solids/g COD removed and is usually stabilized by anaerobic digestion to produce methane at a yield of 450 L/kg digested VS with 65% volatile solids (VS) removal at 30 day of solids retention time with loading rates (OLR) around 1.45 kg/VSS m^3· d (Appels *et al*., 2008). This low digestion rates are due to the flocs' components, being the EPS as digestible as the cell nuclei (46 to 44%) but more biodigestible than cell membranes (34%) and cell walls (27%) as determined by Xiao *et al*. (2015) (9<pH<12) suggesting that when the floc surfaces are exposed at alkaline conditions get negatively charged creating a strong electrostatic repulsion which releases the EPS, disrupting the sludge floc, saponifying and solubilizing the structural lipids of the cell wall and membrane.

WAS pretreatment by steam explosion (SE) destroys the EPS and the microbial cells' wall and membrane releasing proteins, polysaccharides and other soluble substances. This process: a) improves methane yields (17 to 80%) due to augmented digestibility (up to 35%) of dissolved sludge solids (Carrere *et al*., 2016), b) increases AD rates and thus the solids load to the reactor above5 kgVS/ m^3· d at HRT less than 15 d (Barr *et al*. 2008), d) improve the dewaterability of the residual digested sludge, from 20% to 30-40% (Barber, 2016). In order to be energy efficient, it has to be fed with at least 50 g TSS/L as experienced in the field (Cano *et al*., 2015).

Thus, the combination of SE and alkali (A-SE) adds up to break the EPS and the cell wall fibers. Sani-Shehu *et al*. (2012) found an optimal set of conditions at 88.5°C for, 21 min at pH 12 to obtain a 36% increase in biogas yield while Neyens *et al*. (2003) worked at 100°C for 60 min T pH 10 obtaining a dewatered cake of 46% solids.

Another important concept to improve WAS digestibility is an alkaline acidogenesis to increase the production of volatile fatty acids (VFA). At pH 10 and 8 days reaction time, the VFA yield is 256.2 mg CODVFA/mg VSS (with 50% acetic acid), over 4 times that obtained under uncontrolled pH (Yuan *et al*., 2006). The use of lime also precipitates carbonate and phosphate (Xiao *et al*. 2019) but the alkaline conditions can be detrimental to methanogenesis, mainly the acetoclastic reaction which is an advantage when the objective is to produce VFA (Wang *et al*., 2017).

The thermophilic alkaline acidogenesis can take place in an upflow anaerobic sludge blanket (UASB) reactor where the suspended solids are retained in the lower part, within the sludge blanket (Terreros *et al*., 2009), while the effluent has low suspended solids and high VFA. The physical separation of acidogenesis and methanogenesis in two reactors contributes to the stability of anaerobic digestion (AD) because the high overloads given by the hydrolysed solids are buffered in the alkaline acidogenic UASB reactor accumulating high concentrations of VFA anions to be consumed in the second stage, to produce methane (Vigueras *et al*., 2011) at neutral pH. The hydraulics of this reactor can be studied for scaling up purposes using dimensional relantionships (Monroy. *et al*., 2020).

Flow cytometry (FCM) has been used to study damage to cell structure during pretreatments of WAS because it allows a discriminating cell counting (> 1000 cells/sec) to differenciate characteristics like size by light scattering and physiologic state by fluorescence of the stained DNA. It has been used to determine cell integrity and activity, quantifying intact, permeabilized, organic debris or dead cells (Prorot *et al*., 2008 and Foladori *et al*., 2010). A small light deviation of 0.5 to 5° with respect to the laser axis, known as the forward scatter (FSC), is produced by the cell membrane which reflects a cone, an indicator of the cell size (Macey, 2010). Fluorescence, emited by fluorochromes, indentifies between intact and damaged cells; SYBR Green I penetrates all the cells while propidium iodide (PI:$C_{27}H_{34}I_2N_4$) penetrates only wall damaged cells complexing with the DNA. So in these damaged cells, penetrated by both fluorochromes in an energy transfer phenomena, the emission spectra of SYBR Green I is absorbed and invisibilized by the PI spectra (Ziglio *et al*., 2002). Pang *et al*. (2014), measured the effect of alkaline acidogenesis on cell integrity and found that soluble organic matter (OMS) comes only from the flocs disaggregation (breakage of EPS) during acidogenesis at uncontrolled pH while under alkaline conditions there is also a disruption of the cell wall thus adding to the production of OMS.

The aim of this study was to combine alkaline and SE pretreatments (A-SE) with alkaline acidogenesis to improve, above these processes separated, the degradation of WAS. It was done in a batch SE

reactor at pH 9 and 160°C, followed by a continuous thermophilic (at 50°C) alkaline acidogenesis UASB type reactor to continue the cell destruction and obtain high VFA concentrations. To characterize the A-SE pretreatment, the destruction of TSS, which lumps the microbial cells, was assessed by cell damage and average particle diameter. The alkaline acidogenesis was characterized by the rates of VFA production and the of TSS destruction.

2 Material and methods

The effect of time and alkali on the SE of WAS on the TSS reduction was studied in seven batches. The resulting sludges from each treatment (Three reaction at neutral and alkaline conditions) were analysed for TSS by the gravimetric method and particle size distribution (PSD) and cell integrity in a FCM (by light scattering and stained DNA fluorescence). Then the VFA conversion of the pretreated WAS in a continuous acidogenic UASB reactor at alkaline pH was evaluated.

2.1 Waste activated sludge (WAS)

Samples were obtained from the activated sludge return line (connecting the clarifier to the aeration tank) of the Cerro de la Estrella wastewater treatment plant at Iztapalapa, Mexico City. To get rid of excess water they were let to settle on-site and kept at 4°C for 24 h to concentrate to 33% of their original volume (Ts). Finally, they were centrifuged at 15.3 G for 5 min (Cs) The process produced the sludge which was used in the experiments. All samples were characterized (table 1) according to Rice *et al*. (2012).

2.2 Steam explosion pretreatment (SE)

Batches of 4 kg of centrifuged WAS kept in a stainless-steel basket and 0.5 L of water were exploded in a 4 L reactor heated with saturated vapor (160°C, 0.67 MPa absolute pressure) through an external jacket (García-A. *et al*., 2018). The working pressure was reached in 10 min and the depressurization was instantaneous once the relief valve was opened (figure S1). Retention times of 5, 15 and 20 min under neutral (SE) and alkaline (A-SE, 4.25 g $Ca(OH)_2$/kg WAS) conditions were performed. Exploded WAS samples of 100 mL were analyzed.

2.3 A-SE pretreatment assessment

2.3.1 By gravimetry

Standard methods (Rice *et al*., 2012) were used for the characterization of initial and remaining total suspended solids (TSSi and TSSf) and the solids destruction efficiency was calculated: $\eta_{SST} = 1 - \frac{TSS_f}{TSS_i}$.

2.3.2 By flow cytometry (FCM)

a. Suspended solids size reduction was estimated through particle size distribution (PSD) before and after the pretreatments. To release the maximum number of free cells WAS suspensions were disaggregated with a vortex mixer for several agitations of 1 min at 2000 rpm until no visible flocs were noticed. The resulting suspension was diluted with a phosphate buffer solution (3 g K_2HPO_4, 1 g KH_2PO_4 and 8.5 g NaCl per L, pH=7.2) and filtered through 20 μm membranes to eliminate coarse particles (Foladori *et al*., 2010) and collect the free cells filtrate to inject samples into the FCM to measure the forward scatter (FSC) and to prepare them for the scanning electron microscope.

Table 1. WAS concentration process.

Parameter	Unit	WAS	Ts	Cs
TSS	g/L	6.6 ± 0.8	18.1 ± 4.8	62.1 ± 4.8
VSS		4.7 ± 0.7	12.5 ± 2.7	48.1 ± 5.3
COD		8.8 ± 0.7	18 ± 3.2	76.3 ± 2.2
COD/VSS	-	1.87	1.44	1.58
VSS/TSS		71%	69%	77%
pH	-		7.1 ± 0.3	

Ts: thickened WAS, Cs: centrifuged WAS, n (number of samples) = 7

b. Cell integrity was measured by fluorescence emitted by fluorochromes inside the WAS cells in 1 mL samples of the free cells filtrate with 10 μL of IP (1 mg/mL, Thermo Fisher Scientific, Invitrogen, USA) and SYBR Green I (diluted 1:30 with dimethyl sulfoxide; DMSO, Merck, Germany) and incubated in darkness at 25°C for 15 min. The emitted red fluorescence of IP (λ_{ex} = 536 nm, λ_{em} = 617 nm) indicates damaged and dead cells, while the green fluorescence emitted by SYBR-I (λ_{ex} = 495 nm, λ_{em} = 525 nm) indicates undamaged cells. Both signals are registered, amplified and analyzed with a FACScalibur flow cytometer equipped with an Ar laser (488 nm). Thus, quadrant I (Q_I) corresponds to cells positive to both fluorescences (D + U, damaged and undamaged cells), in which small aggregates or damaged cells with incorporated IP were observed (Ziglio *et al.*, 2002), in Q_{II} red fluorescence was identified, which corresponds to damaged cells (D), Q_{III} was negative to both fluorescences and were considered unidentified pretreatment products or particles (P) and in Q_{IV} corresponding to undamaged cells (U), green fluorescence was identified.

Each analysis used 20,000 cells, data were acquired and processed with the BDCellQuest and Flowing Software 2.5.1 (http://flowingsoftware.btk.fi/).

Destruction efficiency was determined as follows:

$$\eta_P(particle) = [P/(P+D+U)];$$

$$\eta_D(damaged\ cells) = [D/(P+D+U)];$$

$$\eta_{P+D} = (\eta_P + \eta_D)$$

2.3.3 *Scanning electron microscopy of the steam exploded WAS*

Fresh and pretreated WAS were observed through a digital scanning electron microscope (SEM) model DSM 940 (Zeiss, Germany) at 200X amplification. Duplicate samples were: chemically fixed with 3.5% glutaraldehyde for 24 h at 4°C, washed three times with a phosphate buffer, post fixed with 1% OsO_4 for 2 h, dehydrated with an ethanol gradient in 10% increments in 10 min intervals up to 100%, dried with supercritical carbonic gas as transitional fluid and finally, mounted and Au metallized (Taheri *et al.*, 2012). Considering the field length (450 μm) of the obtained micrographs, the particle size distribution (PSD) was obtained with the help of the FCM's FSC.

2.4 *Alkaline acidogenesis*

Volumes of 750 mL of the selected A-SE WAS (pH 9), cooled to 50°C were fed to two 1 L batch reactors for the preliminary selection of reaction time and the effect of an inoculum at a ratio of food to inoculum (S_0/X_0) = 4 g COD/g VSS. Anaerobic sludge (20 g VSS/L) from the UASB reactor treating the University campus wastewater was used as inoculum.

Then, after having selected a reaction time a continuous reactor (in a 7 L glass container, figure S2) was started with the batch conditions selected, until the reaction time was reached and then operated at organic loading rates (B_v) from 3 to 7 g COD/L·d.

3 Results and discussion

3.1 *Gravimetry assessment of the A-SE tests*

The WAS treated by A-SE had a better particle destruction (53%) than the treated in N-SE in 15 min (figure 1). The former followed a first order hydrolysis rate (equations 1), meaning that the decreases linearly with time or that the remaining TSS diminishes exponentially with time. On the other hand, the neutral treatment adjusted better to second order kinetics (equation 2) implying that as the reaction proceeds the rate decreases faster until the concentration becomes asymptote to the time axis (changes little with time).

$$r_A = k_A S, R^2 = 0.998 \quad (1)$$

$$r_N = k_N S^2, R^2 = 0.996 \quad (2)$$

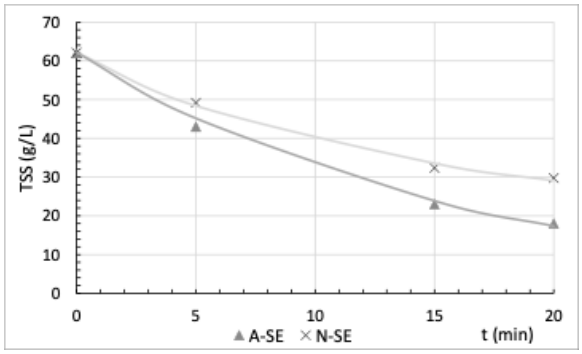

Figure 1. Time and alkali effect on the TSS of centrifuged and steam exploded WAS (N-SE = neutral, A-SE= alkaline) $r_A = k_A S$, $r_N = k_N S^2$.

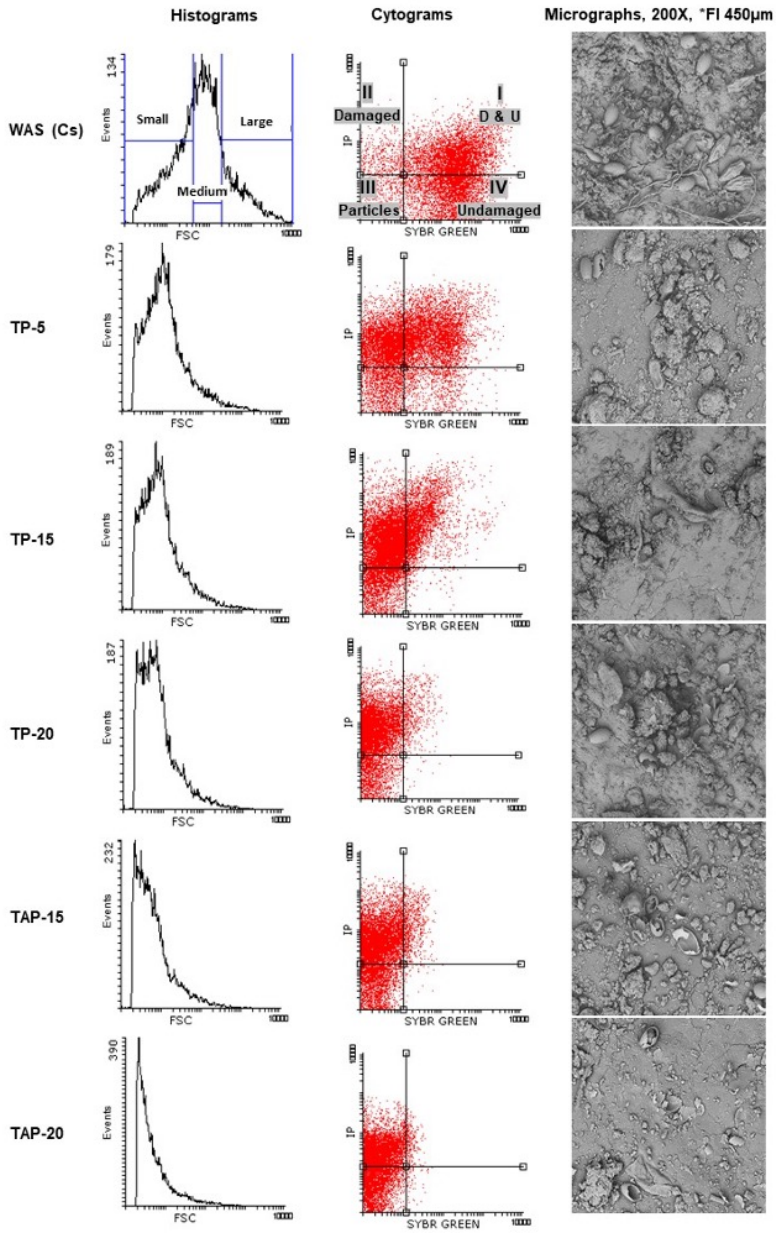

Figure 2. Histograms giving the number of events as a function of the forward scatter, cytograms relating the green and red fluorescences and micrographs *Fl = field length, from the WAS pretreatments.

where r = rate of TSS destruction (g/L·min), S is TSS, k are the specific rate constants: k_A = 0.0637 [min^{-1}] 1st order for A-SE, and k_N = 0.00091 [L g^{-1} min^{-1}] 2nd order for the N-SE.

3.2 FCM assessment of the cells' destruction by A-SE

The samples of the centrifuged WAS (Cs) and those obtained at 5, 15 and 20 minutes, with and without alkali were analyzed for particle size distribution (PSD), as measured with the FSC, the distribution of damaged (D), undamaged (U) cells as measured by FCM fluorescence and the micrographs of the free cell suspensions (figure 2).

Histograms in the 1st column show that the mean PSD moves to the left with increasing treatment time due to particle breakdown. The micrographs (3rd column) show at bare eye the abundance of large particle and the reduction in size and number with time and alkali. To relate the FSC to the particle size an image analysis of the particle micrographs helped to classify them in small (S = 23±13 μm), medium (M = 70±14 μm) and large (L= 98±10 μm) sizes and determine the PSD for each treatment.

Cytograms (2nd column) show the fluorescence signals which assessed the distribution of damaged and undamaged cells (in quadrants (Q) II and IV respectively) together with no DNA debris caused by the SE pretreatments (Q_I). It shows the abundance of U cells in the untreated WAS (WAS Cs). After 5 minutes N-SE (denoted in the figure as TP-5) they have been greatly reduced and almost disappeared in the rest of the treatments, particularly the A-SE treatments (TAP 15 and TAP 20, data of TAP-5 is missing).

With the double staining analysis, it was determined that in the centrifuged WAS (Cs) 44% of the particles are intact (Q_{IV}) and 41% are small aggregates (Q_I), while only 8% are damaged cells (Q_{II}) and 7% are no DNA particles (Q_{III}). At 5 minutes of treatment, the undamaged cells (Q_{IV}) are only 5% and 9% of the total cells until 15 min when there were none but 100% of the cells were damaged (Q_{II}) with small debris associated (Q_{III}). The neutral treatment took 5 more minutes to reach the same results (figure 3). This shows that cell viability is not useful to track the process as they permeabilize faster that the size reduction.

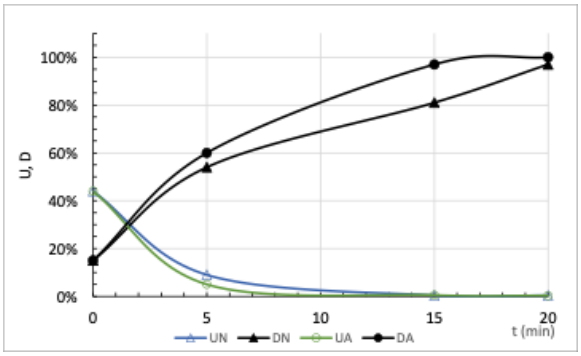

Figure 3. Cell integrity in WAS after SE pretreatments. U = undamaged particles (IV Q), D = damaged and other particles (II+III Q).

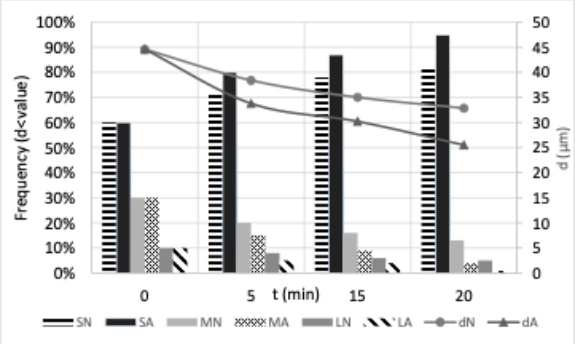

Figure 4. Evolution of the particle size distribution (PSD) after each treatment. S =23±13 μm, M =70±14 μm, L=98±10 μm, d =average diameter, A =A-SE, N=N-SE.

Figure 4 shows how the PSD is displaced in 20 min from 60% small particles (S) to 95% with the A-SE and to 80% with the N-SE treatment, with the concomitant reduction of medium (M) and large (L) sized particles. The weighted average size is also plotted to show the influence of time and alkali on the steam explosion treatments and they follow a first order average diameter (d = μm) reduction with equations 3 and 4.

$$r_{TA} = [0.028 min^{-1}]d \quad (3)$$

$$r_T = [0.016 min^{-1}]d \quad (4)$$

The correlations of the removal efficiencies η_{TSS} with the size reduction and damaged cell efficiencies (η_d and η_D) considering both treatments, with and without alkali (figure 5), obtained from figures 3 and 4, mean that there is a potential use of FCM for the on-line evaluation of the steam explosion treatment instead of the traditional gravimetric method.

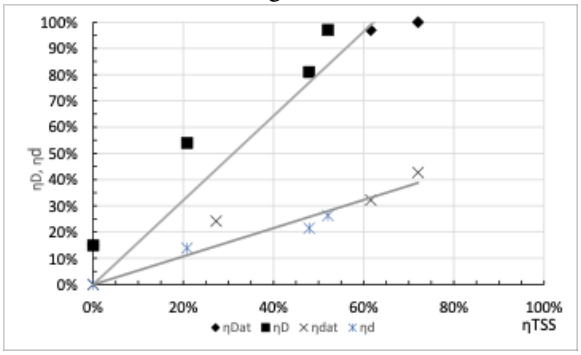

Figure 5. Correlation between η_{TSS} and η_d and η_D by FCM. $\eta_d = 0.537\eta_{VSS}$, $R^2 = 0.99$, $\eta_D = 1.607\eta_{VSS}$ with $R^2 = 0.96$.

Table 2. Characterization of A-SE WAS.

pH	9± 0.1
TSS (g/L)	51 ± 5
VSS (% ST)	73 ± 4
CODT (g/L)	69 ± 5
CODS (g/L)	13 ± 2
n (samples)	15

3.3 Alkaline acidogenesis in UASB reactor (AAR)

3.3.1 Influent preparation

The alkaline steam exploded WAS, 40 batches of approximately 4 kg/run, were stored to 50°C where it settled until it was fed to the continuous alkaline acidogenic reactor (AAR) at 2.5 to three times the concentration obtained from the SE reactor (table 2). The daily feeding flow rate (F = L/d) was calculated according to equation 5

$$F = \frac{B_v V}{S_0} \tag{5}$$

Where V is the reactor volume (7 L) and S_o is the inlet volatile solids COD (g/L).

The pH remained around 9. The soluble COD was low because the supernatant which contained most of the soluble compounds released from the A-SE did not enter the AAR. With this arrangement the full advantage of the alkaline acidogenesis is obtained because with higher VSS concentrations more VFA will be produced with no inhibition because the alkaline media kept them ionized.

3.3.2 Reactor operation

The run was started in batch with a So/X = 4 which meant that 3.25 L of the inoculum (20 g SSV/L) were added to 3.75 L of A-SE WAS (70 g COD/L). After 5 days of batch fermentation, with effluent recirculation, when VFA reached 13 g CODVFA/L (61% acetate) the reactor was started in continuous mode changing the organic loading rates (Bv) from 3 to 7 g COD_{VSS}/L·d (the COD of VSS) by adjusting the hydraulic retention time (HRT) from 20 to 8 days.

During the first OLR run the residual soluble COD (CODs) is 51% and methane is 6% of the VSS solubilization (VSS_0-VSS). Total VFA is 63% of the CODs (figure 6 top). After an OLR increment, to 6.2, the VSS removal decreases with a concomitant decrease in CODs and VFA_t. A drop of OLR to half and then two successive increments does not stop the leveling of VFA_t to 3 g/L. The individual VFA (figure 6 bottom), show in the first run, a high concentration of VFAt peaking to 12 g/L, 62% being acetate and 30% propionate. In subsequent OLR changes the propionic acid is higher than acetic, indicating the presence of H. pH is nearly constant at around 8.5 with a minimum period at 7.5 when VFA are at their highest. Methane is low as expected due to the basic pH as suggested by Wang *et al*. (2017).

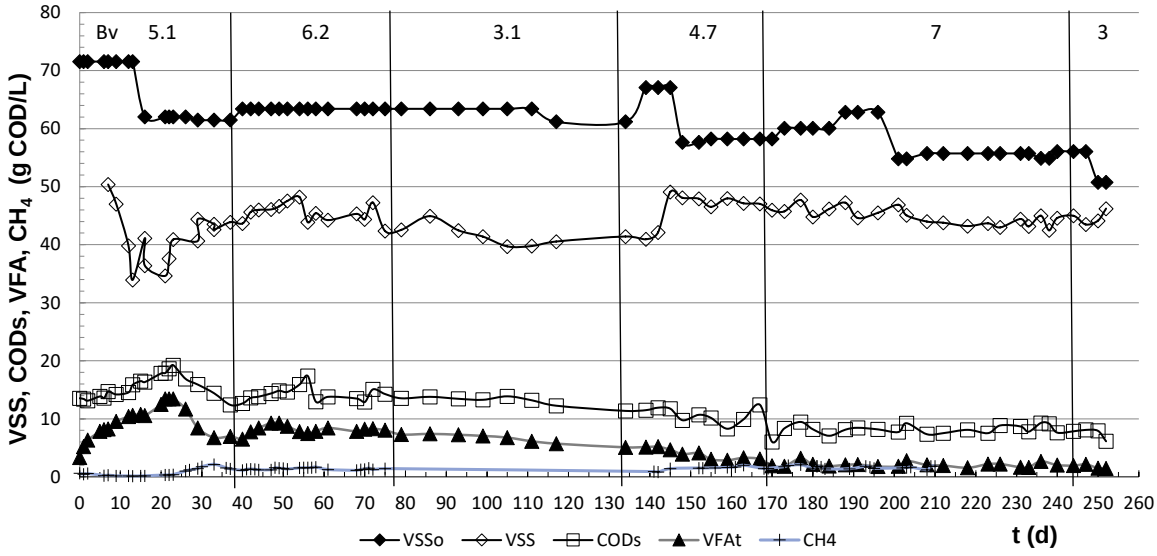

Figure 6. Evolution of alkaline acidogenesis at several Bv (g COD_{VSS}/L·d). VSS_0 (♦), VSS (◊), COD_s (□), total VFA (+), CH_4 (x). The bottom plot shows the VFA in perspective with methane and pH.

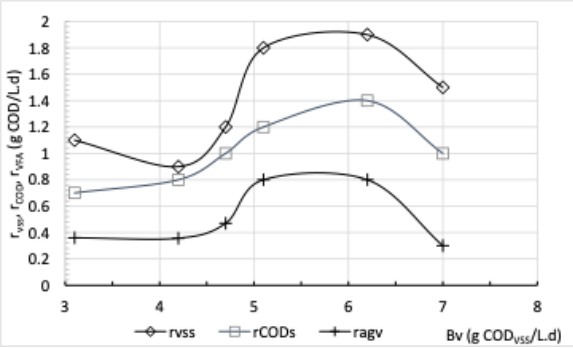

Figure 7. Rates of produced VFA as compared with VSS removal showing an optimal Bv at 5 to 6 g COD_{VSS}/L·d.

By taking five days of constant VSS output as a steady state point for each Bv, the plot of reaction rates as a function of the loading rates is obtained (figure 7). It shows that a OLR of 5 to 6 g COD_{VSS}/g·L is an optimum range to operate an alkaline acidogenesis of WAS with efficiencies of 30% for VSS solubilization and 42% VFA formation from the solubilized VSS. According to these results, WAS treated with A-SE, cooled to 50°C can be fed to a reactor for an alkaline acidogenesis al 60 g TSS/L with 10 days retention time to produce 1.4 g COD_S/L·d with 0.8 g COD_{VFA}/L·d. thus yielding 0.133 g COD_{VFA}/g COD_{VSS} =0.246 g COD_{VFA}/g VSS (table 2), 3 to 4 larger than an acidic acidogenesis (Yuan *et al*., 2006).

Table 3. Material balance of the integrated WAS treatment process in figure 8.

Stream	**1**	**2**	**3**	**4**	**5**	**6**	**7**
V (L)	1000	106	106	condensed steam	60	46	46
TSS (g/L)	6.6	62.1	22		0	51	33.3
CODt (g/L)	9	84	54.3		54.3	69	45
CODs (g/L)	0.05	0.05	13		13	13	15
CODVFA (g/L)	0	0	0		0	0	8

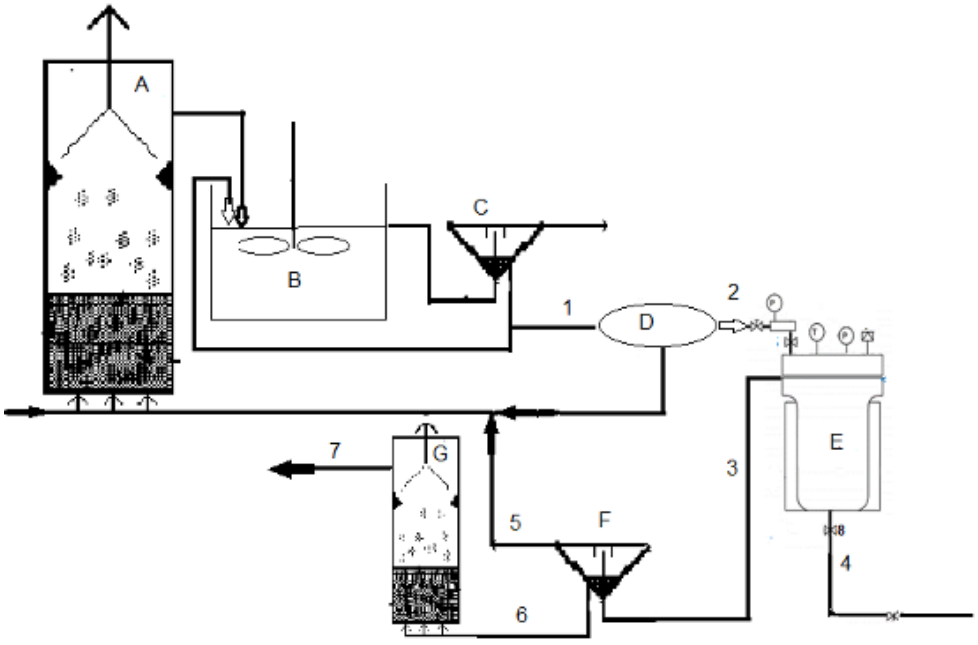

Figure 8. Process flow diagram for the alkaline steam explosion and alkaline acidogenesis of waste activated sludge. A= UASB reactor, B = Activated sludge tank reactor, C = secondary clarifier, D = Centrifuge E = steam explosion reactor, F = consolidation tank, G = alkaline acidogenesis reactor. The streams characteristics are shown in table 3.

Based on these results a process flow diagram is built to appreciate the importance of integrating the alkaline steam explosion with alkaline acidogenesis to reduce the mas of WAS and produce methane and VFA (figure 8, table 3). The process starts at the return line of the clarifier (1) of the activated sludge tank (AST) reactor. The settled sludge (1) is a slurry of about 7 g TSS/L which has to be concentrated about ten times (2) for an efficient heat use in the A-SE reactor which breaks the TSS from 62 to 22 g TSS/L (3). The supernatant which is a secondary effluent is returned to the wastewater treatment process. Stream 3, at 160°C and pH 9 is cooled down to 50°C and concentrated to handle the thermophilic alkaline acidogenic reactor with highest possible load of solids (6). The supernatant can be returned to the WWT process (which if has an anaerobic reactor before the AST, can add to the methane production). Stream 7 can be directed to produce methane, adding to the obtained from stream 5, or for VFA extraction (15 g/L). The alkaline steam explosion alone gives 65% TSS removal and the alkaline acidogenesis yields 35% TSS removal. The overall process produces 77% removal.

Conclusions

A positive effect of the alkaline steam explosion (pH 9, 15 min, 0.67 MPa absolute pressure, 160°C) on the TSS size reduction was found to be concentration dependent (first order rate solids destruction) which is related to a smaller particle size as measured by average particle diameter in a flow cytometer. These results show that the alkaline pre-treatment can double methane production by increasing the WAS digestibility.

Assessing cell integrity by FCM fluorometry did not allow the follow-up of the WAS destruction because with only 5 min of pretreatment, 86% presented damages in their cellular integrity without really breaking down the cells and reducing the particles sizes. On the other hand, light scattering FCM can be implemented on line to assess the VSS destruction of WAS by steam explosion as there is a good correlation with the time-consuming gravimetric analysis of VSS (R^2 = 0.98).

The alkaline steam explosion of waste activated sludge destroys 60% solids in 15 min leaving a stream with high COD concentration and another of solids which needs to be concentrated for high VFA production rates.

The study of the separated unit operations is useful to integrate a process with solid experimental basis.

Supplementary material

https://www.dropbox.com/s/8pylv2gyjt2cvy5/Tafolla2021Supplementary%20Material.docx?dl=0

Acknowledgements

This work was supported by "Fondo de Sustentabilidad Energética CONACYT-SENER (Mexico)", through the project CEMIE-Bio Cluster Gas Biofuels # 247006.

To CONACYT for scholarship No. 300613 to the first author within the Biotechnology Posgraduate Program at UAM.

References

Appels, L., Baeyens J., Degreve, J. and Dewil, R. (2008). Principles and potential of the anaerobic digestion of waste-activated sludge. *Progress in Energy and Combustion Science 34(6)*, 755-781. https://doi.org/10.1016/j.pecs.2008.06.002

Barber, W.P.F. (2016). Thermal hydrolysis for sewage treatment: A critical review. *Water Research 104*, 53-71. https://doi.org/10.1016/j.watres.2016.07.069

Barr, K.G., Solley, D.O., Starrenburg, D.J. and Lewis, R.G. (2008). Evaluation, selection and initial performance of a large scale centralised biosolids facility at Oxley Creek Water Reclamation Plant, Brisbane. *Water Science and Technology 57 (10)*, 1579-1586, https://doi.org/10.2166/wst.2008.041

Cano, R., Pérez-E., S.I. and Fdz-Polanco, F. (2015). Energy feasibility study of sludge pre-treatments. *Applied Energy 149*, 176-185. http://dx.doi.org/10.1016/j.apenergy.2015.03.132

Carrere, H., Georgia, A., Affes, R., Passos, F., Battimelli, A., Lyberatos, G. and Ferrer, I. (2016). Review of feedstock pretreatment strategies for improved anaerobic digestion:

from lab-scale research to full-scale application. *Bioresource Technology 199*, 386-97. http://dx.doi.org/10.1016/j.biortech.2015.09.007

Foladori, P., Bruni, L., Tamburini, S. and Ziglio G. (2010). Direct quantification of bacterial biomass in influent, effluent and activated sludge of wastewater treatment plants by using flow cytometry. *Water Research 44(13)*, 3807-3818. https://doi.org/10.1016/j.watres.2010.04.027

García-A., R., Hernández, S., Ortiz, I. and Cercado B. (2019). Assessment of microbial electrolysis cells fed hydrolysate from agave bassase to determine the feasibility of bioelectrohydrogen production. *Revista Mexicana de Ingeniería Química 18(3)*, 865-874. https://doi.org/10.24275/uam/izt/dcbi/revmexingquim/2019v18n3/Garcia

Macey M. (2010). Principles of flow cytometry. In: *Flow Cytometry: Principles and Applications*, 3rd Ed. Human Press, New Jersey, EUA.

Monroy-O., S.G., Jimenez-G., A., Gutierrez-R., M. and Medina-M., S. A. (2020). Fundamentals in the design and scaling of biodigesters with mixing by hydraulic recirculation of wastewater for biogas production using dimensional analysis. *Revista Mexicana de Ingeniería Química 19*, Sup. 1, 81-99. https://doi.org/10.24275/rmiq/Bio1545

Pang, L., Ni, J., and Tang, X. (2014). Fast characterization of soluble organic intermediates and integrity of waste activated sludge. *Biochemical Engineering Journal 86*, 49-56. http://dx.doi.org/10.1016/j.bej.2014.03.005

Prorot, A., Eskicioglu, C., Droste, R., Dagot, C. and Leprat, P. (2008). Assessment of physiological state of microorganisms in activated sludge with flow cytometry: application for monitoring sludge production minimization. *Journal of Industrial Microbiology and Biotechnology 35(11)*, 1261-1268. http://dx.doi.org/10.1007/s10295-008-0423-9

Rice, E.W., Baird, R.B. Eaton, A.D. and Clesceri L.S. (2012). *Standard Methods for the Examination of Water and Wastewater*. 22th Ed. American Public Health Association, American Water Works Association, Water Environment Federation, Washington, DC. ISBN: 978087553o130

Sani-Shehu, M. S., Abdul-Manan, Z. and Wan-Alwi, S. R. (2012). Optimization of thermo-alkaline disintegration of sewage sludge for enhanced biogas yield. *Bioresource Technology 114*, 69-74. http://dx.doi.org/10.1016/j.biortech.2012.02.135

Taheri E., Khiadani (Hajian) M.H., Amin, M. M., Nikaeen, M. and Hassanzadeh, A. (2012). Treatment of saline wastewater by a sequencing batch reactor with emphasis on aerobic granule formation. *Bioresource Technology 111*, 21-26, http://dx.doi.org/10.1016/j.biortech.2012.01.164

Terreros-M., J., Olmos, A., Noyola R., A., Ramírez V., F., and Monroy H., O. (2009). Anaerobic digestion of primary and secondary sludge in two serial UASB reactors. *Revista Mexicana de Ingeniería Química 8(2)*, 153-161.

Vigueras, S., Ramírez, F., Noyola, A. and Monroy, O. (2011). Effect of the thermal alkaline pretreatment on the mesophilic and thermophilic anaerobic digestion of waste actived sludge. *Revista Mexicana de Ingeniería Química 10(2)*, 247-255.

Wang D., Liu Y., Huu Hao Ngo, H.H. Zhang C., Yang, Q., Lai Peng, He D., Zeng G., Li, X. and Ni, B.-J. (2017). Approach of describing dynamic production of volatile fatty acids from sludge alkaline fermentation. *Bioresource Technology 238*, 343-351, http://dx.doi.org/10.1016/j.biortech.2017.04.054

Xiao, B., Liu, C., Liu, J. and Guo, X. (2015). Evaluation of the microbial cell structure damages in alkaline pretreatment of waste activated sludge. *Bioresource Technology 196*, 109-115. http://dx.doi.org/10.1016/j.biortech.2015.07.056

Xiao Ma., Jiongjiong Ye, Li Jiang, Liang Sheng, Jianyong Liu, Yu-You Li and Zhi Ping Xu (2019). Alkaline fermentation of waste activated sludge with calcium hydroxide to improve short-chain fatty acids production and extraction efficiency via layered double hydroxides.

Bioresource Technology 279, 117-123. https://doi.org/10.1016/j.biortech.2019.01.128

Yuan H., Chen Y., Zhang H., Juang S., Zhou Q. and Gu G. (2006) Improved bioproduction of short-chain fatty acids (SCFAs) from excess sludge under alkaline conditions. *Environmental Science and Technology 40(6)*, 2025-2029. https://doi.org/10.1021/es052252b

Ziglio, G., Andreottola, G., Barbesti, S., Boschetti, G., Bruni, L., Foladori, P. and Villa, R. (2002). Assessment of activated sludge viability with flow cytometry. *Water Research 36*, 460-468.

Biomass and Bioenergy 142 (2020) 105753

Contents lists available at ScienceDirect

Biomass and Bioenergy

journal homepage: http://www.elsevier.com/locate/biombioe

Research paper

Hydrothermal pretreatment of agave bagasse for biomethane production: Operating conditions and energy balance

Abigail Hernández-Vázquez [a], Sergio Hernández [b], Irmene Ortíz [b,*]

[a] Posgrado en Ciencias Naturales e Ingeniería, Universidad Autónoma Metropolitana-Cuajimalpa, Mexico
[b] Depto. Procesos y Tecnología, Universidad Autónoma Metropolitana-Cuajimalpa, Av. Vasco de Quiroga 4871, Col. Santa Fe, C.P. 05348, México City, Mexico

ARTICLE INFO

Keywords:
Lignocellulosic biomass
Biochemical methane potential (BMP)
Energy balance
Steam explosion
Biogas
Severity factor

ABSTRACT

In this study, agave bagasse (a lignocellulosic residue) was pretreated by steam explosion to increase the solubility of carbohydrates in the hydrolysates. The operational variables studied were pressure (0.28, 0.47, and 0.67 MPa, corresponding to 116, 142, and 154 °C, respectively) and pretreatment time (5, 10, 15, and 20 min). The conditions that favored the highest solubilization of glucose (66 ± 4 mg L^{-1}), arabinose (160.31 ± 3.2 mg L^{-1}), and the chemical oxygen demand (COD, 4395.71 ± 22.44 mg L^{-1}) were 154 °C and 10-min. On the other hand, the maximum solubilization of total carbohydrates (TC, 2177.99 ± 197.22 mg L^{-1}) and xylose (43 ± 2.8 mg L^{-1}) was obtained at 154 °C and 15-min. Pretreatments catalyzed with H_2SO_4 at 154 °C and 10-min resulted in 3, 2.7, and 100-times TC, glucose and xylose concentrations, respectively, as compared to the uncatalyzed pretreatment. However, concentrations of potential inhibitor compounds (i.e., acetic acid, furfural, and hydroxymethylfurfural) increased as well, 26, 120 and 18-times, respectively. A biochemical methane potential (BMP) test of the hydrolysates resulting from the 154 °C-10 min conditions was used to calculate the energy balance of their conversion to methane. When considering only the energy invested in the pretreatment, the process showed an efficiency of 247%, thus being energetically feasible. The integration of methane production to the tequila processes could be implemented using the steam flow already present in the process, improving energy efficiency and reducing the environmental impact of this industry.

1. Introduction

Lignocellulosic biomass is any plant material with complex structured fractions of cellulose, hemicellulose, and lignin that form a highly recalcitrant three-dimensional mesh. The biomass can be used directly as a source of energy via combustion with low energy recovery and negative environmental effects due to the emissions of CO_2. Therefore, the processing of biomass to access primary or secondary metabolites is energy and environmentally more attractive and efficient [1]. Energy conversion from lignocellulosic biomass includes a stage of biomass pretreatment to increase the accessibility of sugars for their subsequent processing. The pretreatment of biomass could represent up to 40% of the global cost of second-generation biofuels, but this process is required to access the carbohydrates [2]. The pretreatments can be physical, chemical, physicochemical, biological, or various combinations thereof [3].

According to data from the Food and Agricultural Organization of the United Nations, around 41,000 tons per year of agave fibers were produced globally from 2015 to 2018 with an average total cultivated area of 57500 ha [4]. The main producers of *Agave* are Colombia (~37%), Central America (~30%), Mexico (15%), Cuba, and the Philippines (~9% each). The genus Agave is endemic to the American continent with approximately 200 species and 254 taxa worldwide [4]. Therefore, it has been identified as a potential feedstock for biofuel production [5]. It can be used as raw a material to obtain alcoholic beverages, organic acids, composts, paper, fuel, string fibers (ixtle), animal feed, and, more incipiently, as a low-cost carbon source for the production of biopolymers and carbohydrates as well as for obtaining phenolic compounds from the lignin present in its fibers [6]. In Mexico, particularly, the *Agave tequilana* (blue agave) is used for the production of tequila (a distillate with the appellation of origin). The production of tequila is divided into six main steps: harvesting, cooking (100–120 °C), fermentation, distillation, aging, and bottling [7]. This industry reported consumption of *Agave* of 1340 thousand tons in 2019, which represents approximately 540 thousand tons of agave bagasse generated (considering 40% of the processed agave on dry basis) [5,7]. This amount of

* Corresponding author.
E-mail address: irmene@cua.uam.mx (I. Ortíz).

https://doi.org/10.1016/j.biombioe.2020.105753
Received 15 April 2020; Received in revised form 14 August 2020; Accepted 25 August 2020

feedstock could be significantly higher if other *Agave* varieties and related industries were taken into account. The agave bagasse has been studied as a potential raw material for the production of non-fossil fuels such as ethanol, H_2 and biogas via biological conversion [5]. Hydrogen production is still under development, but it is attractive because of its higher energy content compared to natural gas and the fact that its combustion releases only water vapor [5]. Following the above idea, the continuous production of H_2 and methane in a two-stage process using agave bagasse as substrate has reported 105 mL H_2 g^{-1} and 225 mL CH_4 g^{-1} of agave bagasse, respectively [8]. Likewise, a biochemical methane potential (BMP) of 178 mL CH_4 per gram of chemical oxygen demand (COD) added has been reported in hydrolysates of agave bagasse wastes generated in the production of second-generation ethanol and pretreated by steam explosion [9]. Pretreatment of agave bagasse by steam explosion and subsequent enzymatic hydrolysis for ethanol production has been also reported, obtaining 126 g L^{-1} of glucose that resulted in 65.26 g L^{-1} of ethanol after 10 h of fermentation [10].

The steam explosion pretreatment consists of subjecting the material to high pressures (0.7–4.8 MPa) and temperatures (150–240 °C) for a short period (seconds to minutes) and subsequent, sudden depressurization of the system, which changes the biomass structure [2]. The main effects of the steam explosion on lignocellulosic biomass are the solubilization of hemicellulose and the transformation of the lignin fractions [11]. The optimal solubilization of hemicellulose during this pretreatment could be achieved under two conditions: high temperatures with a short time of pretreatment or lower temperatures with a longer time of pretreatment. The latter method has the advantage of reducing the formation of inhibitor compounds for the next steps of biofuel production [12].

The explosion of steam has been used for the pretreatment of various crops, forest, and agricultural residual biomasses such as sugar cane bagasse, poplar, eucalyptus chips, sorghum bagasse, wheat straw, maize stalk, bamboo, winter rye, oilseed rap, faba bean, corn stover, and others [13–22]. These studies have evidenced that the process of steam explosion, up to a certain level, can effectively release hemicellulosic sugars, improving the efficiency of ethanol or methane conversion. Thus, this technology is one of the most used in demonstration pilot plants and industrial-scale plants for the production of second-generation ethanol in Sweden, USA, Italy, and Canada, among others [3]. Some of the advantages of steam explosion are that it is a relatively simple process, it does not generate residual streams that need to be treated, and the concentrations of inhibitors like furfural, hydroxymethylfurfural, and acetic acid are not toxic, in general, for subsequent stages [10]. Steam explosion can be improved by adding some chemical compounds such as acids (H_2SO_4) or bases (NaOH) that serve as catalysts [2]. However, this addition usually carries a drawback of generating inhibitory products for subsequent biological processes.

Thus, the objective of this work was to determine the temperature and reaction time conditions of agave bagasse pretreatment by steam explosion that favor the solubilization of carbohydrates in hydrolysates and to calculate the energy balance of the reactor and the process based on the obtained BMP of the hydrolysates.

2. Materials and methods

2.1. Experimental aspects

2.1.1. Biomass

The bagasse of *Agave tequilana* Weber blue variety was supplied by the Institute for Scientific and Technological Research of San Luis Potosi (IPICYT) and was obtained from a tequila company from Amatitán, state of Jalisco, Mexico.

2.1.2. Biomass characterization prior to pretreatment

The physicochemical biomass characterization consisted of determining total solids, ash, extractives, structural carbohydrates, and lignin. Total solids were determined by eliminating humidity from the sample in a muffle furnace at 110 °C for 5 h [23]. Ash was measured by calcination of a sample in a muffle furnace at 510 °C for 5 h [24]. Extractives were determined using Soxhlet equipment. First, there was an extraction with water for 12 h at a temperature of 90–100 °C and a second extraction with ethanol for 16 h at a temperature of 70 °C; extractives were concentrated by using a rotary evaporator [25]. Structural carbohydrates and furans were quantified by High-Pressure Liquid Chromatography (HPLC, Varian ProStar 210) with a UV–vis detector (Varian ProStar PS 325, 278 nm), using an AMinex HPX-87H column [26]. The column temperature was maintained at 60 °C and H_2SO_4 5 mM was used as the eluent at a flow of 0.6 mL min^{-1}. The soluble lignin was extracted by hydrolysis with 72% sulfuric acid followed by heating in a water bath at 30 °C for 1 h, then neutralization, and finally 1 h in an autoclave at 121 °C and 15 psi [26].

2.1.3. Characterization of hydrolysates

The characterization of the hydrolysates consisted of quantifying the COD [27], total carbohydrates (TC) [28], glucose, and xylose by using a biochemical analyzer YSI 2700. It also included furans, which were quantified by HPLC as previously described, phenols by the 4-aminoantipyrine method [29], and pH using a potentiometer (Conductronic PC 45).

2.1.4. Experimental system

The experimental system consisted of a 3 HP boiler that supplied steam to the jacket of the pretreatment reactor to heat the reactor and take it to the operating pressure. The 4 L stainless steel reactor (Sch. 10S, ASTM A312 TP 316L) was provided with a relief valve to carry out sudden depressurization in an expansion tank (92 L) where the hydrolysates were collected. Liquefied pretroleum gas (LPG) was used as boiler fuel and quantified to determine the consumption during each pretreatment condition tested.

2.1.5. Design of experiments and statistical analysis

Pretreatments by steam explosion were carried out using 55 g of dry biomass and 2 L of water. Operational variables were temperature and time of pretreatment, which varied between 116, 142, and 154 °C (0.28, 0.47, and 0.67 MPa, absolute pressure) and between 5, 10, 15, and 20 min, respectively. These operational conditions were selected to minimize the formation of potential inhibitors and favoring the energy balance, considering that the agave bagasse has already been submitted to a temperature of 100–120 °C during cooking in the process of tequila production. Therefore, the approach of this study was the use of lower pressure values and longer reaction times than those typically reported for steam explosion pretreatment [30]. Furthermore, catalyzed pretreatments were also carried out with H_2SO_4 (2% v/v) at 154 °C for 5 and 10 min.

Based on this information, the severity factors (R_0) of the pretreatments were determined according to Equation (1). Whereas, in the case of pretreatments catalyzed, the combined severity factor (CSF) was determined using Equation (2) [31].

$$R_0 = t * e^{(T-100)/14.75} \quad (1)$$

where R_0 is the severity factor, t is the time in minutes, and T is the pretreatment temperature in °C.

$$CSF = \log Ro - pH \quad (2)$$

where *CSF* is the combined severity factor and the pH is that of hydrolysate.

The R_0 values obtained were classified as low, medium, and high. Table 1 shows the conditions of 9 pretreatments carried out (3 of each level of R_0). The table includes logarithmic values of severity ranging between 1.17 and 2.89, which are in the range of those reported for biochemical conversion to biofuels [32].

Table 1
Experimental conditions and severity factor of the pretreatments.

No. Exp	Pressure (MPa)	Time (min)	Internal reactor temperature (°C)	Severity Factor (Ro)	Log Ro	pH
1	0.28	5	116	14.79	1.17	5.10
2	0.28	15	116	44.38	1.65	5.07
3	0.47	5	142	86.22	1.94	4.44
4	0.47	10	142	172.44	2.24	4.40
5	0.47	15	142	258.66	2.41	4.00
6	0.47	20	142	344.88	2.54	4.06
7	0.67	10	154	389.01	2.59	4.55
8	0.67	15	154	583.51	2.77	4.66
9	0.67	20	154	778.02	2.89	4.76
10[a]	0.67	5	154	194.50	1.44[b]	0.85
11[a]	0.67	10	154	389.01	1.68[b]	0.91

[a] Catalyzed with 2% H_2SO_4 (v/v)
[b] CSF

The significant differences in pretreatments regarding COD and TC for hydrolysates were determined by Duncan's multiple range tests using Statistical Analysis System (SAS) software.

2.1.6. Biochemical methane potential (BMP) test

The BMP test was used to evaluate, in a relatively fast way, the methane production under controlled conditions without other factors such as the configuration and operational conditions of the anaerobic digestor reactors and inoculum specialization.

Based on the results at different conditions of pretreatment, the BMP evaluation was performed on hydrolysates obtained at 154 °C for 10 min using 110 g of dry biomass and 2 L of water. The tests were performed at the University Center for Exact Sciences and Engineering CUCEI-Guadalajara. They were done using an automatic system for methane potential evaluation (AMPTSII, Bioprocess Control, Sweden) in which the volume of methane produced during the anaerobic digestion process was quantified accordingly to the protocols reported previously [33]. The test was run in triplicate with a volume of 360 mL of hydrolysates whose pH was adjusted to 7.5. The inoculum to solid ratio was 1:2, considering 5 g L^{-1} of COD and 10 gSV L^{-1} (grams of volatile solids) for the inoculum. This inoculum consisted of granular sludge from a UASB reactor used to treat tequila vinasses. The anaerobic digestion conditions were as follows: 37 °C, continuous stirring at 150 rpm, and a 60% methane concentration in the biogas [33].

3. Theoretical aspects

3.1. The overall energy yield of the process

The overall process efficiency was calculated on the basis of the methane energy that can be obtained from hydrolysates (COD) using the BMP test versus the energy consumed during the pretreatment, i.e., LPG consumption, as described in Equation (3) [34]. This calculation did not include the energy required for the anaerobic digestion, since this study considered the BMP test approach to estimate the methane production.

$$\eta_{overall} = \frac{E_{produced}}{E_{consumed}} \tag{3}$$

where $\eta_{overall}$ is the overall process efficiency (%), $E_{produced}$ is the energy produced in the process (J), and $E_{consumed}$ is the energy consumed during pretreatment (J).

The energy produced by conversion to methane was estimated using the volume of methane obtained in the BMP test and the inferior calorific power (ICP) of methane. The calculation of energy consumed during pretreatment considered the LPG consumption during the time of each pretreatment. The ICP of LPG was determined using the densities and ICPs of propane and butane.

3.2. Macroscopic energy balance

This calculation requires first determining the heat supplied to the reactor as steam through the jacket and the heat transferred to the reactor interior. So, the heat used by the system was calculated with the contributions of the change of energy as heat due to the temperature change of the liquid water, the change of state of aggregation, and the change of steam temperature, considering latent and sensible heat as detailed in Equation 4

$$Q_1 = \left(m_{ow} * C_p * \Delta T\right)_w + \left(m_{ow} * L_s\right) + \left(m_{ow} * C_p * \Delta T\right)_s \tag{4}$$

where Q_1 = heat used by system (J); m_{ow} = operating water mass (kg); C_p = heat capacity (J kg^{-1} K^{-1}); ΔT = temperature difference (K); L_s = latent heat of vaporization (J kg^{-1}); w, water; s, steam.

On the other hand, the heat transferred to the reactor (Q_2) was quantified considering the contributions of steam supplied to the reactor jacket in the pretreatment according to Equation (5):

$$Q_2 = -\left(m_{condens} * L_s\right) + \left(m_{steam} * C_p * \Delta T\right)_s \tag{5}$$

where Q_2 = heat transferred to the reactor (J); $m_{condens}$ = mass of condensed steam at the jacket outlet (kg); L_s = latent heat of vaporization (J kg^{-1}); m_{steam} = steam mass supplied to the jacket (kg); C_p = heat capacity (J kg^{-1} K^{-1}); ΔT = temperature difference (K); s, steam.

So, the macroscopic energy efficiency was calculated as the ratio of the heat used by the system (Q_1) and the heat transferred toward it (Q_2), according to Equation (6):

$$\eta_{macro} = \left|\frac{Q_1}{Q_2}\right| * 100 \tag{6}$$

3.3. Microscopic energy balance

In the microscopic balance, the heat lost through the non-insulated reactor lid was calculated. In that way, the (real) energy efficiency of the reactor was also determined. That analysis was performed using an approximation for the composite walls and a calculation of the convection coefficients of the reactor's interior and exterior.

The considerations of the microscopic balance were as follows:

1. Heat transfer by conduction and convection
2. Steady-state conditions of the process, where the heat flow is proportional to the area measured normal to the direction of heat flow.
3. Reactor geometry as a cylinder, which can be approximated to a vertical plate, if and only if the condition of Equation (7) is satisfied so that vertical plate ratios can be used [35].

$$D \geq \frac{35 L_c}{Gr_L^{1/4}} \tag{7}$$

where D = reactor diameter (m); L_c = characteristic length of the reactor (m); Gr_L = Grashof number.

4. The temperature difference between the reactor and the steam from the boiler causes an increase or decrease in steam density, which gives rise to buoyancy, and thus natural convection is assumed [35].

The resolution of the balance between the jacket, where the steam circulates, and the interior and the exterior of the reactor was formulated as a problem of composite walls and their analogy with thermal resistances as described below.

The system was checked for satisfying the condition of Equation (7) by calculating Gr_L for the jacket, the interior, and the exterior of the reactor (Equation (8)). This proved that the cylinder diameter was large enough to minimize the effects of curvature and thus permit the approximation of the pretreatment reactor as a vertical plate.

$$Gr_L = \frac{g*\beta(T_s - T_\infty)*L_c^3}{v^2} \tag{8}$$

where g = gravitational acceleration (m s^{-2}); β = volumetric expansion coefficient (K^{-1}) for ideal gases $\beta = T^{-1}$; T_s = surface temperature (K); T_∞ = temperature of the fluid far enough from the surface (K); L_c = characteristic length (m); v^2 = kinematic viscosity (m^2 s^{-1}).

The approximation of reactor walls as composite plates and their analogy to thermal resistances are shown in Fig. 1a, which also exhibits the internal wall of the reactor (**A**), the jacket space (**B**), the mineral wool insulation (**C**), the external wall of the reactor (**D**), temperatures (T_i), conduction coefficients (k_i), convection coefficients (h_i), and thicknesses of the plates (δ_i). Fig. 1b displays the plot of thermal resistances for reactor walls. Table 1S (supplementary material) shows the thickness and thermal conductivity data of the reactor walls (Fig. 1b).

The heat transfer mechanisms prevailing in the reactor are conduction and convection. Based on Fourier's law, the conduction heat is represented by Equation (9):

$$\dot{Q}_{conduction} = -kA\frac{dT}{dx} \tag{9}$$

The temperature through the wall varies linearly with respect to position x, so by separating and integrating the variables, we obtain Equation (10):

$$\dot{Q}_{conduction} = -kA\frac{(T_2 - T_1)}{L} \tag{10}$$

where $\dot{Q}_{conduction}$ = heat transferred by conduction (W); k = thermal conductivity (W m^{-1} K^{-1}); A = heat transfer area (m^2); L = wall thickness (m).

On the other hand, heat transfer by convection is expressed using Newton's law of cooling (Equation (11)):

$$\dot{Q}_{convection} = hA_s(T_s - T_\infty) \tag{11}$$

where $\dot{Q}_{convection}$ = heat transferred by convection (W); h = coefficient of heat transfer by convection (W m^{-2} K^{-1}); A_s = surface area (m^2); T_s = surface temperature (K); T_∞ = temperature of the fluid far enough from the surface (K).

Drawing the analogy between thermal resistances and the mechanisms of heat transfer by conduction and convection, Equations (12) and (13) were formulated.

$$\dot{Q}_{conduction} = \frac{T_1 - T_2}{R_{wall}} \tag{12}$$

$$\dot{Q}_{convection} = \frac{T_6 - T_\infty}{R_{convection}} \tag{13}$$

where $R_{wall} = \delta k^{-1}A^{-1}$, conduction resistance of the wall (K W^{-1}); $R_{convection} = h^{-1}A_s^{-1}$, resistance by convection (K W^{-1}).

Heat losses are considered to take place from the reactor jacket toward the exterior and are expressed by Equation (14):

$$Q_{loss} = \frac{T_J - T_{\infty 2}}{\frac{1}{h_{jacket}} + \frac{\delta_3}{k_2} + \frac{\delta_4}{k_3} + \frac{\delta_5}{k_4} + \frac{1}{h_{air}}} \tag{14}$$

Since the heat transfer is constant, the lost heat can also be expressed by Equation (15):

$$Q_{loss} = h_{air}(T_6 - T_{\infty 2}) \tag{15}$$

where Q_{loss} is the heat flux lost through the reactor walls (W m^{-2}); h_{air} is the convection coefficient of air (W m^{-2} K^{-1}); T_6 is the exterior temperature of the reactor (K); and $T_{\infty 2}$ is the environmental temperature (K).

On the other hand, heat losses due to the reactor lid were determined using Equation (16):

$$Q_{loss-lid} = h_{reactor}(T_1 - T_{\infty 1}) \tag{16}$$

where $Q_{loss-lid}$ is the heat flux lost through the lid (W m^{-2}); $h_{reactor}$ is the convection coefficient of the reactor interior (W m^{-2} K^{-1}); T_1 is the temperature of the rector internal wall (K); and $T_{\infty 1}$ is the temperature of the reactor interior (K).

Analogously, the heat transferred from the jacket toward the interior of the reactor is expressed through Equations (17) and (18):

$$Q_{transf} = h_{jacket}(T_v - T_2) \tag{17}$$

$$Q_{transf} = h_{reactor}(T_1 - T_{\infty 1}) \tag{18}$$

where Q_{transf} is the heat flux transferred to the reactor.

Once Equations (17) and (18) were calculated, the efficiency was determined on the basis of the microscopic balance as expressed in Equation (19):

$$\eta_{micro} = \frac{Q_{transf} - Q_{loss-lid}}{Q_{transf} + Q_{loss}} \tag{19}$$

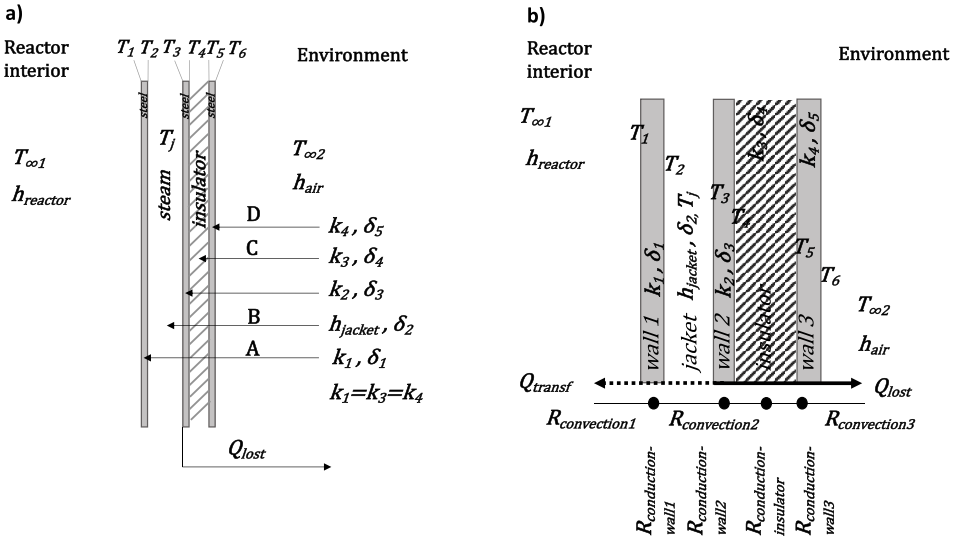

Fig. 1. a) Composite walls approximation of the reactor; b) Diagram of thermal resistances in the reactor.

The microscopic balance was solved by taking into account the heat used by the reactor (Q_1) and the heat transferred toward the reactor (Q_2) as well as Q_{loss}, which served to calculate the convection coefficient of air (h_{air}). However, the transferred heat (Q_2) was used to obtain the convection coefficient of the jacket (h_{jacket}) and the convection coefficient of the reactor interior ($h_{reactor}$). The heat lost through the reactor lid was achieved using Equation (16), which allowed calculating the energy efficiency at a microscopic level (Equation (19)).

4. Results and discussion

4.1. Agave bagasse composition

The biomass analyses demonstrated that the initial composition (w/w) was 46% ± 1 cellulose, 23.1% ± 1 hemicellulose, 15.24% ± 1 lignin, 6.84% ± 1.37 total extractives, 4.31% ± 1.15 humidity, and 2.94% ± 1.18 ash. This composition is similar to that reported by other authors with a variation of 4–6% [36,37]. These differences can be attributed to the composition of agave bagasse affected by environmental and nutritional factors during its growth, which changes depending on the region and harvest year, as well as by the conditions under which the tequila making process was carried out [38].

4.2. Characterization of hydrolysates

The quantification of COD and TC of hydrolysates, after each pretreatment performed, as a function of temperature and time of pretreatment are shown in Fig. 2a and b. The observed behavior indicates that the increase in temperature and time of pretreatment favors higher solubility of the organic matter, which increases the TCs and COD in the hydrolysates until reaching a maximum point (Fig. 2a and b) indicating the solubilization of hemicellulose, as reported for the range of temperatures used in this study [18,39–41]. The COD values obtained at 116 °C increased 2 and 3 times for temperatures of pretreatment at 142 °C and 154 °C, respectively. The increment in time of pretreatment also resulted in an increment of COD concentration until reaching a maximum between 15 and 20 min at lower temperatures (116–142 °C) and around 15 min at higher temperatures (146–154 °C) (Fig. 2a). From that point on, the effects are negative, possibly because carbohydrates are degraded to undesirable products due to the combined effect of temperature and time (severity factor) as will be discussed further below. The TC concentration has a similar behavior; it increased as a function of temperature and reached a maximum at around 15 min of treatment (Fig. 2b).

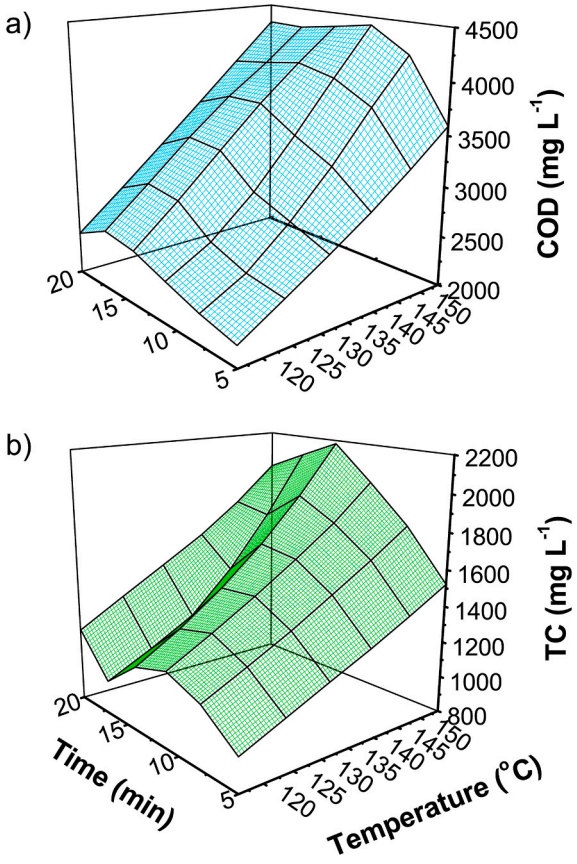

Fig. 2. Hydrolysate concentration of a) COD; b) TC as a function of temperature and time of treatment.

The effect of temperature and time of pretreatment (correlated by severity factor Log Ro) indicated an increase in COD and TCs, as is shown in Fig. 3. The maximum concentrations of COD (4395.71 ± 22.44 mg L^{-1}), glucose (66 ± 4 mg L^{-1}), arabinose (160.31 ± 3.2 mg L^{-1}) were obtained in hydrolysates at 154 °C and 10 min (Log Ro = 2.59) while the overall yield expressed as grams of TC g^{-1} of biomass was 7%. This result is important from the energy point of view because the highest concentrations did not require the most severe conditions. However, it is also important to mention that arabinose was only solubilized at conditions of Log Ro > 2.59. This behavior was correlated with the decrease in the pH of the medium, as can be seen in Fig. 4. This was a result of xylan deacetylation to form acetic acid after being depolymerized. However, this also favors the degradation of carbohydrates, as could be seen at more severe pretreatment conditions [10].

Furthermore, the maximum concentrations of TC (2177.99 ± 197.22 mg L^{-1}) and xylose (43 ± 2.8 mg L^{-1}) were achieved at Log Ro = 2.77 (154 °C and 15 min), Fig. 3. Under such conditions, the overall yield expressed as grams of TC g^{-1} of biomass was 8%, the highest yield obtained in uncatalyzed pretreatments; whereas, the highest yield of grams TC g^{-1} of biomass for catalyzed pretreatments was 19%. Based on the statistical tests carried out, it was concluded that TC concentrations in hydrolysates at 154 °C for 10 min (Log Ro = 2.59) are not significantly different (P = 0.005) from pretreatments at the same temperature but with longer testing times.

Another study reported that 0.24 g of glucose per gram of agave bagasse was obtained from hydrolysates resulting from a pretreatment by steam explosion and subsequent enzymatic hydrolysis, using agave bagasse at 180 °C, 0.67 MPa and 30 min. This higher amount of glucose obtained can be attributed to enzymatic hydrolysis [42]. For xylose, however, the authors report 2.9 mg of xylose per gram of bagasse, while in our study 4.94 mg of xylose per gram of bagasse were obtained. Still

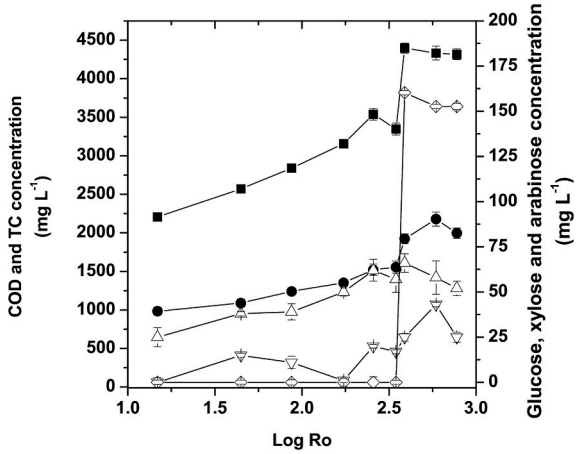

Fig. 3. Concentration of COD (■), TC (●), glucose (△), xylose (▽), and arabinose (◇) as a function of severity factor.

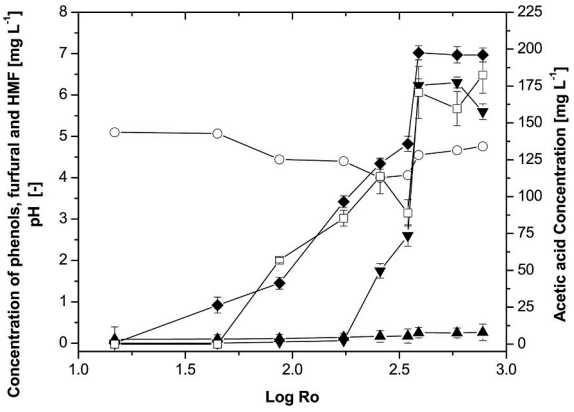

Fig. 4. Concentration of phenols (▲), furfural (▼), hydroxymethylfurfural (◆), acetic acid (□), and pH (○) in hydrolysates as a function of severity factor.

another study indicated a xylose concentration of 4.69 g L^{-1} in hydrolysates of agave bagasse pretreated by steam explosion at 180 °C for 50 min; so, the energy requirements should be considered to evaluate the feasibility of this study [38].

As mentioned earlier, the pretreatment conditions (temperature and time of reaction) used in this study were selected to minimize the formation of potential inhibitors. In this regard, the presence of inhibitors exhibited a linear ascending behavior with respect to the increase in severity factor (Fig. 4). This was the case for the concentration of phenols that increased from 0.093 to 0.26 mg L^{-1}, whereas furfural went up from 0.03 to 6.3 mg L^{-1} and HMF from 0.92 to 7 mg L^{-1}. Finally, the concentration of acetic acid increased from 56.89 to 182.4 mg L^{-1} in all cases within the range of Log Ro tested (1.17–2.89). The maximum concentrations of the abovementioned inhibitors were obtained for the most severe pretreatments (Log R_0 > 2.59) where the pH value was 4.5. On this matter, no generation of furfural in agave bagasse hydrolysates was reported at temperatures between 140 and 160 °C when using a pretreatment by steam explosion, which is consistent with the data obtained herein [10]. The inhibition of methanogenic microorganisms at acetic acid concentrations above 1619.47 mg L^{-1} has been reported [43]. So, the concentration of acetic acid present in hydrolysates in this work would not represent problems for anaerobic digestion. For phenols, concentrations above 1.2 g L^{-1} have been reported to inhibit anaerobic digestion [44]. In this study, the concentrations of phenols present in uncatalyzed pretreatments did not represent inhibition problems.

4.3. Pretreatments catalyzed with a dilute acid

Based on the previous results, pretreatments catalyzed with H_2SO_4 were carried out for the conditions of 154 °C for 5 and 10 min, and their results are shown in Table 2.

TC concentrations present in the pretreatments with acid were 3-fold higher; whereas those of glucose and xylose were 2.7 and 100 times greater, respectively, as compared to the uncatalyzed pretreatment at 154 °C for 10 min. This fact indicated that the addition of sulfuric acid as a catalyst for the pretreatment had positive effects on increasing the compounds of interest. However, concentrations of acetic acid, furfural, and HMF increased as well. The concentration of acetic acid (6087 mg L^{-1}) generated in the catalyzed pretreatment would inhibit the process of anaerobic digestion according to the data reported [43]. On the other hand, the conditions of acid hydrolysis and methane production by anaerobic digestion, using agave bagasse as a substrate, have been evaluated [45]. The evaluation included the step of HMF elimination because even though its concentration did not inhibit the process, the synergistic effect between HMF and other inhibitors has been reported.

Table 2
Concentration of carbohydrates and inhibitors in pretreatments catalyzed by H_2SO_4 (2% v/v).

	CSF = 1.44 (154 °C 5 min)	CSF = 1.68 (154 °C 10 min)
pH	0.85 ± 0.1	0.91 ± 0.1
COD (mg L^{-1})	5101.9 ± 325	4990.8 ± 168
TC (mg L^{-1})	6262.7 ± 108	5943.2 ± 115
Glucose (mg L^{-1})	169 ± 10	180 ± 8
Xylose (mg L^{-1})	3227	2529
Phenols (mg L^{-1})	NA	NA
Furfural (mg L^{-1})	468	749
Hydroxymethylfurfural (mg L^{-1})	82	129
Acetic acid (mg L^{-1})	6087	4409

CSF- combined severity factor.

An inhibiting effect on biogas production at low furfural concentrations (>1 g of furfural L^{-1}) and a stimulating effect at high furfural concentrations have been reported [9]. The maximum concentration of furfural obtained in this study was 749 mg L^{-1} (Table 2); so, accordingly, there would be inhibition [9]. For this reason, in the catalyzed pretreatment by steam explosion, it is necessary to either evaluate the concentrations of the compounds of interest and the inhibitors as well as their possible effects on the subsequent processes for biofuel production or for implementing strategies of chemical, physical, or biological detoxification.

4.4. BMP

For BMP evaluation the hydrolysates pretreated at 154 °C and 10 min (Log Ro = 2.59) were used; the values of pH, COD, and TC were 3.20 ± 0.2, 9875 ± 88 mg L^{-1}, and 4499 ± 35 mg L^{-1}, respectively. The COD yield was 0.135 g COD g^{-1} dry biomass, which was comparable to 0.138 g COD g^{-1} dry biomass obtained in the set of experiments discussed above. This hydrolysate was selected since no significant differences in TC were observed using the same temperature and different times of pretreatment.

The results of the BMP test indicated a COD consumption of 63.59% ± 0.5 and a value of 215.24 ± 15.88 mL of CH_4 produced per g of COD added. The latter data are comparable with the value of 290 mL CH_4 g^{-1} of COD reported for *A. tequilana* Weber bagasse pretreated by steam explosion [46]. However, it should be taken into consideration that the pressure and time of reaction used in that study were 1.6-fold and 2.2-fold greater than in this work. The BMP value obtained is also comparable to those obtained by acid and enzymatic hydrolysis [45,47,48]. On the other hand, the BMP of the hydrolysates from the pretreatment at the most severe conditions studied (Log Ro = 2.89) was 167.27 ± 7.3 CH_4 g^{-1} COD added [49]. This indicates again that the most severe condition was not the most favorable one. Furthermore, since the BMP tests indicated the digestibility of the hydrolysates under controlled and favorable conditions, an increase in COD concentration in hydrolysates or BMP value does not necessarily imply an increase in methane production in anaerobic digesters where operational conditions and inoculum specialization play a major role [9,48]. Likewise, it is important to analyze the energy expenditure necessary to obtain these values of COD, and thus set it against the energy that can be obtained from those hydrolysates, as discussed in the next section where the obtained values were used to calculate the corresponding energy balances.

4.5. Energy by conversion to methane

On the basis of the best experimental results, the Log Ro pretreatment of 2.59 (154 °C during 10 min) was used as a reference. Taking into consideration the volume of the recovered hydrolysate, the concentration of COD, and its BMP, it was calculated that 1657 mL of methane (30127 mL of methane kg^{-1} of dry biomass) could be obtained from the

whole hydrolysate batch. While the calorific power of hydrolysates was calculated considering the ICP of methane (34.02 MJ m^{-3}) and the volume of methane obtained in the BMP test. It was determined that the batch of hydrolysates could produce 56381 J. Likewise, it was calculated that the Log Ro pretreatment of 2.89 (154 °C during 20 min) could provide 1223 mL of methane, meaning that 41606 J could be produced from that batch of hydrolysates. These results confirmed the observation that less severe conditions could result in higher energy production. Further, in a study in which straw was pretreated by steam explosion, an 11% higher BMP was reported at 140 °C compared to other pretreatments at 160 °C and 178 °C [19].

4.6. Energy consumed during the pretreatment by steam explosion

The results regarding the characterization of the boiler in terms of gas consumption, the time required to bring the temperature from 0 to 154 °C, and reactor operating costs are shown in Table 2S of the supplementary material. The quantification of LPG consumption in the boiler indicated a linear behavior (Fig. 1S, supplementary material), resulting in a gas consumption rate of 0.052 L min^{-1}. The analysis of the time needed to reach the operating temperature showed that 42% of the time was employed to reach 0.13 MPa and 58% of the time to achieve the operating pressure of 0.67 MPa. The gas consumption necessary to reach the working pressure and the one needed for pretreatment duration were recorded as well. Based on the above data, it was concluded that the time necessary to reach the working pressure has a greater impact on gas consumption than the pretreatment duration. The quantification of LP gas consumption allowed us to calculate the energy invested in the pretreatment and contrast it with the energy produced by the BMP test. This resulted in an energetically positive balance since 56381 J can be recovered from methane, which is 247% of the energy invested in the time of pretreatment. It is important to point out that this result only considers the energy used in the pretreatment to obtain the hydrolysates, as discussed in the next section.

4.7. The overall energy yield of the process

The calculation of density and ICP of LPG (42% butane and 58% propane) resulted in 2.304 kg m^{-3} and 46.103 MJ kg^{-1}, respectively. The gas consumption for the reference pretreatment (Log Ro = 2.59) was 0.215 L (22837.6 J), and the pretreatment energy efficiency obtained by Equation (3) was 247%, considering the energy obtained from conversion to methane calculated in section 4.5. Meanwhile, the gas consumption for pretreatment Log Ro of 2.89 was 0.197 L (20926 J), thereby resulting in pretreatment energy efficiency (Equation (3)) of 199%. It is therefore concluded that more severe conditions of pretreatment resulted in a detriment to the energy efficiency in the process.

On the other hand, the energy obtained by methane produced in this study corresponded to only 10.73 and 6.26% of the energy reported for combustion of raw and pyrolyzed agave bagasse (9.55 and 16.35 and kJ g^{-1}, respectively) [50,51]. Indicating that despite the positive energy balance of the process, the low solubilization yield obtained needs to be improved, and the carbohydrates remaining in the solid fraction should also be utilized since they are more available after the pretreatment. The overall yield of the solid fraction was 0.669 g TC g^{-1} dry biomass.

4.8. Macroscopic energy balance

This analysis determined the energy efficiency in the reactor by calculating the heat supplied toward the reactor for the reference pretreatment and the heat used in the reactor. For that pretreatment, the steam temperature (T_j) measured was 163 °C, whereas the temperature of the reactor interior ($T_{\infty 1}$) was 154 °C (Fig. 1). These temperatures were used to calculate the energy efficiency at the macroscopic and microscopic levels.

The heat consumed by the reactor (Q_1) involved the heat due to the change of temperature (the first and third term of Equation (4)) and the change of state of aggregation (the latent heat of vaporization, the second term of Equation (4)). On the other hand, the volume of steam transferred through the jacket during pretreatment was quantified by condensation from the volume of water recovered. Also, the heat supplied to the reactor (Q_2), which considered the latent heat of condensation (the first term of Equation (5)) and the heat due to the change of temperature (the second term of Equation (5)), was determined. These data were used to calculate the energy efficiency in the reactor by Equation (3).

Equation (4) was also used to calculate Q_1 of 2400 kJ, which took into consideration the temperature range from 17 °C to 154 °C, the density of saturated water, the volume of water used for pretreatment, and the latent heat of vaporization (L_s) at 154 °C as well as water properties in the vapor state (at an average temperature of 159 °C). Finally, the heat used by the system during the 10 min of treatment resulted in 4 kW.

On the other hand, Q_2 was calculated by quantifying the volume of vapor condensed at experimental conditions (0.0025 m^3) and considering the density at ambient temperature in the liquid state, the latent heat of vaporization, and steam properties at an average temperature of 132 °C. Thus, the heat consumed by the system during the 10 min of treatment was – 4.4 kW (Equation (5)).

Finally, the macroscopic energy efficiency in the reactor was calculated by Equation (6), revealing that 90.9% of the heat transferred to the reactor was used, and 9.1% of the heat was lost or dissipated to the surroundings through the reactor walls. However, the heat losses through the (non-insulated) lid were not considered; so, a more thorough analysis will be done in the following section, taking into account these losses as well.

4.9. Microscopic energy balance

The average environmental temperature in Cuajimalpa, Mexico City, in June 2018 (when the experiments were carried out) was 18 ± 0.47 °C ($T_{\infty 2}$), which was therefore taken as the environmental temperature. However, as was already mentioned, at 0.67 Mpa, the temperature in the interior of the reactor ($T_{\infty 1}$) was 154 °C, and steam temperature in the jacket (T_j) was 163 °C.

The results of the diameter condition (Equation (7)) are shown in Table 3.

Additionally, this condition was checked for each reactor section considering the temperatures in the reactor interior, exterior, and jacket to calculate the Grashof number, which allowed us to calculate the dissipated heat during the pretreatment (10 min) from the macroscopic balance, which resulted in 0.4 KW. So, to obtain the heat flux, the areas corresponding to Q_{loss}, $Q_{loss-lid}$, and Q_{transf} of 0.42, 0.042, and 0.223 m^2, respectively, were considered. Therefore, the flux of $Q_2 - Q_{transf}$ was 19739.94 W m^{-2}, and that of Q_{loss} was 952.38 W m^{-2}.

Equation (15) was used to calculate the air convection coefficient of 95.23 W m^{-2} K^{-1}, whereas the convection coefficient of the jacket (h_{jacket}) of 2192.32 W $m^{-2}K^{-1}$ was determined by Equation (17) and the convection coefficient of reactor interior ($h_{reactor}$) of 29101.68 W m^{-2} K^{-1} by Equation (18). Thence, the $Q_{loss-lid}$ was 828.69 W m^{-2} (Equation (16)). Lastly, this value allowed recalculating the heat transfer efficiency

Table 3
Diameter condition for vertical plate approximation of the reactor (Equation (7)).

	$D \geq \frac{35L_c}{Gr_L^{1/4}}$ [m]
Reactor interior	0.219 ≥ 0.0477
Jacket	0.264 ≥ 0.0383
Reactor exterior	0.273 ≥ 0.1378

in the reactor of 74% (Equation (19)).

Energy balances indicate that if the losses due to the lid are taken into account, the efficiency decreases from 90% to 74%. That is, the heat lost through the lid is equivalent to 16% of the heat transferred to the reactor, which shows that the lid should be insulated to increase energy efficiency.

Furthermore, most of the studies on steam explosion focus on optimizing the carbohydrate extraction, and little information on the energy balance is provided [41]. Energy balances are relevant to assess the feasibility and sustainability of the process. This feedstock also has the opportunity to be integrated into the tequila production process since steam is already used in the cooking, distillation, and rectification (second distillation) stages. Furthermore, considering that the estimated annual consumption of fossil energy is 2800 TJ and 110 GWh for the whole *Agave* culture-tequila productive chain, this integration could improve the energy efficiency and contribute to the sustainability goal proposed by the sector of reducing 25% of the CO_2 emissions (3 kg CO_2 eq per liter of tequila) by 2030 [52].

5. Conclusions

The concentrations of COD and structural carbohydrates increased in the hydrolysates as the severity of pretreatment increased up to a maximum indicating the solubilization of the hemicellulose fraction and its degradation under most severe conditions (Log Ro = 2.89). The maximum concentrations of COD, glucose, and arabinose were obtained in the hydrolysates pretreated at 154 °C and 10-min (Log Ro = 2.59). At the same temperature (154 °C) with a longer time of pretreatment (15 min) corresponding to a Log Ro of 2.77, the maximum concentrations of TC and xylose were achieved. The range of inhibitors (phenols, furfural, HMF and acetic acid) concentrations quantified in the hydrolysates has not been reported as toxic in the literature. On the other hand, the pretreatment catalyzed with H_2SO_4 at 154 °C and 10-min resulted in TC, glucose, and xylose concentrations that were 3, 2.7, and 100- times higher, respectively, as compared to the uncatalyzed pretreatment. However, the concentrations of potential inhibitor compounds increased as well, 26, 120 and 18 times, respectively. Furthermore, the normalized BMP value achieved (215.24 NmL g^{-1} of COD added) was comparable to the values reported in other research that used higher pressures and longer reaction times than those employed in this study.

The energy balance of the process proved to be feasible (247%) even with heat losses of 16% resulting from the non-insulated reactor lid and the low glucose and xylose recovery obtained. This result indicates the importance of insulation in this type of process for its industrial application. Thus, the use of agave bagasse as a raw material for biofuel production is promising, but further studies in anaerobic digestors are needed to assess its potential. Furthermore, the implementation of methane production including a steam explosion pretreatment in the tequila industry might be feasible, considering that current tequila production schemes already use steam at the conditions suggested in this study for the cooking, distillation, and rectification stages of production, which could enhance the energy efficiency of both processes. Finally, there are many reports on biomass treatment by steam explosion, but only a few deals with energy balance; hence, the relevance of this study that included micro and macro energy balances.

Funding

This work was financed by the Mexican Department of Energy (SENER) through Gaseous Biofuels Cluster Project 247006.

Individual author contributions

A Hernández carried out the research, analyzed the data, prepared the visuals, and wrote the first draft.

S Hernández supervised the pretreatment experimentation and energy balance calculations.

I Ortíz did the conceptualization, supervised the research, analyzed the data, and wrote the final draft.

Acknowledgments

The Mexican Council of Science and Technology (CONACYT) is acknowledged for the national Master's study scholarship No. 798752.

Appendix A. Supplementary data

Supplementary data to this article can be found online at https://doi.org/10.1016/j.biombioe.2020.105753.

References

[1] X. Han, Y. Guo, X. Liu, Q. Xia, Y. Wang, Catalytic conversion of lignocellulosic biomass into hydrocarbons: a mini review, Catal. Today 319 (2018) 2–13, https://doi.org/10.1016/j.cattod.2018.05.013.
[2] I. Ortíz, R. Quintero, V.K. Gupta, C.P. Kubicek, J. Saddler, F. Xu, in: M. G (Ed.), Bioenergy Research: Advances and Applications, Elsevier, London, 2014, p. 57.
[3] P. Bajpai, Pretreatment of Lignocellulosic Biomass for Biofuel Production, 1rd. ed., Springer Singapore, 2016.
[4] Data. FAOSTAT. Food and Agricultural. http://www.fao.org/faostat/en/#data.
[5] S.C. Davis, F.G. Dohleman, S.P. Long, The global potential for Agave as a biofuel feedstock, Global Change Biol. 3 (2011) 68–78, https://doi.org/10.1111/j.1757-1707.2010.01077.x.
[6] Y. González García, O. González Reynoso, J. Nungaray Arellano, Potential del bagazo de Agave tequilero para la producción de biopolímeros y carbohidrasas por bacterias celulolíticas y para la obtención de compuestos fenólicos, e-Gnosis. 3 (2005) 1–18. Available at: https://www.redalyc.org/articulo.oa?id=73000314.
[7] CRT, Consejo Regulator del Tequila, Información Estadística, revised in, December 2018. Available at: https://www.crt.org.mx/EstadisticasCRTweb/.
[8] V. Montiel Corona, E. Razo-Flores, Continuous hydrogen and methane production from Agave tequilana bagasse hydrolysate by sequential process to maximize energy recovery efficiency, Bioresour. Technol. 249 (2018) 334–341, https://doi.org/10.1016/j.biortech.2017.10.032.
[9] G. Buitrón, A. Hernández-Juárez, M.D. Hernández-Ramírez, A. Sánchez, Biochemical methane potential from lignocellulosic wastes hydrothermally pretreated, Ind. Crop. Prod. 139 (2019) 1–7, https://doi.org/10.1016/j.indcrop.2019.111555.
[10] L.J. Rios-González, T.K. Morales-Martínez, M.F. Rodríguez-Flores, J.A. Rodríguez-De la Garza, D. Castillo-Quiroz, A.J. Castro-Montoya, A. Martinez, Autohydrolysis pretreatment assessment in ethanol production from agave bagasse, Bioresour. Technol. 242 (2017) 184–190, https://doi.org/10.1016/j.biortech.2017.03.039.
[11] M.A. Kabel, G. Bos, J. Zeevalking, A.G.J. Voragen, H.A. Schols, Effect of pretreatment severity on xylan solubility and enzymatic breakdown of the remaining cellulose from wheat straw, Bioresour. Technol. 98 (2007) 2034–2042, https://doi.org/10.1016/j.biortech.2006.08.006.
[12] J. Singh, M. Suhag, A. Dhaka, Augmented digestion of lignocellulose by steam explosion, acid and alkaline pretreatment methods: a review, Carbohydr. Polym. 117 (2015) 624–631, https://doi.org/10.1016/j.carbpol.2014.10.012.
[13] E. Ruiz, C. Cara, P. Manzanares, M. Ballesteros, E. Castro, Evaluation of steam explosion pre-treatment for enzymatic hydrolysis of sunflower stalks, Enzym. Microb. Technol. 42 (2008) 160–166, https://doi.org/10.1016/j.enzmictec.2007.09.002.
[14] M. Ballesteros, J.M. Oliva, M.J. Negro, P. Manzanares, I. Ballesteros, Ethanol from lignocellulosic materials by a simultaneous saccharification and fermentation process (SFS) with Kluyveromyces marxianus CECT 10875, Process Biochem. 39 (2004) 1843–1848, https://doi.org/10.1016/j.procbio.2003.09.011.
[15] X.F. Sun, F. Xu, R.C. Sun, Z.C. Geng, P. Fowler, M.S. Baird, Characteristics of degraded hemicellulosic polymers obtained from steam exploded wheat straw, Carbohydr. Polym. 60 (1) (2005) 15–26, https://doi.org/10.1016/j.carbpol.2004.11.012.
[16] H. Chen, L. Liu, X. Yang, Z. Li, New process of maize stalk amination treatment by steam explosion, Biomass Bioenergy 28 (4) (2005) 411–417, https://doi.org/10.1016/j.biombioe.2004.06.010.
[17] B. Ch Schumacher, H.E. Oechsner, T. Senn, T.U. Jungbluth, Thermo-mechanical pre-treatment of ripe triticale for biogas production, Landtechnik 62 (2007) 162–163. http://www.landtechnik-net.com/gbindex.htm.
[18] A. Bauer, P. Bösch, A. Friedl, T. Amon, Analysis of methane potentials of steam exploded wheat Straw and estimation of energy yields of combined ethanol and methane production, J. Biotechnol. 142 (2009) 50–55, https://doi.org/10.1016/j.jbiotec.2009.01.017.
[19] F. Theuretzbacher, J. Lizasoain, Ch Lefever, M.K. Saylor, R. Enguidanos, N. Weran, A. Gronauer, A. Bauer, Steam explosion pretreatment of wheat straw to improve methane yields: investigation of the degradation kinetics of structural compounds during anaerobic digestión, Bioresour. Technol. 179 (2015) 299–305, https://doi.org/10.1016/j.biortech.2014.12.008.

[20] F. Kobayashi, H. Take, Ch Asada, Y. Nakamura, Methane production from steam-exploded bamboo, J. Biosci. Bioeng. 97 (6) (2004) 426–428, https://doi.org/10.1016/S1389-1723(04)70231-5.
[21] A. Petersson, M.H. Thomsen, H. Hauggaard-Nielsen, A.B. Thomsen, Potential bioethanol and biogas production using lignocellulosic biomass from winter rye, oilseed rape and faba bean, Biomass Bioenergy 31 (2007) 812–819, https://doi.org/10.1016/j.biombioe.2007.06.001.
[22] M. Galde, G. Zacchi, in: T. Scheper (Ed.), Advances in Biochemical Engineering/Biotechnology, Springer, Berlin, 2007, p. 41.
[23] A. Sluiter, B. Hames, D. Hyman, C. Payne, R. Ruiz, C. Scarlata, J. Sluiter, D. Templeton, J. Wolfe, Determination of Total Solids in Biomass and Total Dissolved Solids in Liquid Process Samples, Revised, NREL, Golden, Colorado, March 2008. Available at: https://www.nrel.gov/docs/gen/fy08/42621.pdf.
[24] A. Sluiter, B. Hames, R. Ruiz, C. Scarlata, J. Sluiter, D. Templeton, Determination of ash in biomass, NREL, Golden, Colorado, Revised, Available at: https://www.nrel.gov/docs/gen/fy08/42622.pdf, January 2008.
[25] A. Sluiter, R. Ruiz, C. Scarlata, J. Sluiter, D. Templeton, Determination of Extractives in Biomass, National Renewable Energy Laboratory, Golden, Colorado, 2008. Available at: https://www.nrel.gov/docs/gen/fy08/42619.pdf.
[26] A. Sluiter, B. Hames, R. Ruiz, C. Scarlata, J. Sluiter, D. Templeton, D. Crocker, Determination of Structural Carbohydrates and Lignin in Biomass, Revised, NREL, Golden, Colorado, August 2012. Available at: https://www.nrel.gov/docs/gen/fy13/42618.pdf.
[27] Hach Company, Chemical oxygen demand, in: Water Analysis Manual, 2000, pp. 182–189.
[28] M. Dubois, K.A. Gilles, J.K. Hamilton, P.A. Rebers, F. Smith, Colorimetric method for determination of sugars and related substances, Anal. Chem. 28 (3) (1956) 350–356, https://doi.org/10.1021/ac60111a017.
[29] APHA, Standard Methods for the Examination of Water and Wastewater, eighteenth ed., American Public Health Association (APHA), American Water Works Association (AWWA) and Water Pollution Control Federation (WPCF), Washington DC, 1992.
[30] J. Singh, M. Suhag, A. Dhaka, Augmented digestion of lignocellulose by steam explosion, acid and alkaline pretreatment methods: a review, Carbohydr. Polym. 117 (2015) 624–631, https://doi.org/10.1016/j.carbpol.2014.10.012.
[31] R. Kataria, A. Mol, E. Schulten, A. Happel, S.I. Mussatto, Bench scale steam explosion pretreatment of acid impregnated elephant grass biomass and its impacts on biomass composition, structure and hydrolysis, Ind. Crop. Prod. 106 (2016) 48–58, https://doi.org/10.1016/j.indcrop.2016.08.050.
[32] K. Wang, J. Chen, Shao-NiSun, Run-CangSun, in: A. Pandei, S. Negi, P. Binod, C. Larroche (Eds.), Pretreatment of Biomass Processes and Technologies, Elsevier, Ámsterdam, 2015, p. 75.
[33] I. Angelidaki, W. Sanders, Assessment of the anaerobic biodegradability of macropollutants, 0, Rev. Environ. Sci. Biotechnol. 3 (2004) 117–129, https://doi.org/10.1007/s11157-004-2502-3.
[34] D.M. Mousdale, Chemistry, Biochemistry, and Microbiology of Lignocellulosic Biomass, CRC Press, Boca Raton, 2008.
[35] Y.A. Cengel, Transferencia de calor y masa, fourth ed., Mc Graw Hill, México, 2011.
[36] J. Saucedo-Luna, A.J. Castro-Montoya, J.L. Rico, J. Campos-García, Optimization of acid hydrolysis of bagasse from agave tequilana Weber, Revista Mexicana de Ingeniería Química 9 (2010) 91–97.
[37] M.A. Robles-García, C.L. Del-Toro-Sánchez, E. Márquez-Ríos, A. Barrera-Rodríguez, J. Aguilar, J.A. Aguilar, F.J. Reynoso-Marín, I. Ceja, R. Dórame-Miranda, F. Rodríguez-Félix, Nanofibers of cellulose bagasse from *Agave tequilana* Weber var. *azul* by electrospinning: preparation and characterization, Carbohydr. Polym. 192 (2018) 69–74, https://doi.org/10.1016/j.carbpol.2018.03.058.
[38] D.L. Aguilar, R.M. Rodríguez-Jasso, E. Zanuso, D. Jasso de Rodríguez, L. Amaya-Delgado, A. Sanchez, H. Ruiz, Scale-up and evaluation of hydrothermal pretreatment in isothermal and non-isothermal regimen for bioethanol production using agave bagasse, Bioresour. Technol. 263 (2018) 112–119, https://doi.org/10.1016/j.biortech.2018.04.100.
[39] P. Kumar, D.M. Barrett, M.J. Delwiche, P. Stroeve, Methods for pretreatment of lignocellulosic biomass for efficient hydrolysis and biofuel production, Ind. Eng. Chem. Res. 48 (8) (2009) 3713–3729, https://doi.org/10.1021/ie801542g.
[40] R.P. Chandra, R. Bura, W.E. Mabee, A. Berlin, X. Pan, J.N. Saddler, in: T. Scheper (Ed.), Advances in Biochemical Engineering/Biotechnology, Springer, Verlag Berlin Heidelberg, 2007, p. 67.
[41] K. Kucharska, P. Rybarczyk, I. Hołowacz, R. Łukajtis, M. Glinka, M. Kamiński, Pretreatment of lignocellulosic materials as substrates for fermentation processes, Molecules 23 (11) (2018) 2937, https://doi.org/10.3390/molecules23112937.
[42] J.A. Perez-Pimienta, C.A. Flores-Gómez, H.A. Ruiz, N. Sathitsuksanoh, V. Balan, L. Sousa, B.E. Dale, S. Singh, B. Simmons, Evaluation of agave bagasse recalcitrance using AFEX, autohydrolysis, Bioresour. Technol. 211 (2016) 216–223, https://doi.org/10.1016/j.biortech.2016.03.103.
[43] K.K. Xiao, C.H. Guo, Y. Zhou, Y. Maspolim, J.Y. Wang, W.J. Ng, Acetic acid inhibition on methanogens in a two-phase anaerobic process, Biochem. Eng. J. 75 (2013) 1–7, https://doi.org/10.1016/j.bej.2013.03.011.
[44] A. Barakat, F. Monlau, J.-P. Steyer, H. Carrere, Effect of lignin-derived and furan compounds found in lignocellulosic hydrolysates on biomethane production, Bioresour. Technol. 104 (2012) 90–99, https://doi.org/10.1016/j.biortech.2011.10.060.
[45] J. Arreola-Vargas, V. Ojeda-Castillo, R. Snell-Castro, R. Corona-González, F. Alatriste-Mondragón, H.O. Méndez-Acosta, Methane production from acid hydrolysates of Agave tequilana bagasse: evaluation of hydrolysis conditions and methane yield, Bioresour. Technol. 181 (2015) 191–199, https://doi.org/10.1016/j.biortech.2015.01.036.
[46] B. Weber, A. Estrada-Maya, A.C. Sandoval-Moctezuma, I.G. Martínez-Cien fuegos, Anaerobic digestion of extracts from steam exploded Agave tequilana bagasse, J. Environ. Manag. 245 (2019) 489–495, https://doi.org/10.1016/j.jenvman.2019.05.093.
[47] J. Arreola-Vargas, A. Flores-Larios, V. González-Álvarez, R.I. Corona-González, H. O. Méndez-Acosta, Single and two-stage anaerobic digestion for hydrogen and methane production from acid and enzymatic hydrolysates of Agave tequilana bagasse, Int. J. Hydrogen Energy 41 (2) (2016) 897–904, https://doi.org/10.1016/j.ijhydene.2015.11.016.
[48] L. Breton-Deval, H.O. Méndez-Acosta, V. González-Álvarez, R. Snell-Castro, D. Gutiérrez-Sánchez, J. Arreola-Vargas, Agave tequilana bagasse for methane production in batch and sequencing batch reactors: acid catalyst effect, batch optimization and stability of the semi-continuous process, J. Environ. Manag. 224 (2018) 156–163, https://doi.org/10.1016/j.jenvman.2018.07.053.
[49] I. Valdez-Vazquez, F. Alatriste-Mondragón, J. Arreola-Vargas, G. Buitrón, J. Carrillo-Reyes, E. León-Becerril, H.O. Mendez-Acosta, I. Ortíz, B. Weber, A comparison of biological, enzymatic, chemical and hydrothermal pretreatments for producing biomethane from Agave bagasse, Ind. Crop. Prod. 145 (2020), https://doi.org/10.1016/j.indcrop.2020.112160.
[50] L. Chávez-Guerrero, Uso de bagazo de la industria mezcalera como materia prima para generar energía, Ingenierias 13 (2010), 1405-0676. Available at: http://eprints.uanl.mx/10432/1/47_Uso_de_bagazo.pdf.
[51] A. Liñán-Montes, S. Parra-Arciniega, M. Garza-González, R. García-Reyes, E. Soto-Regalado, F. Cerino-Córdova, Characterization and thermal analysis of agave bagasse and malt spent grain, J. Therm. Anal. Calorim. 115 (1) (2014), https://doi.org/10.1007/s10973-013-3321-y.
[52] CMO. Centro Mario Molina, Sustainability strategy for the 2016 agave-tequila production chain. Available at: http://centromariomolina.org/english2/wp-content/uploads/2016/12/Estrategia-de-Sustentabilidad-2016-eng.pdf.

Nomenclature

β: Dilatation coefficient [K^{-1}]
δ_i: Thickness [m]
ΔT: Temperature difference [K]
$\eta_{overall}$: Overall process efficiency [%]
η_{micro}: Microscopic reactor energy efficiency [%]
η_{macro}: Macroscopic reactor energy efficiency [%]
v^2: Kinematic viscosity [$m^2\ s^{-1}$]
A: Area [m^2]
A_s: Surface area [m^2]
C_p: Heat capacity [$J\ kg^{-1}K^{-1}$]
CS: combined severity factor
D: Diameter of the reactor [m]
g: Gravity force [$m\ s^{-2}$]
Gr_L: Grashof Number, [dimensionless]
h: Convective coefficient [$W\ m^{-2}\ K^{-1}$]
h_{air}: Convective coefficient of the air [$W\ m^{-2}K^{-1}$]
h_{jacket}: Convective coefficient of the jacket [$W\ m^{-2}\ K^{-1}$]
$h_{reactor}$: Convective coefficient of the reactor [$W\ m^{-2}\ K^{-1}$]
k: Thermal conductivity [$W\ m^{-1}K^{-1}$]
L: Length [m]
L_c: Characteristic length [m]
L_s: Latent heat of vaporization [$J\ kg^{-1}$]
m_{ow}: Operating water mass [kg]
$m_{condens}$: Mass of condensed steam at the jacket outlet [kg]
m_{steam}: Mass of steam supplied to jacket [kg]
$\dot{Q}_{conduction}$: Heat transferred by conduction [W]
$\dot{Q}_{convection}$: Heat transferred by convection [W]
Q_{loss}: Lost heat through the reactor walls [$W\ m^{-2}$]
$Q_{loss-lid}$: Lost heat through the lid [$W\ m^{-2}$]
Q_{transf}: Heat transferred to the reactor [$W\ m^{-2}$]
Q_1: Heat used by the reactor [J]
Q_2: Heat transferred to the reactor [J]
$R_{convection}$: Convection resistance [$K\ W^{-1}$]
Ro: Severity factor
R_{wall}: Conduction resistance of the wall [$K\ W^{-1}$]
t: Time [min]
T: Temperature [K]
T_j: Steam temperature in the jacket [K]
T_s: Surface temperature [K]
T_1: Reactor internal wall temperature [K]
T_2: Reactor internal wall temperature next to the jacket [K]
T_6: Reactor external wall temperature [K]
T_∞: Temperature far from the wall [K]
$T_{\infty 1}$: Reactor interior temperature [K]
$T_{\infty 2}$: Environmental temperature [K]
Note: the temperatures were measured in °C and converted to K for energy balance calculations

AMIDIQ

Academia Mexicana de Investigación y Docencia en Ingeniería Química A.C.

XLI Encuentro Nacional

La Ingeniería Química, el Desarrollo Nacional y la Responsabilidad Social

Otorga el presente

RECONOCIMIENTO

a:

Adriana Lizeth Casanova-Olguín, Sonia Cabrera, Sergio Hernández-Jiménez, Irmene Ortíz

Por la presentación del trabajo:

Evaluación de la capacidad degradadora de endosulfan por cepas bacterianas aisladas de suelo hortícola con historial de uso de plaguicidas

ID: 880

Dra. María del Rosario Enríquez Rosado
PRESIDENTE DEL AMIDIQ Y DEL COMITÉ ORGANIZADÓR

Dr. Tomás Viveros García
PRESIDENTE DEL COMITÉ TÉCNICO

Evento virtual del 22 al 24 de octubre 2020

2nd LATIN AMERICAN & CARIBBEAN YOUNG WATER PROFESSIONALS CONFERENCE

IWA the international water association

La Universidad Católica de Manizales

CERTIFIES

That:

M. Vital Jácome, I. Ortíz, G. Buitrón.

with the work entitled:

Methane production from Agave bagasse by using chemical, biological, and hydrothermal pretreatments.

Participated as **SPEAKERS** with an **ORAL PRESENTATION**, within the framework of the 2nd Latin American & Caribbean Young Water Professional Conference, which took place from 8th to the 12th of November 2020, in Manizales, Colombia.

Mgra. Hna. María Elizabeth Caicedo Caicedo O.P.
Rectora
Universidad Católica de Manizales

Mgra. Catalina Triana Navas
Secretaria General
Universidad Católica de Manizales

Ph.D. Juan Sebastian Arcila Henao
Presidente Comité Organizador
IWA- Young water Latinoamerica and Caribbean professionals

Organiza Universidad® Católica de Manizales

En alianza

Dado en Manizales (Colombia) el 12 de noviembre de 2020

AMIDIQ
Academia Mexicana de Investigación y Docencia en Ingeniería Química A.C.

XLII Encuentro Nacional
Desafíos actuales en la investigación y docencia en ingeniería química

19 de mayo de 2021

Estimado(a) **Sergio Hernández Jiménez**

Agradecemos sinceramente el interés por participar en el XLII Encuentro Nacional de la Academia Mexicana de Investigación y Docencia en Ingeniería Química A.C. (AMIDIQ) y por este conducto nos complace informarle que su trabajo:

Simulación de la producción de fitasa utilizando un hongo del género Aspergillus

Cuyos autores son:

Miguel Ángel Tomate Hernández, Sergio Hernández Jiménez, Irmene Ortiz López

Ha sido aceptado para su presentación en la sesión de **Educación** en la modalidad **CARTEL**. Para ser acreedor de la constancia de participación de requiere que al menos uno de los **autores esté inscrito**, y que el **trabajo haya sido efectivamente presentado**. Para que el trabajo sea publicado en las memorias del congreso, es necesario cumplir con los criterios anteriores y haber enviado su trabajo en extenso.

En fechas posteriores podrá consultar el programa completo en nuestra página web www.amidiq.com para conocer el día y hora precisa de su presentación. Recuerde que tiene hasta el sábado 19 de junio de 2021 para sustituir el resumen de dos páginas por su trabajo en extenso en la plataforma OpenConf.

A nombre de la AMIDIQ le agradecemos su participación y esperamos tener la oportunidad de saludarlo durante el evento.

Atentamente
COMITÉ TÉCNICO AMIDIQ 2021

AMIDIQ

Academia Mexicana de Investigación y Docencia en Ingeniería Química A.C.

XLII Encuentro Nacional

Desafíos actuales en la investigación y docencia en ingeniería química

19 de mayo de 2021

Estimado(a) **Irmene Ortiz López**

Agradecemos sinceramente el interés por participar en el XLII Encuentro Nacional de la Academia Mexicana de Investigación y Docencia en Ingeniería Química A.C. (AMIDIQ) y por este conducto nos complace informarle que su trabajo:

EVALUACIÓN TÉCNICO-ECONÓMICA DEL PRETRATAMIENTO DE RESIDUOS DE PODA Y VEGETACIÓN URBANA PARA LA PRODUCCIÓN DE ETANOL

Cuyos autores son:

Luis Enrique Angulo Sierra, Sergio Hernández Jiménez, Irmene Ortiz López

Ha sido aceptado para su presentación en la sesión de **Ingeniería Ambiental** en la modalidad **CARTEL**. Para ser acreedor de la constancia de participación de requiere que al menos uno de los **autores esté inscrito**, y que el **trabajo haya sido efectivamente presentado**. Para que el trabajo sea publicado en las memorias del congreso, es necesario cumplir con los criterios anteriores y haber enviado su trabajo en extenso.

En fechas posteriores podrá consultar el programa completo en nuestra página web www.amidiq.com para conocer el día y hora precisa de su presentación. Recuerde que tiene hasta el sábado 19 de junio de 2021 para sustituir el resumen de dos páginas por su trabajo en extenso en la plataforma OpenConf.

A nombre de la AMIDIQ le agradecemos su participación y esperamos tener la oportunidad de saludarlo durante el evento.

Atentamente
COMITÉ TÉCNICO AMIDIQ 2021

Asunto: Aceptación trabajo libre XIX Congreso Nacional de Biotecnología y Bioingeniería
Fecha: lunes, 19 de julio de 2021, 20:21:25 hora de verano central
De: Sociedad Mexicana de Biotecnología y Bioingeniería
A: irmene@cua.uam.mx

Estimados:

- **Adriana Casanova**
- **Sonia Cabrera**
- **Marta Zubillaga**
- **Carmen Wacher**
- **Gloria Díaz-Ruiz**
- **Sergio Hernandez**
- **Irmene Ortiz**

El Comité Científico del XIX Congreso Nacional de Biotecnología y Bioingeniería se complace en informarle que su resumen titulado: **EVALUACIÓN DE LA CAPACIDAD de Achromobacter spanius, Peribacillus Simplex y Bacillus pseudomycoides PARA DEGRADAR ENDOSULFAN**

Fue aceptado para su presentación en el área **V. Biotecnología ambiental**.

Las instrucciones detalladas para la presentación de su trabajo puede encontrarlas en el archivo anexo y serán publicadas en la página de la SMBB a partir del 30 de junio de 2021.

- Se le recuerda que para que su resumen sea incluido en las memorias del XIX Congreso Nacional, **alguno de los autores deberá de cubrir su cuota de inscripción: Pagos SMBB**
- **La cuota de inscripción de un participante avala la presentación DE DOS TRABAJOS LIBRES.**
- Lo invitamos a registrar su asistencia al XIX Congreso Nacional a través del siguiente sitio: **Registrarme**

Descargar instrucciones para presentación de trabajos

Por el Comité Científico del XIX Congreso Nacional,

Dra. Romina Rodríguez
Presidenta del Comité Científico

Dr. Jaime Ortega López
Presidente del Comité Organizador XIX Congreso Nacional

Asunto: Aceptación trabajo libre XIX Congreso Nacional de Biotecnología y Bioingeniería
Fecha: sábado, 17 de julio de 2021, 16:11:02 hora de verano central
De: Sociedad Mexicana de Biotecnología y Bioingeniería
A: irmene@cua.uam.mx

Estimados:

- **Verónica Duran-Cruz**
- **Sergio Hernandez**
- **Irmene Ortiz**

El Comité Científico del XIX Congreso Nacional de Biotecnología y Bioingeniería se complace en informarle que su resumen titulado: **EVALUACIÓN DE LAS CONDICIONES DE PRETRATAMIENTO POR EXPLOSIÓN DE VAPOR E HIDRÓLISIS ENZIMÁTICA DE BAGAZO DE AGAVE PARA LA PRODUCCIÓN DE BIOMETANO**

Fue aceptado para su presentación en el área **VI. Bioenergía y biocombustibles**.

Las instrucciones detalladas para la presentación de su trabajo puede encontrarlas en el archivo anexo y serán publicadas en la página de la SMBB a partir del 30 de junio de 2021.

- Se le recuerda que para que su resumen sea incluido en las memorias del XIX Congreso Nacional, **alguno de los autores deberá de cubrir su cuota de inscripción: Pagos SMBB**
- **La cuota de inscripción de un participante avala la presentación DE DOS TRABAJOS LIBRES.**
- Lo invitamos a registrar su asistencia al XIX Congreso Nacional a través del siguiente sitio: **Registrarme**

Descargar instrucciones para presentación de trabajos

Por el Comité Científico del XIX Congreso Nacional,

Dra. Romina Rodríguez
Presidenta del Comité Científico

Dr. Jaime Ortega López
Presidente del Comité Organizador XIX Congreso Nacional

La Ingeniería Química, el Desarrollo Nacional y la Responsabilidad Social

Programa del XLI Encuentro Nacional de la AMIDIQ

22 al 24 de Octubre de 2020

AMIDIQ

Academia Mexicana de Investigación y Docencia en Ingeniería Química A.C.

XLI Encuentro Nacional

La Academia Mexicana de Investigación y Docencia en Ingeniería Química (AMIDIQ)

Otorga el presente

RECONOCIMIENTO

A: Dra. Adela Irmene Ortiz López

Por su participación como miembro del Comité Técnico del XLI Encuentro Nacional de la AMIDIQ

Dra. María del Rosario Enríquez Rosado
PRESIDENTA DEL AMIDIQ Y DEL COMITÉ ORGANIZADOR

Dr. Tomás Viveros García
PRESIDENTE DEL COMITÉ TÉCNICO

Ixtapa Zihuatanejo, Gro., México. 5 al 8 de mayo de 2020

COMITÉ TÉCNICO
AMIDIQ 2020

Tomás Viveros García
Presidente

Adela Irmene Ortiz López
Adrián Bonilla-Petriciolet
Agustín Jaime Castro Montoya
Agustín Ramón Uribe Ramírez
Aida Alejandra Pérez Fonseca
Alma Hortensia Serafin Muñoz
Aurora Valdés Fragoso
Claudia Gutiérrez Antonio
David Contreras López
Eduardo Jaime Vernon Carter
Eduardo Salvador Pérez Cisneros
Enrique Arriola Guevara
Fernando Israel Gómez Castro
Guadalupe de la Rosa Álvarez
Guadalupe María Guatemala Morales
Héctor Fernando Puebla Núñez
Héctor Hernández Escoto
Hugo Joaquín Ávila Paredes
Hugo Mujica Paz
Hugo Pérez Pastenes
Ignacio René Galindo Esquivel

Janett Betzabe González Campos
Jesús Alberto Ochoa Tapia
Jesús Isaac Minchaca Mojica
Jorge Ramón Robledo Ortiz
José Antonio de los Reyes Heredia
José María Ponce Ortega
Juan Gabriel Segovia Hernández
Lada Domratcheva Lvova
Marco Antonio Sánchez Castillo
María del Rosario Enríquez Rosado
Mauricio Sales Cruz
Miguel Ángel Morales Cabrera
Nelly Ramírez Corona
Ricardo Lobo Oemhnichen
Ricardo Morales Rodríguez
Rubén González Núñez
Sara Núñez Correa
Teresa del Carmen Flores Flores
Vicente Rico Ramírez
Zeferino Gamiño Arroyo
Ignacio René Galindo Esquivel

AMIDIQ

Academia Mexicana de Investigación y Docencia en Ingeniería Química A.C.

XLII
Encuentro Nacional

Desafíos actuales en la investigación
y docencia en ingeniería química

PROGRAMA TÉCNICO

PROGRAMA TÉCNICO del XLII Encuentro Nacional del AMIDIQ

Evento virtual del 08 al 11 de septiembre de 2021

COMITÉ TÉCNICO
AMIDIQ 2021

Tomás Viveros García
Presidente

Adela Irmene Ortiz López
Agustín Ramón Uribe Ramírez
Aida Alejandra Pérez Fonseca
Alfonso Mauricio Sales Cruz
Alma Hortensia Serafin Muñoz
Aurora Valdés Fragoso
Claudia Gutiérrez Antonio
Didilia Ileana Mendoza Castillo
Eduardo Salvador Pérez Cisneros
Enrique Arriola Guevara
Fernando Israel Gómez Castro
Francisco Raúl Carrillo Pedroza
Guadalupe de la Rosa Álvarez
Guadalupe María Guatemala Morales
Hugo Joaquín Ávila Paredes
Hugo Mujica Paz
Hugo Pérez Pastenes
Ignacio René Galindo Esquivel
Adela Irmene Ortiz López
Agustín Ramón Uribe Ramírez
Aida Alejandra Pérez Fonseca
Janett Betzabe González Campos
Jesús Alberto Ochoa Tapia
Jesús Isaac Minchaca Mojica
Jorge Ramón Robledo Ortiz
José María Ponce Ortega
Juan Gabriel Segovia Hernández
Marco Antonio Sánchez Castillo
María del Rosario Enríquez Rosado
Miguel Ángel Morales Cabrera
Nelly Ramírez Corona
Ricardo Morales Rodríguez
Rubén González Núñez
Salvador Hernández Castro
Sara Núñez Correa
Teresa del Carmen Flores Flores
Tomás Viveros García
Zeferino Gamiño Arroyo
Janett Betzabe González Campos
Jesús Alberto Ochoa Tapia
Jesús Isaac Minchaca Mojica

COMITÉ REVISOR
AMIDIQ 2021

Addi Rhode Navarro Cruz
Adrian Bonilla-Petriciolet
Adriana Medina Ramirez
Agustín Jaime Castro Montoya
Agustín Ramón Uribe Ramírez
Aida Alejandra Pérez Fonseca
Alejandro Ruiz Marin
Alicia Román Martínez
Alma Hortensia Serafin Muñoz
Ana Angelica Feregrino Perez
Andrea Quetzalli Cerdán Pasarán
Antioco López-Molina
Antonio Bernabé Antonio
Antonio Rodríguez Martínez
Araceli Guadalupe Romero Izquierdo
Araceli Jacobo Azuara
Areli del Carmen Ortega Martínez
Arodí Bernal Martínez
Arturo Rangel Gonce
Arturo Sanchez
Avelina Franco Vega
Beatriz Gutiérrez Rivera
Beatriz Ruiz Camacho
Brenda Huerta Rosas
Carlos Enrique Alvarado Rodríguez
Carolina Conde Mejía
Cesar Gomez
Christian O. Díaz-Ovalle
Cintia Karina Rojas Mayorga
Claudia Gutiérrez Antonio
Claudia Martínez Gómez
Constanza Machín Ramírez
Daniel Álvarez Barrera
David Contreras López
Denis Rodrigue
Diana Bustos Martínez
Didilia Ileana Mendoza Castillo
Dolores Gabriela Martínez Vázquez
Edgar José López Naranjo
Edgar Omar Castrejón González
Edgar Vázquez-Núñez
Edilberto Murrieta Luna
Eduardo Alberto López Maldonado
Eduardo Sánchez-Ramírez
Enrique Arriola Guevara
Enrique Palou
Erasmo Herman y Lara
Erika Yudit Rios Iribe
Eunice Yáñez Barrientos
Fabricio Napoles Rivera
Fernando Israel Gómez Castro
Francisco Lopez-Villarreal
Francisco Manuel Pacheco Aguirre
Francisco Raul Pedroza
German Cuevas
Guadalupe María Guatemala-Morales
Gustavo Rangel-Porras
Héctor A. Ruiz
Hector Hernandez Escoto
Heidi Patricia Medorio Garcia
Hilda Elizabeth Reynel Avila
Horacio Inchaurregui Méndez
Hugo Joaquín Ávila Paredes
Ignacio René Galindo Esquivel
Irmene Ortíz López
Irving Israel Ruiz López
Ismael Alejandro Aguayo Villarreal
Ivan Luzardo
J. Betzabe González
J. Carlos Cárdenas Guerra
Javier Fontalvo
Jazmín Cortez González
Jorge Arturo Alfaro Ayala
Jorge Ramón Robledo Ortíz
José de Jesús Ramírez Minguela
José Enrique Botello Álvarez
José Lemus Ruiz
José María Ponce-Ortega
Jose-Antonio Colin-Luna
Josefina Vergara Sánchez
Juan Antonio Noriega Rodríguez
Juan Antonio Sánchez Márquez
Juan Gabriel Segovia Hernandez
Juan José Quiroz Ramírez
Julio Armando de Lira Flores
Lada Domratcheva Lvova
Lorena Eugenia Sánchez Cadena.
Luis Mario González Rodríguez
Ma. del Carmen Chávez Parga
Ma. Guadalupe de la Rosa Alvarez
Marco Antonio Sánchez Castillo
Maria Antonieta Rios Corripio
María De La Luz Xochilt Negrete Rodríguez
María del Rosario Galindo González
María Elena Sosa Morales
Maria Guadalupe Aguilar Uscanga
Mario Alberto Rodríguez Angeles
Martín Esteban González López
Martín Picón Núñez
Mauricio Sales Cruz
Mayra Agustina Pantoja Castro
Mayra Ruiz Reyes
Micael Gerardo Bravo Sánchez
Midory Samaniego Hernández
Miguel Ángel Morales Cabrera
Myrna H. Matus
Nadia Renata Osornio Rubio
Nancy del Pilar Medina Herrera
Nancy Eloísa Rodríguez Olalde
Nancy Velasco Alvarez
Nelly Flores Ramirez
Norma Leticia Gutiérrez Ortega
Obdulia Vera López
Oscar Andrés Prado-Rubio
Radamés Trejo Valencia
Rafael Huirache
Raul Carrera Cerritos
Raúl Reyes-Bautista
Rene Loredo-Portales
Ricardo Morales Rodríguez
Roberto Gutiérrez-Guerra
Rodolfo Murrieta Dueñas
Rosa Isela Corona González
Rosa Maria Camacho Ruiz
Rubén González Núñez
Salvador Marmolejo Cervantes
Salvador Tututi-Avila
Sara Núñez Correa
Silvia Yudith Martinez Amador
Susana Figueroa Gerstenmaier
Teresa del Carmen Flores Flores
Ulises Paramo Garcia
Ulrich Vasconcelos
Valaur Ekbalam Márquez Baños
Vicente Rico Ramírez
Yuridiana Rocio Galindo Luna
Zeferino Gamiño Arroyo

Casa abierta al tiempo
UNIVERSIDAD AUTÓNOMA METROPOLITANA

C.A. 1801/18

5 de noviembre, 2018

DRA. ADELA IRMENE ORTIZ LÓPEZ
P r e s e n t e

Por este conducto le comunico que el Colegio Académico en la Sesión Número 449, celebrada el día 31 de octubre del año en curso, después de analizar los documentos correspondientes, y en el ejercicio de la facultad que le confiere el artículo 7 del Reglamento para la Transparencia de la Información Universitaria, acordó ratificarlo como *Titular* del Comité de Transparencia, periodo 2018-2020.

Atentamente

Casa abierta al tiempo

Dr. José Antonio De los Reyes Heredia
Secretario del Colegio Académico

DPT.230.20
Ciudad de México, a 7 de diciembre de 2020

A quien corresponda:

Por la presente certifico que la **Dra. Adela Irmene Ortiz López** adscrita al Departamento de Procesos y Tecnología, **co-dirigió** la formación de recursos humanos de la licenciatura en Ingeniería Biológica, fungiendo como **co-asesora** del Proyecto Terminal que se describe a continuación:

Proyecto:	Evaluación técnico-económica del pretratamiento de residuos de poda y vegetación urbana para la producción de etanol
Alumno:	Luis Enrique Angulo Sierra
Institución:	UAM-Cuajimalpa
Nivel:	Licenciatura en Ingeniería Biológica
Fecha de conclusión:	23 de noviembre de 2020

Cabe mencionar que la fecha de terminación estuvo sujeta a ajustes en las modalidades de enseñanza debido a la pandemia por la COVID-19. Asimismo, es importante señalar que este tipo de proyectos tiene un gran impacto en la formación de los alumnos ya que aplican los conocimientos teóricos y/o experimentales adquiridos a lo largo de su licenciatura, para el desarrollo de temáticas diversas en el marco de su campo profesional. El trabajo realizado se encuentra reflejado en un informe escrito final equivalente a tesis de licenciatura.

Sin más por el momento, aprovecho para enviarle un cordial saludo, quedando de usted para cualquier aclaración al respecto.

Atentamente
Casa abierta al tiempo

Dra. Marcia Guadalupe Morales Ibarría
Jefa de Departamento
Departamento de Procesos y Tecnología

Casa abierta al tiempo
UNIVERSIDAD AUTÓNOMA METROPOLITANA
Unidad Cuajimalpa

CONSTANCIA DE ASESORIA DE SERVICIO SOCIAL
6 de Septiembre, 2021.

A QUIEN CORRESPONDA:

La Sección de Servicio Social de la Universidad Autónoma Metropolitana Unidad Cuajimalpa, a través de la instancia de Servicio Social, hace constar que la profesora **DRA. ADELA IRMENE ORTIZ LOPEZ**, con No. Eco. 31055 adscrita al Departamento de **PROCESOS Y TECNOLOGIA**, de la División **CIENCIAS NATURALES E INGENIERIA**, Unidad **CUAJIMALPA**, asesoró a la siguiente alumna durante la prestación de su Servicio Social en el Proyecto: **Capacidad degradadora de plaguicidas por microorganismos aislados de suelo.**

	MATRICULA	NOMBRE DE ALUMNO LICENCIATURA DEPENDENCIA	FECHAS INICIO	 TERMINO	 ACREDITACIÓN
1	2153032316	CASANOVA OLGUIN ADRIANA LIZETH INGENIERIA BIOLOGICA UNIVERSIDAD AUTÓNOMA METROPOLITANA (UAM)	19/Oct/2020	19/Abr/2021	29/Abr/2021

Se expide la presente para los usos legales correspondientes.

Atentamente
Casa abierta al tiempo

LIC. MARIA DEL CARMEN SILVA ESPINOSA
JEFA DE LA SECCIÓN DE SERVICIO SOCIAL

UNIVERSIDAD AUTONOMA METROPOLITANA
Casa abierta al tiempo
UNIDAD CUAJIMALPA
SECCION DE SERVICIO SOCIAL

Casa abierta al tiempo
UNIVERSIDAD AUTÓNOMA METROPOLITANA
Unidad Cuajimalpa

CONSTANCIA DE ASESORIA DE SERVICIO SOCIAL
6 de Septiembre, 2021.

A QUIEN CORRESPONDA:

La Sección de Servicio Social de la Universidad Autónoma Metropolitana Unidad Cuajimalpa, a través de la instancia de Servicio Social, hace constar que la profesora **DRA. ADELA IRMENE ORTIZ LOPEZ**, con No. Eco. 31055 adscrita al Departamento de **PROCESOS Y TECNOLOGIA**, de la División **CIENCIAS NATURALES E INGENIERIA**, Unidad **CUAJIMALPA**, asesoró al siguiente alumno durante la prestación de su Servicio Social en el Proyecto: **Capacidad degradadora de plaguicidas por microorganismos aislados de suelo.**

	MATRICULA	NOMBRE DE ALUMNO LICENCIATURA DEPENDENCIA	FECHAS INICIO	 TERMINO	 ACREDITACIÓN
1	2163072233	TOMATE HERNANDEZ MIGUEL ANGEL INGENIERIA BIOLOGICA UNIVERSIDAD AUTÓNOMA METROPOLITANA (UAM)	20/Ene/2021	20/Jul/2021	17/Ago/2021

Se expide la presente para los usos legales correspondientes.

Atentamente
Casa abierta al tiempo

LIC. MARIA DEL CARMEN SILVA ESPINOSA
JEFA DE LA SECCIÓN DE SERVICIO SOCIAL

UNIVERSIDAD AUTONOMA METROPOLITANA
SECCION DE SERVICIO SOCIAL

Casa abierta al tiempo
UNIVERSIDAD AUTÓNOMA METROPOLITANA

C.A. 1084/20

18 de diciembre, 2020

DRA. ADELA IRMENE ORTIZ LÓPEZ
P r e s e n t e

Por este conducto le comunico que el Colegio Académico en la Sesión Número 488, celebrada el día 16 de diciembre del año en curso, después de analizar los documentos correspondientes, y en el ejercicio de la facultad que le confiere el artículo 7 del Reglamento para la Transparencia de la Información Universitaria, acordó ratificarla como *Titular* del Comité de Transparencia, periodo 2020-2022.

Atentamente

Casa abierta al tiempo

Dr. José Antonio De los Reyes Heredia
Secretario del Colegio Académico

KCM/FVI'S

Sociedad Mexicana de Biotecnología y Bioingeniería

XIX CONGRESO NACIONAL DE BIOTECNOLOGÍA Y BIOINGENIERÍA

MODALIDAD VIRTUAL

27 SEPTIEMBRE - 1º OCTUBRE, 2021

OTORGA LA PRESENTE

CONSTANCIA A:

Dra. Adela Irmene Ortíz López

Por su participación en la evaluación de trabajos libres del área

V. Biotecnología ambiental

del XIX Congreso Nacional de Biotecnología y Bioingeniería,
27 de septiembre - 1° de octubre, 2021

Dr. Jaime Ortega López
PRESIDENTE SMBB

Dra. Romina Rodríguez Sanoja
PRESIDENTA COMITÉ ORGANIZADOR

Dr. Álvaro R. Lara
PRESIDENTE COMITÉ CIENTÍFICO